LOS ANGELES PUBLIC LIBRARY
AUG 18 1955

JOURNAL
OF THE
AIR POLLUTION CONTROL
ASSOCIATION
Founded 1907

STACKS

SCIENCE AND TECHNOLOGY

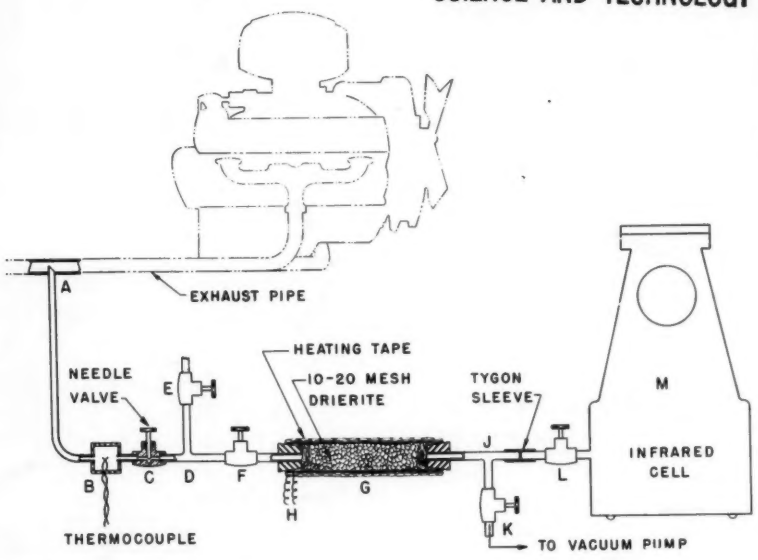

Vol. 5, No. 2 August 1955

The internal Combustion Engine—are exhaust gases an air pollution problem?

AIR REPAIR

FOUNDED 1907

JOURNAL OF THE AIR POLLUTION CONTROL ASSOCIATION

Formerly "Air Repair"

A QUARTERLY JOURNAL DEVOTED TO AIR PURIFICATION

Printed in the United States
Editor: H. C. BALLMAN
Editorial Asst.: JANE MILLER
Technical Associate: DR. W. L. NELSON

Copyright 1955
AIR POLLUTION CONTROL ASSOCIATION
4400 FIFTH AVENUE
PITTSBURGH 13, PA.

Publications Committee 1955-56
HENRY E. ALDRICH, Chairman
B. E. SAWYER, JOSEPH McCABE, D. H. HUTCHISON,
E. Q. CAMP, W. A. CARTER, ROBERT L. CHASS
Technical Review Committee 1955-56
W. C. L. HEMEON, Chairman
C. A. BISHOP, M. D. THOMAS

AUGUST 1955 **CONTENTS** **Vol. 5, No. 2**

Engine Variables and Their Effects on Exhaust Gas Composition . . . . . *J. M. Chandler, W. A. Cannon, J. C. Neerman, A. Rudolph* 65

An Inventory of Automobile Gases . . . . . *D. H. Hutchison, F. R. Holden* 71

Application of Infrared Spectroscopy to Exhaust Gas Analysis . . . . . *S. B. Twiss, D. M. Teague, J. W. Bozek, M. V. Sink* 75

Study of the Distribution and Effects of Auto Exhaust Gases . *G. P. Larson, J. C. Chipman, E. K. Kauper* 84

Flame Photographs of Light Load Combustion Point the Way to Reduction of Hydrocarbons in Exhaust Gas . . . . . *J. T. Wentworth, W. A. Daniel* 91

The Composition of Exhaust Gases from Diesel, Gasoline, and Propane Powered Motor Coaches . . . . . *M. A. Elliott, G. J. Nebel, F. G. Rounds* 103

Some Effects of Engine-Fuel Variables on Exhaust Gas Hydrocarbon Content . . . . . *F. G. Rounds, P. A. Bennett, G. J. Nebel* 109

A Rapid General Purpose Centrifuge Sedimentation Method for Measurement of Size Distribution of Small Particles—Apparatus and Methods . . . . . *K. T. Whitby* 120

A Technique for the Rapid Solution of An Air-Pollution Equation . . . . . *F. T. Bodurtha, Jr.* 127

The Editor welcomes writers interested in air pollution problems and encourages them to use the pages of this journal for the expression of their opinions. But neither he nor the Association assumes responsibility for the validity of the opinions expressed herein.

Journal of the Air Pollution Control Association is published quarterly, with editorial and executive offices at 4400 Fifth Avenue, Pittsburgh 13, Pa. Printed in U.S.A. by General Press Corporation and entered at the Post Office, Tarentum, Pa., as third class matter, P. L. & R. 34.66

Engine Variables and Their Effects on Exhaust Gas Composition*

J. M. Chandler, W. A. Cannon, J. C. Neerman, and Arthur Rudolph
Ford Motor Company
Dearborn, Michigan

Recent reports on air pollution[1-2-3], particularly those concerned with the Los Angeles smog, have indicated that hydrocarbons might be important smog-forming compounds, and that automobile exhaust could be an important source of hydrocarbons in the Los Angeles area. Surveys have been made to determine the composition of automobile exhaust, and tests have been run attempting to simulate smog under controlled conditions by combining automobile exhaust with either ozone or oxides of nitrogen. Plants which are known to be susceptible to smog damage have then been exposed to these artificial "smogs," and attempts have been made to correlate plant damage with hydrocarbons in automobile exhaust[4].

A broad program on automobile exhaust and air pollution has been active in our company for some time. We have conducted surveys of our products to determine composition of exhaust gas, we have developed several techniques for exhaust gas analysis, and we have tried several methods for reducing hydrocarbons in automobile exhaust. This paper is essentially a progress report describing some of the results we have obtained to date.

Analysis Techniques

All the data reported in this paper were obtained using a Consolidated Mass Spectrometer Model 21-103 B (Fig. 1). During the course of our mass spectrometric analysis of exhaust gas it became apparent that a significant amount of apparently unchanged gasoline is found in the exhaust. The relative proportion of unchanged gasoline to "cracked" or partly burned materials varies with the engine operating conditions, being highest on deceleration and lowest on cruising. This proportion, however, remains relatively constant for any given type of engine operation.

The gasoline actually used in each test was scanned in the mass spectrometer and treated as a "compound" in the analysis of exhaust gas samples obtained in that test. This is the quantity designated as "Unburned Fuel" in the test results. Data are thus reported either as total hydrocarbons, weight percent of supplied fuel, or as unburned fuel, mole per cent. Total hydrocarbons were determined to provide basic knowledge of exhaust gas composition, whereas the unburned fuel values were used for all comparative testing of devices for reducing hydrocarbon emission in automobile exhaust gas.

Sampling Methods

Most of our exhaust gas samples were collected in 300 ml. evacuated (below 1 mm. Hg.) flasks equipped with special high-vacuum stopcocks. To obtain a sample, a standard taper joint on the flask was inserted into a matching stainless steel taper mounted in the wall of the exhaust pipe (Fig. 2 shows a test car mounted on a chassis dynamometer, and Fig. 3 shows how the exhaust gas sample is actually taken). At the desired moment, the stopcock was opened, and the flask allowed to fill with exhaust gas to atmospheric pressure. Moisture usually condenses on the inside walls of the flasks; hence, subsequent analysis of the water in the gaseous portion of the sample does not represent all of the water originally present. Some water-soluble compounds (i.e., H_2S, HCl, SO_2) may also be removed. Recognizing these limitations, the sampling procedure seems quite satisfactory for the problem at hand; that is, the evaluation of the effect of engine variables on the hydrocarbon content of the exhaust.

Fig. 1 Mass Spectrometer used to analyze exhaust gases.

(1) Haagen-Smit, A. J., "Chemistry and Physiology of Los Angeles Smog," *Ind. Eng. Chem., 44,* 1342-46 (1952).

(2) Magill, P. L., Hutchison, D. H., and Stormes, J. M., "Hydrocarbon Constituents of Automobile Exhaust Gases," Proc. Second National Air Pollution Symposium, p. 71, 1952.

(3) Viets, F. H., Fischer, G. I., and Fudurich, A. P., "Hydrocarbon Pollution from Automobile Exhaust Gases, A Report of Test 668 and Associated Work," Air Pollution Control District, County of Los Angeles, Sept. 12, 1952.

(4) Conn, G. R., Noble, W. M., and Larson, G. P., "Detection of Smog-Forming Hydrocarbons in Automobile Exhaust Gases Using Plants as Indicators," *Air Repair, 4,* 31-34 (1954).

*Presented at the 48th Annual Meeting of the Air Pollution Control Association, Detroit, Michigan, May 22-26, 1955.

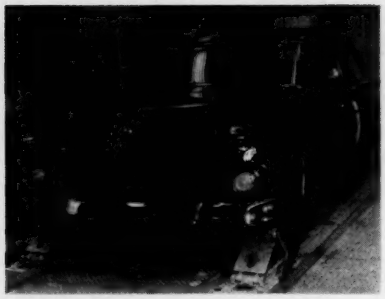

Fig. 2. Test vehicle on chassis dynamometer.

Fig. 3. Exhaust gas sampling technique.

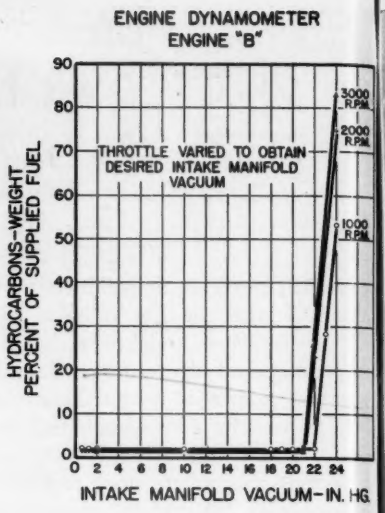

Fig. 4. Effect of intake manifold vacuum on hydrocarbon emission. ➡

During deceleration, exhaust gas flow and composition change so rapidly that it is difficult to get reproducible "grab samples," and we questioned whether a "grab sample" would be representative of the total deceleration cycle. It therefore seemed desirable to collect a deceleration sample throughout an entire cycle. Mass spectrometric procedures did not seem readily adaptable to this sort of sampling, so a chemical method was developed.

A portion of the exhaust gas flow was diverted through a dry-ice-cooled trap and thence to a wet test meter. A solenoid valve actuated by a microswitch attached to the throttle linkage accurately timed the flow of exhaust through the cold trap, starting at the moment the throttle was closed (thus initiating the deceleration cycle). The condensate was analyzed for combustible materials by an adaptation of the combustion methods of MacFarlane[5] and Lloyd[6]. Results obtained by this chemical procedure are compared with a mass spectrometric analysis of a "grab sample" (taken approximately 6 seconds after closing throttle) on deceleration cycles with the same car:

	Volume Per Cent Hydrocarbons (C_4 and Higher)
Chemical Method	1.4
Mass Spectrometer	1.8

This comparison between a "grab sample" analyzed on the mass spectrometer and a sample collected during the entire deceleration cycle, analyzed by the combustion method, verifies that a "grab sample" taken six seconds after the start of deceleration is a reasonable indication of the average hydrocarbon emission during a typical deceleration.

Hydrocarbon Emissions—Standard Engines

Having established test procedures, we then proceeded to survey our production engines to determine the hydrocarbon content of their exhaust gas. The results from this phase of the program are interesting in that they confirm previously published results obtained by another automobile manufacturer, particularly identifying the deceleration cycle as the one emitting the most hydrocarbons.

For test purposes, engines were mounted on an engine dynamometer and samples were taken from a standard car exhaust system attached to the engine.

Fig. 4 shows a plot of intake manifold vacuum versus hydrocarbon emission (weight per cent of supplied fuel) for several engine speeds. These curves indicate that the hydrocarbon emission is approximately 2% by weight from full throttle until idling manifold vacuum is exceeded.

Above 21 in. Hg. manifold vacuum, the hydrocarbon emission rises steeply as shown. In this operating range, the engine is not developing power, but must be turned by the dynamometer, similar to a car deceleration or a coast down a hill with the clutch engaged and the throttle closed. It should be noted that the points on the extreme left hand side of the curve, at wide open throttle, would be almost equivalent to a full power acceleration on the road, while the center portion represents cruising at various speeds. Of interest here is the reason for the abrupt increase in hydrocarbon emission at the high-manifold-vacuum conditions existing during deceleration.

Illuminating contributions in this respect were given in 2 papers presented at the SAE Annual Meeting last January[7-9]. Of fundamental interest were the flame photographs which showed the suspected partial or incomplete combustion during high-vacuum conditions. Limits were also established beyond which no more combustion takes place. The reason for the lack of burning was found to be the extensive exhaust gas dilution of the charge, or "low concentration of reactants," due to the

(5) MacFarlane, J. J., "The Application of Chemical Analysis to the Investigation of Gas Turbine Combustion Problems," Proc. International Congress of Pure and Applied Chemistry, 1947.

(6) Lloyd, P., *Transactions Am. Soc. Mech. Eng., 70,* 335-41 (1948).

(7) Rounds, F. G., Bennett, P. A., and Nebel, G. J., "Some Effects of Engine-Fuel Variables on Exhaust Gas Hydrocarbon Content," J. Air Poll. Control Assoc., *5,* this issue (August 1955).

(8) "Automotive Exhaust Testing Procedures and Efficiency Studies in the Evaluation of a Catalytic Muffler," Los Angeles County Air Pollution Control District Publication No. *51,* July 30, 1954.

(9) Wentworth, J. T., and Daniel, W. A., "Flame Photographs of Light-Load Combustion Point the Way to Reduction of Hydrocarbons in Exhaust Gas," J. Air Poll. Control Assoc., *5,* (1955).

← *Fig. 5. Ionization gap spark plug.*

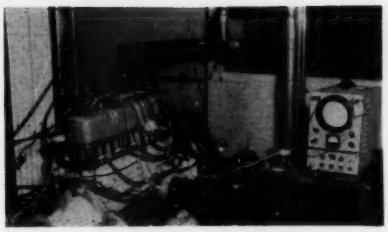

Fig. 6. Dynamometer test installation using Socony engine analyzer.

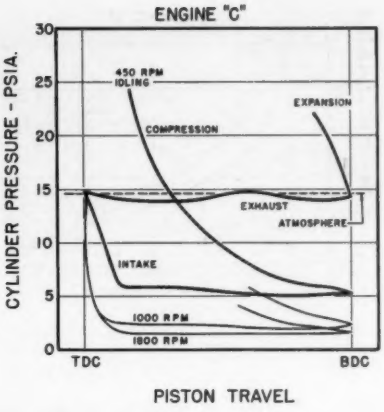

Fig. 7. P-V diagram comparision at ⟵ idling and during simulated decelerations at 1000 and 1800 R.P.M.

high manifold vacuum rather than just high vacuum itself. It has been our contention that an alternate burning and non-burning takes place during deceleration, inasmuch as non-burning for a few cycles should create a charge with less dilution, which in turn should burn in a normal manner.

Hydrocarbon emission is dependent on the failure of the charge to burn completely. It is, therefore, desirable to determine whether and to what extent burning takes place in the combustion chamber during a normal deceleration of the car, or during over-ride conditions on the dynamometer, simulating deceleration. Three methods were applied to detect the occurrence of combustion.

They were:

1. The ionization gap.
2. Indicator diagrams.
3. Dynamometer beam loads.

The ionization gap method gave a good indication of firing and non-firing for each cylinder, and could be used on the dynamometer as well as on the road. A Socony Engine Analyzer was used, connected to ionization gaps located within the spark plugs (and in some cases also in the quench area) to determine burning throughout the chamber (Fig. 5 and 6). The ionization gap method proved to be a valuable tool for determining the existence and/or completeness of combustion, both under standard operating conditions and during the preliminary evaluation of carburetor devices. It does not, however, replace exhaust gas analysis as the final test to determine the effectiveness of a device designed to reduce hydrocarbon emission.

Indicator diagrams taken with a strain-gage-type pressure pick-up and an oscilloscope show cycle-to-cycle pressure events. Of interest in this connection are the diagram portions which represent the exhaust and intake strokes. A special low-pressure pickup was used in connection with a continuous-recording X-Y indicator and a sampling valve. The results in this case are average values for many cycles. An example is shown in Fig. 7, converted to a pressure-volume diagram. It was taken at 450 rpm. idling. The suction strokes for 1000 and 1800 rpm. simulated decelerations are superimposed. While the pressure during the exhaust stroke is near atmosphere in each case, it drops to depressions as they exist in the manifold as soon as the intake valve opens.

The cylinder charge at the end of the suction stroke, therefore, consists of residual gases having a volume equal to the combustion chamber volume—expanded to the vacuum and temperature existing in the cylinder—plus fresh charge equal to the remainder of the total cylinder volume. Thus, the amount of fresh charge will decrease in comparison with the residual gas volume as the cylinder depression increases, thus increasing exhaust gas dilution. This increased dilution is responsible for lack of combustion, thereby causing hydrocarbon emission to increase with an increased manifold vacuum.

Dynamometer beam loads were used to explore engine variables which might affect hydrocarbon emission, particularly spark advance, as shown on Fig. 8. Here we have plotted braking torque (or engine friction) with the throttle closed versus engine rpm. The lower curve shows braking torque with standard 3 to 5.5° spark advance (closed throttle). The upper curve shows the reduction in braking torque, or improvement in burning, which is accomplished by advancing the spark until a maximum reduction in torque has been attained. As can be seen, the per cent improvement is greatest at the lower engine speeds, decreasing with increasing engine rpm. Fig. 9, however, shows a plot of hydrocarbon emission versus engine speed under the same engine operating conditions. In this case the upper curve represents hydrocarbon emission using the automatic spark advance setting, the lower curve, the reduced hydrocarbon emission resulting from increasing spark advance for least braking. It appears from this curve that the per cent reduction in hydrocarbon emission increases with engine speed, even though the per

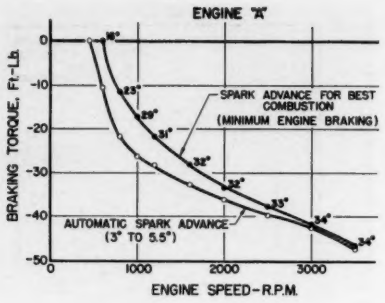

Fig. 8 Effect of spark advance on engine braking.

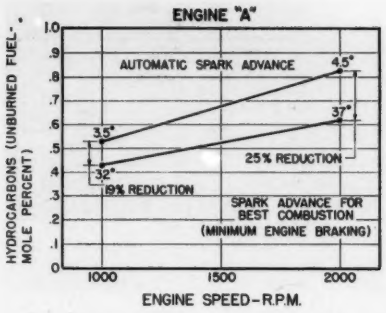

Fig. 9. Effect of spark advance on hydrocarbon emission during closed throttle deceleration.

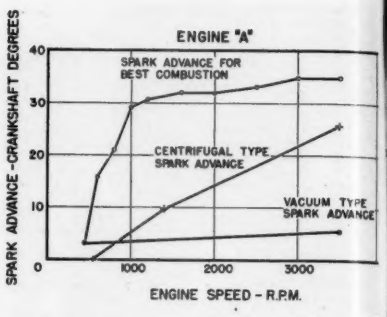
ENGINE "A"
SPARK ADVANCE - CRANKSHAFT DEGREES
SPARK ADVANCE FOR BEST COMBUSTION
CENTRIFUGAL TYPE SPARK ADVANCE
VACUUM TYPE SPARK ADVANCE
ENGINE SPEED - R.P.M.

Fig. 10. Spark advance during closed throttle deceleration.

cent reduction in braking torque decreases with engine speed, as on the previous curve. This test indicates some advantage, not yet fully explored, in advancing the spark beyond the automatic setting during deceleration.

Fig. 10 shows the spark advance required for best burning throughout the speed range with closed throttle. It can be seen that the spark settings required are beyond present settings for either centrifugal or full-vacuum-advance distributors.

Having noted the high rates of hydrocarbon emission during idling operation as published in the literature[2-3], and having noted that many of the cars tested were old and in poor mechanical condition, it became of interest to us to determine the effect of engine condition on air-fuel ratio at idle. Since good correlation exists between air-fuel ratio and hydrocarbon emission at idle, as shown in Fig. 11, it was apparent that air-fuel ratio, which is relatively easy to measure, could be a guide for estimating hydrocarbon emission.

For this information a parking lot survey of customer cars was considered. A second approach was conceived, however, which led us to examine a large number of company-owned pool cars for air-fuel ratio at idle, both as the car was received, and after the idle spark advance and carburetor settings were readjusted to best idle at manufacturer's specifications. It was reasoned that if the company pool cars, which are current models and in good mechanical condition, were in the air-fuel range of low hydrocarbon emission, then cars in the field could also be considered to be in the same range *if* they too were in good mechanical condition and properly tuned. In this survey 46 vehicles were tested, and the results are shown in Fig. 12, superimposed on the previous curve. Here we see that these cars not only were at a relatively low hydrocarbon emission rate as received, but were also in good adjustment, as tuning did not bring about a large improvement. (It should be noted that these cars were *not* test cars, but company pool cars used throughout the Detroit area for transportation.)

Concurrent with the field surveys and the testing on the engine dynamometer was our test program on the chassis dynamometer. Exhaust gas samples were taken from standard test cars under various operating conditions. Cruising and idling are steady state conditions, but the transient conditions during deceleration posed the need for a continuous exhaust gas analyzer. We patterned our sampling technique after the one developed by the Los Angeles Air Pollution Control District. We felt that they had done a considerable amount of work to arrive at their procedure, and we also wanted data obtained on a comparable basis. Thus, our deceleration samples were taken in evacuated flasks, at a point ahead of the muffler, 6 seconds after the start of the deceleration.

Fig. 13 indicates some of our results during cruising, idling, and deceleration. The results were as expected, cruising having the lowest hydrocarbon emission, idling

(2) See footnote 2, page 65.
(3) See footnote 3, page 65.

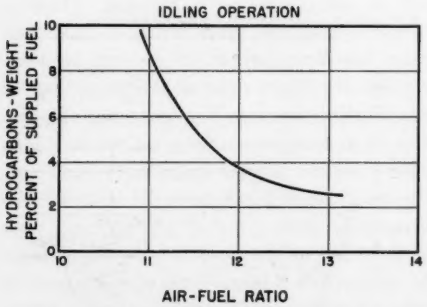

Fig. 11. Effect of air-fuel ratio on hydrocarbon emission.

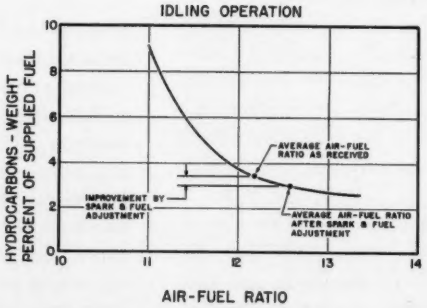
IDLING OPERATION
HYDROCARBONS - WEIGHT PERCENT OF SUPPLIED FUEL
AVERAGE AIR-FUEL RATIO AS RECEIVED
IMPROVEMENT BY SPARK & FUEL ADJUSTMENT
AVERAGE AIR-FUEL RATIO AFTER SPARK & FUEL ADJUSTMENT
AIR-FUEL RATIO

Fig. 12. Effect of air-fuel ratio on hydrocarbon emission.

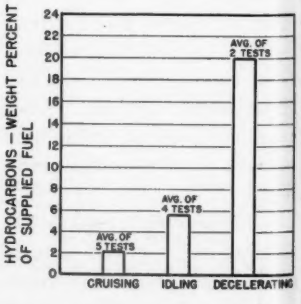

Fig. 13. Effect of engine operating conditions on hydrocarbon emission.

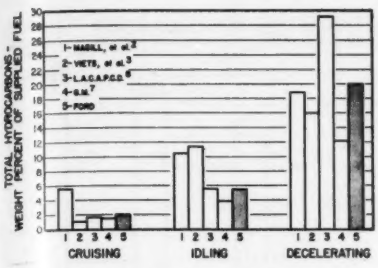

Fig. 14. Comparison of results with previous studies.

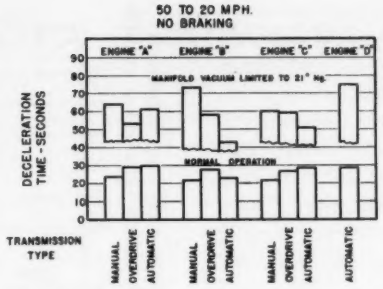

Fig. 15. Effect of vacuum limiter on closed throttle deceleration time.

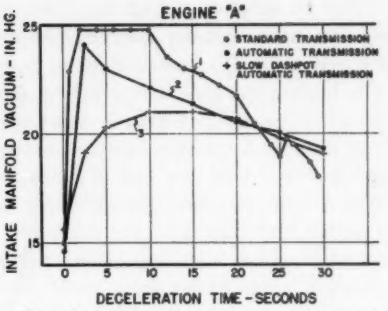

Fig. 16. Level road deceleration tests intake manifold vacuum vs. deceleration time from 50 M.P.H.

slightly more, and deceleration considerably more. Fig. 14 comparing our results with those of 4 other investigators, shows good correlation of results[2-3-7-8].

From the results shown in Fig. 13 and 14, it appears that cruising and idling have low rates of hydrocarbon emission for vehicles in good operating condition. The major area for reduction of hydrocarbon emission through engine design appears to be in the range of high manifold vacuum during deceleration.

Reducing Hydrocarbon Emission During Deceleration

Of the various methods devised for decreasing hydrocarbon emission during deceleration, limiting the manifold vacuum has many interesting features. Referring back to Fig. 4, we can see that below 21 in. Hg. the hydrocarbon emission is in the 2% range, far below the emission rate of a normal deceleration. If a spring-loaded diaphragm were attached to the throttle linkage and actuated by manifold vacuum, it could be set to keep the throttle sufficiently open during a run-down to prevent the manifold vacuum from exceeding 21 in. Hg.

In order to estimate the potential of such a device, road tests were run on each of our products to measure deceleration time under normal driving conditions, and also with the throttle held open to hold the manifold vacuum at or below 21 in. Hg.

As shown in Fig. 15, the time required for a non-braking deceleration with an automatic torque-converter transmission and a manifold-vacuum limiter averaged almost twice the time required for a normal non-braking deceleration from 50 to 20 mph. Overdrive transmissions also averaged almost twice as long, and the manual transmission with the manifold-vacuum limiter took nearly 3 times as long as normal. In other words, in order to stop a vehicle in the same amount of time, more braking would be required with a vacuum-limiter-equipped vehicle than with a standard vehicle.

However, the potential reduction in hydrocarbon emission from a vacuum limiter is worth consideration. Since we have already seen that operation below 21 in. Hg. manifold vacuum averages 2% hydrocarbon emission, (weight per cent of supplied fuel), and that normal decelerations average up to 20% hydrocarbon emission, a substantial reduction in emission rate is readily apparent with the manifold vacuum limited to 21 in. Hg. during a deceleration. Based on equal deceleration times, and on the fact that fuel flow is 2 to 3 times as much during "limited vacuum" deceleration as during normal deceleration, an estimated reduction in hydrocarbon emission of 70 to 80% can be calculated. Operation with the vacuum limiter will, of course, result in a need for increased braking.

(2) See footnote 2, page 65.
(3) See footnote 3, page 65.
(7) See footnote 7, page 66.
(8) See footnote 8, page 66.

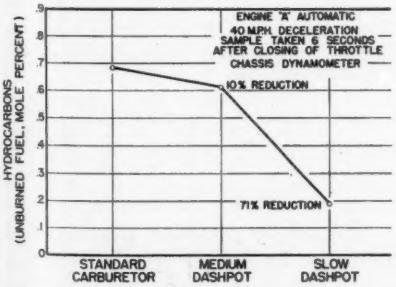

Fig. 17. Effect of carburetor devices on hydrocarbon emission.

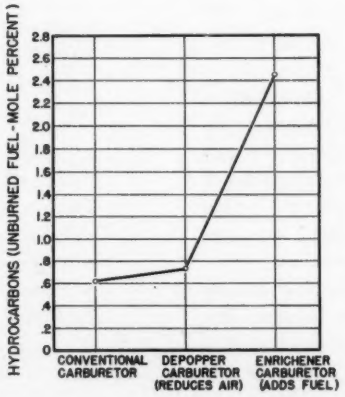
HYDROCARBONS (UNBURNED FUEL - MOLE PERCENT)
CONVENTIONAL CARBURETOR
DEPOPPER CARBURETOR (REDUCES AIR)
ENRICHENER CARBURETOR (ADDS FUEL)

Fig. 18. Effect of carburetor devices on hydrocarbon emission.

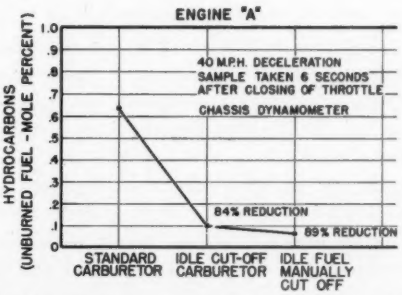

Fig. 19. Comparison of carburetor idle fuel cut-off device on hydrocarbon emission.

Fig. 16 shows a plot of manifold vacuum versus deceleration time utilizing an even simpler type of manifold vacuum limiter, a slow-leakage dashpot on the carburetor. The highest vacuum is reached by a manual transmission vehicle (Curve 1). Curve 2 shows the reduction in manifold vacuum for a standard automatic transmission, indicating the reason for less hydrocarbon emission from a vehicle equipped with an automatic transmission. Curve 3 shows the vacuum-time curve for a dashpot with a slower leakage rate calibrated to keep the manifold vacuum below 21 in. Hg.

Fig. 17 indicates the effect on per cent hydrocarbons in the exhaust gas using dashpots with 3 leakage rates, standard, medium, and slow. It is to be emphasized, of course, that the reductions indicated are for samples taken 6 seconds after the start of the deceleration. Until we have looked further into the field of analyzing transient operating conditions, we will not know the hydrocarbon emission versus deceleration time curve which is required for adequate evaluation of any device designed to reduce hydrocarbon emission during deceleration.

In our pursuit of devices involving more extensive carburetor changes, several different approaches were conceived and tried, some utilizing components already existing. Since the goal was to improve combustion during deceleration, 2 carburetors previously designed to eliminate run-down "popping" in the exhaust manifold were tested on the chassis dynamometer for their effects on combustion. The first, a "de-popper" carburetor, was designed to eliminate backfiring by decreasing the air from the carburetor during deceleration, thereby producing an enriched mixture during high manifold vacuums. The second carburetor was designed for the same use, but achieved richness by actually increasing fuel flow during deceleration. Fig. 18 indicates the negative results attained with each of these devices, since both resulted in more hydrocarbon emission during deceleration.

One of the more promising devices from the standpoint of test results is the idle fuel cut-off carburetor. This carburetor can be set to decrease or cut off entirely the flow of fuel when the manifold vacuum exceeds a pre-set level, usually in the neighborhood of 20 to 22 in. Hg. Such a device has an additional advantage of saving the fuel normally wasted during deceleration (an estimated 3% savings for the Los Angeles APCD test route).

Methods applied to shut off the idle fuel are either a positive shut off valve, or a valve which bleeds a sufficient amount of atmospheric air into the idle system to cancel the suction for the idle fuel. A combination of both methods is also feasible. In either case the valve must be operated by the increased manifold vacuum existing during deceleration and override conditions.

It is understandable that with no fuel flowing during deceleration, the intake manifold and ports become dry after a certain period, and that a lack of combustible mixture then exists, if sudden normal operation is demanded. No trouble in this respect was encountered with the idle-cut off carburetor during acceleration after a deceleration. The accelerating pump apparently takes care of supplying sufficient fuel.

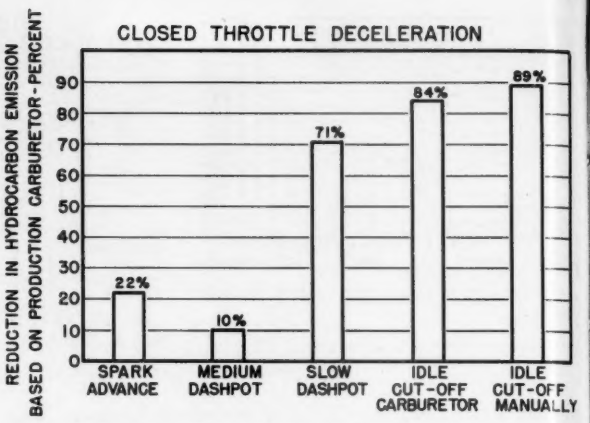

Fig. 20. Summary of methods for reducing hydrocarbon emission.

Idling after deceleration poses a more serious problem and in many cases a "drooping" of the engine or even stalling is encountered. It was found that much can be done to improve the time of recovery after a period of deceleration by making changes in the idle system which would tend to create a quicker response.

The depressions at which the idle fuel shuts off and cuts back in should be nearly the same in order to keep the period of functioning as long as possible. The sensitivity, or lack of hysteresis, depends on the design of the valve and the friction opposing its operation.

Cutting off the fuel during deceleration has a good effect on reducing hydrocarbon emission, as noted in Fig. 19. Here we see a reduction in hydrocarbon emission of 84% at the 6 second sampling point. This 84% reduction is compared with an 89% reduction when the fuel is manually cut-off, indicating some hydrocarbon emission from the fuel residue in the intake manifold and exhaust system.

Summary

From the data presented it can be concluded that:

1. Hydrocarbon emission from well-tuned engines in good mechanical condition is lowest during cruising, next lowest at idle, and highest during deceleration (Fig. 13).
2. An advanced spark setting during deceleration offers an apparent reduction in hydrocarbon emission (Fig. 20).
3. Hydrocarbon emission during deceleration can be substantially reduced by limiting the manifold vacuum to a pre-set level, limiting the manifold vacuum by a slow-leak dashpot, or by cutting off fuel flow during deceleration (Fig. 20).

It is to be emphasized that the data reported in this

(Continued on page 108)

An Inventory of Automobile Gases*

DALE H. HUTCHISON AND FRANCIS R. HOLDEN
Stanford Research Institute
Stanford, California

Large quantities and many types of impurities are emitted daily into the atmospheres of our cities. The pollutants may be solid, liquid, or gaseous—usually there are combinations of the 3 types. The magnitude of each pollution problem is a function of many meteorological factors, each contributing to the available capacity of the atmosphere as a dump. Pollution is most troublesome when the air mass becomes stagnant with great stability for an appreciable period.

Air pollution problems, in the past, have resulted primarily from smoke and fly ash produced by the combustion of fuels used for heating purposes. London, Pittsburgh, Cincinnati, and St. Louis are examples of communities where the major sources of pollution are domestic and industrial heating plants. This type of pollution may be controlled by dust collection, by modification of heating plants, and by restrictions on the use of high volatility fuels.

Of more recent origin is the type of air pollution represented by Los Angeles smog. In the latter, the smog effects are eye irritation, crop damage, and reduced visibility. These smog manifestations, initiated by sunlight, are caused by the reaction products of combustion effluents, primarily hydrocarbons and ozone. These gases and vapors are held in place by the topographical and meteorological conditions in the Los Angeles Basin.

The portion of this area generally known as the south coastal basin is bounded by an arc of mountains on 3 sides, while the ocean with its on-shore winds is on the fourth side. During the period May through November, a mass of air settles over the coast of California from high above the Pacific Ocean. As this mass of air moves downward, it warms to 75° to 90° F, forming a layer of warm air over the cooler air at ground level. This condition is known as a temperature inversion. The base of the inversion in the Los Angeles area is generally 1000 to 2000 feet above ground level[1]. It rises and lowers depending upon the meteorological conditions. If the inversion is preceded by several days when the daily wind movement is less than the normal 125 miles, the pollutants are held captive. Under these conditions, they accumulate as gases and aerosols with the latter consisting of a combination of liquid droplets and particles in the sub-micron range[2]. These materials may react with one another, under the influence of sunlight to produce the plant damage and eye irritation so widely associated with smog[3]. In Los Angeles County these conditions exist about 260 days out of the year, and the pollutants may become sufficiently dense to restrict visibility to less than one mile[4].

Although the entire coastal basin occupies an area of about 1700 mi.^{2}, the air pollution is primarily concentrated in an area of 1200 mi.^{2}, which includes Greater Los Angeles, Pasadena, and Long Beach. The height to which the smog actually rises is unknown, but the upper limit of high concentrations of pollutants is generally considered to be at the base of the inversion, or about 0.2 mile on the average[1]. The volume of smog can be estimated from these figures to be approximately 240 mi.^{3}

The major source of air pollution in Los Angeles County is the incomplete combustion of over 50,000 tons of organic materials and fuels each day by the general public and industry. This combustion pours over 1,000,000 tons of contaminated gas every day into the atmosphere, containing more than 2,600 tons of organic materials, aldehydes, ammonia, and oxides of nitrogen and sulfur[5]. In addition to the organics and other materials put into the air by combustion processes, an amount estimated at 440 tons of hydrocarbons is evaporated into the air each day. Approximately 220 tons of this come from the production, manufacture, and distribution of petroleum products. The other 220 tons come from the evaporation of gasoline from service stations and autos[5].

The Committee on Smoke and Fumes of the Western Oil and Gas Association completed in March 1954 a survey of losses from petroleum-handling operations and automobiles. These figures are shown in Table I.

Of the more than 3,000 tons of organic contaminants emitted to the Los Angeles atmosphere each day by all sources[5], 1456 tons, or about 50%, are hydrocarbons which arise from the producing, refining, marketing, and automotive usage of petroleum. Of these 1456 tons of hydrocarbons, 1016 tons, or 70%, are the products of automobile exhaust. Automobile exhaust therefore contributes one-third of the total organic contamination of 3,000 tons each day, and is the largest single source of

(1) Robinson, Elmer, "Some Air Pollution Aspects of the Los Angeles Temperature Inversion," *Bull. Amer. Met. Soc. 33*, 247-50 (1952).

(2) Stanford Research Institute, "The Smog Problem in Los Angeles County," p. 107, Western Oil and Gas Association, Los Angeles, Calif., 1954.

*Presented at the Anunal Meeting of the Society of Automotive Engineers at Detroit, Michigan, January 10-14, 1955.

(3) Cadle, Richard D., and Johnston, Harold S., "Chemical Reactions in Los Angeles Smog," *Proceedings Second National Air Pollution Symposium*, pp. 28-34, Stanford Research Institute, Stanford, Calif., 1952.

(4) Stanford Research Institute, "The Smog Problem in Los Angeles County," p. 29, Western Oil and Gas Assoc., Los Angeles, Calif., 1954.

(5) Larson, G. P., Fisher, G. I., and Hamming, W. J., "Evaluating Sources of Air Pollution," *Ind. Eng. Chem. 45*, 1070 (1953).

TABLE I

Hydrocarbon Emissions to the Atmosphere from the Producing, Refining, Marketing, and Automotive Usage of Petroleum Products in Los Angeles County

Source of Hydrocarbons	Total Hydrocarbons		Olefins, Amylenes and Heavier	
	Tons per day	Percent	Tons per day	Percent
Hydrocarbons from production, refining, marketing	224	15.4	12	3.6
Service station operation	52	3.6	6	1.8
Evaporation from automobile tanks and carburetors	164	11.0	20	6.1
Automobile exhaust	1,016	70.0	292	88.5
Total	1,456	100.0	330	100.0

hydrocarbon pollutants to the Los Angeles atmosphere and also the most effective distribution system.

The importance of hydrocarbons in the atmosphere is related to the strong oxidizing effect of Los Angeles smog. It is reported by Haagen-Smit, Shepherd and others[6-9] that unsaturated hydrocarbons (olefins), especially those containing 5, 6, and 7 carbon atoms, can react with nitrogen oxides or ozone in sunlight to produce substances causing characteristic effects of smog. These products are considered to be ozonized hydrocarbons or peroxides. As is shown in Table I, automobile exhaust contributes 88% of the olefins found in the Los Angeles atmosphere.

In addition, Haagen-Smit has recently shown[10] that the automobile exhaust gases are capable of forming ozone in the air at concentrations in the same order as those measured in the Los Angeles atmosphere.

Thirty-seven percent of the nitrogen oxides in the air are emitted to the atmosphere from automobile exhaust[5], making this one of the major contributors of oxides of nitrogen to the atmosphere.

The amounts of hydrocarbons and nitrogen oxides discharged in automobile exhaust gases daily in Los Angeles County would result in concentrations of 0.25 ppm. hydrocarbons and 0.06 ppm. nitrogen oxides in the 240 mi.^{3} of polluted air. These values may be compared with 0-3 ppm. hydrocarbons and 0.2-0.4 ppm. of nitrogen oxides measured under conditions of intense smog[5].

The range of measured concentrations of hydrocarbons and nitrogen oxides in the Los Angeles atmosphere demonstrates the variability of smog. It is of interest that the calculated concentrations of the same constituents contributed by automobile exhaust are in reasonable agreement with the measured values. The estimated concentrations assume complete mixing of the exhaust gases in the 240 mi.^{3} of air. The maximum reported concentration of hydrocarbons is 12 times the calculated average and the maximum reported concentration of nitrogen oxides is 6.7 times the calculated average.

It therefore appears that automobile exhaust gases are a substantial source of the hydrocarbons and nitrogen oxides present in the atmosphere during the intense smogs.

As part of the continuing study on the Los Angeles smog problem by Stanford Research Institute, mass spectrometer analyses have been made to estimate the nature and amounts of hydrocarbons exhausted by passenger cars into the Los Angeles County atmosphere. The ultimate objective of these investigations was to arrive at an estimate of the amount of hydrocarbons released into the Los Angeles atmosphere by gasoline-burning vehicles.

Five pre-war and 5 post-war automobiles were used, and were chosen at random without regard to the mechanical condition of the motor. The makes of the automobiles and their ages were selected as typical of the automobile population, according to the passenger car count compiled by the Department of Motor Vehicles of the State of California. A rough indication of the mechanical condition of the cars was obtained by measuring the air-to-fuel ratio, the intake manifold vacuum under idling conditions, and the cylinder pressure. The mechanical condition of the group of cars selected was believed to be roughly representative of the cars on the highway.

Regular-grade, premium-grade, and straight-run gasolines were used. The straight-run was especially prepared and contained no unsaturated hydrocarbons. Runs were also made on composite samples prepared from regular and from premium-grade gasolines produced by 6 major petroleum companies in the Los Angeles area.

Four driving conditions were considered typical of an automobile operating either in Los Angeles city or suburban traffic:

Acceleration (full throttle)	10 to 30 mph.
Steady driving	30 mph.
Deceleration	30 to 10 mph.
Idling	Normal idle

From inspection of the traffic patterns in the city and in the country, a traffic density of about 30,000 or greater on a 16 hr./day basis seemed representative of suburban areas. It was assumed that one-half of the total gasoline was consumed in city driving, and the other half in suburban driving. These densities were arrived at after a study of the traffic counts made annually for Los Angeles County by the Highway Department of the State of California. The division of gasoline consumption was arrived at by numerous visual inspections of the traffic density and discussions with informed traffic engineers.

A route was selected in the county as being repre-

(5) See footnote 5, page 71.

(6) Shepherd, Martin, Rock, S. M., Howard, Royce, and Stormes, John, "Isolation, Identification, and Estimation of Gaseous Pollutants of Air," *Anal. Chem., 23,* 1431-40 (1951).

(7) Haagen-Smit, A. J., Darley, Ellis F., Zaitlin, Milton, Hull, Herbert, and Noble, Wilfred, "Investigation on Injury to Plants from Air Pollution in the Los Angeles Area," *Plant Physiology 27,* 18-34 (1952).

(8) Haagen-Smit, A. J., "The Air Pollution Problem in Los Angeles," *Engineering and Science* (Calif. Inst. Tech.) *14,* 7-13 (December 1950).

(9) Haagen-Smit, A. J., "Chemistry and Physiology of Los Angeles Smog," *Ind. Eng. Chem. 44,* 1342-46 (1952).

(10) Haagen-Smit, A. J., and Fox, M. M., "Photochemical Ozone Formation with Hydrocarbons and Automobile Exhaust," *Air Repair 4,* 105 (November 1954).

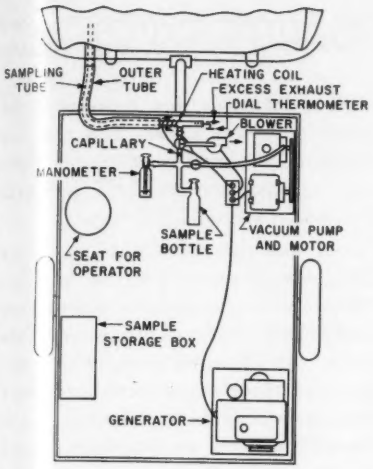

Fig. 1. Apparatus used for automobile exhaust sampling.

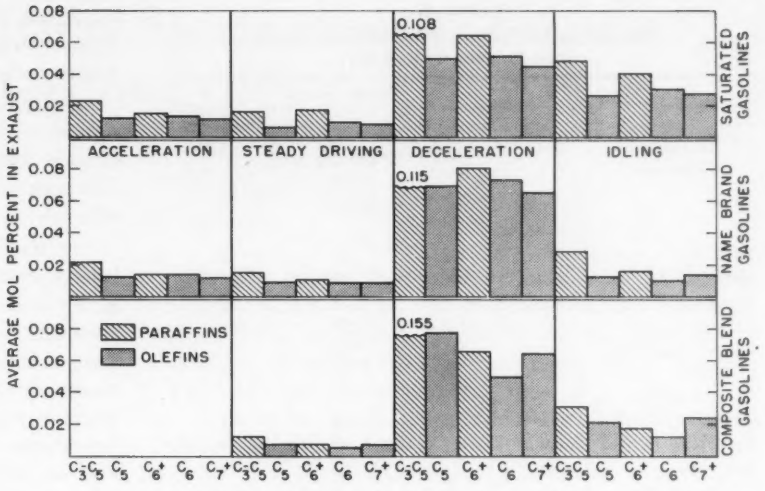

Fig. 2. Average exhaust analyses for different gasolines.

sentative of city and suburban traffic patterns. The amount of gasoline consumed in each of the traffic patterns and under the 4 driving conditions was determined while the vehicle was in operation in the selected traffic routes. A recording tachometer measured the car speed and the distance traveled.

As the automobiles were operating under the 4 driving conditions, exhaust samples for analysis by the mass spectrometer were collected by use of an apparatus mounted in a trailer drawn by the test vehicle. A diagrammatic sketch of the apparatus is shown in Fig. 1.

The automobile exhaust was conducted to the trailer in a double tube to guard against condensation of water. The sample was taken from the inner tube in a 250-ml sample bottle which had previously been evacuated, by raising the pressure in the bottle from 1 to 100 mm. mercury with the exhaust gas.

Twenty to forty samples of exhaust emitted during each driving condition were collected and analyzed to obtain a measure of the variation of results and to permit statistical estimation of the precision.

All samples were analyzed by the Consolidated Engineering Corporation, Pasadena, California, with a mass spectrometer within one to three hours after being collected. A detailed discussion of these analyses is presented in a Stanford Research Institute Report[11]. It has been estimated by the Consolidated Engineering Corporation that the precision of the analyses is ± 0.1 mol. percent for inorganic gases and ± 0.01 percent for volatile hydrocarbons. Statistical analysis of the data confirmed this estimate.

Exhaust sample data for test cars using regular, premium, saturated, and composite gasolines are shown in Fig. 2. It is noteworthy that both saturated and unsaturated gasolines produced almost identical amounts of C_5, C_6, and C_7 + olefins in the exhaust gases. In fact, the olefin content was approximately the same for all grades of gasoline used, including the blends of 6 of the leading gasoline producers in the area.

The average exhaust composition for all components analyzed by the mass spectrometer for each of the 4 driving conditions is shown in Fig. 3. Of interest is the result that the concentrations of methane and acetylene produced under idling conditions are greater than those obtained under conditions of acceleration, steady driving, or deceleration. Ethane and ethene do not fall into this pattern.

Using the data that have been obtained and certain simplifying assumptions, it is possible to obtain an estimate of the amount of hydrocarbon vapors released daily into the Los Angeles atmosphere by approximately 2,000,000 cars[5] burning 12,000 tons (4,000,000 gallons)

(11) Magill, Paul L., Hutchison, Dale H., and Stormes, John M., "Hydrocarbon Constituents of Automobile Exhaust Gases," *Proceedings Second National Air Pollution Symposium*, pp. 70-83, Stanford Research Institute, Stanford, Calif., 1952.

(5) See footnote 5, page 71.

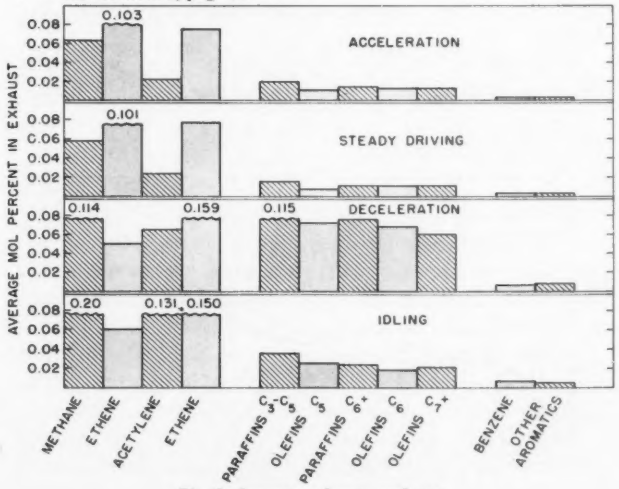

Fig. 3. Average exhaust analyses.

TABLE II
Tons of C_1 to C_7 Hydrocarbons Discharged Daily from Automobile Exhaust

Hydrocarbon Discharged	Mol. Wt.	Routes Tested		
		Figueroa St. Sunset Blvd. to Florence Ave. and Return	Foothill Blvd. from Sunland to U.S. Highway 6	22 Congress St. to Arroyo Seco Pkwy to Adobe St. and Return
Methane	16	61	54	55
Ethane	30	146	166	165
Acetylene	26	52	36	37
Ethene	28	150	124	127
C_3 — C_5 paraffins	58	116	62	68
C_5 olefins	70	84	39	43
C_6 + paraffins	93	128	67	73
C_6 olefins	84	106	58	64
C_7 + olefins	100	117	68	73
Benzene	78	117	114	114
Other aromatics	92	21	16	17
Total		998 (1000)	704 (700)	736 (730)

of gasoline. It was assumed that the results were representative of the Los Angeles automobile population during the test period (1951-52), that half of the gasoline was consumed in city driving and half in suburban driving, and that each car produced 1,000 ft.^{3} of dry exhaust gas/gallon of fuel burned.

Using these assumptions, the total hydrocarbons emitted to the atmosphere from automobile exhaust were calculated. The tons of exhaust products emitted daily under the 4 driving conditions are tabulated in a previously published Stanford Research Institute Report[11]. This tabulation shows that over the range of driving conditions encountered in city traffic, there is a loss of hydrocarbons out of the exhaust ranging from 5% of the weight of fuel entering the carburetor under conditions of steady driving to 19% during periods of deceleration.

Table II shows the estimated amount of C_1 to C_7 + hydrocarbons discharged daily from automobile exhausts.

If all driving had been done exclusively on one of the three different patterns (Figueroa Street, Foothill Boulevard, and Arroyo Seco Parkway) the emissions would then correspond to 1,000 tons, 700 tons, and 730 tons respectively.

It was determined that 700 tons/day represents the minimum daily emission of hydrocarbons into the Los Angeles atmosphere from the automobile exhaust in 1951. The increased gasoline consumption for 1953 indicates that the daily emission would exceed 1,000 tons.

The frequency of smog and the severity of its effects have increased markedly during recent years in Los Angeles County, and it is interesting to consider the manner in which this trend follows the increase in gasoline consumption in the county. An effect of smog which has become more extensive and more pronounced each year is injury to vegetable crops and other herbaceous plants. According to Middleton[12], injury to vegetable leaves was first noted in 1944.

Most of the types of injury observed in the Los Angeles area were duplicated by laboratory fumigations[13]. Typical smog injury was obtained by fumigating plants either with the reaction products of ozone and unsaturated hydrocarbons, or ozone and automobile exhaust, when the reagents were mixed in high concentration and the products diluted to low concentrations. No other fumigant was found which would produce this type of injury.

In Fig. 4 is shown the number of automobile registrations for the State of California from 1935 to 1953[14]. Thirty-five to 40% of the registrations were in Los Angeles County during this period. Although the county had an increase of 400,000 registrations between 1935 and 1944, there were 1,000,000 additional registrations from 1944 to 1953.

The gasoline consumption for California from 1935 through 1953 is shown in Fig. 5. Consumption data for Los Angeles County for the same time period are not

(Continued on page 118)

(11) See footnote 11, page 73.

(12) Middleton, John T., Kendrick, J. B. Jr., and Schwalm, H. W., "Injury to Herbaceous Plants by Smog or Air Pollution," *Plant Disease Reporter 34*, 245-52 (1950).

(13) Stanford Research Institute, "The Smog Problem in Los Angeles County," p. 64, Western Oil and Gas Association, Los Angeles, Calif., 1954.

(14) McCoy, G. T., *"Annual Traffic Count,"* Calif. State Printing Office, Sacramento, Calif., 1951.

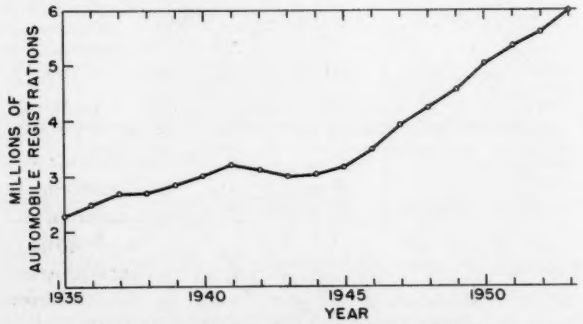

Fig. 4. Automobile registrations, State of California.

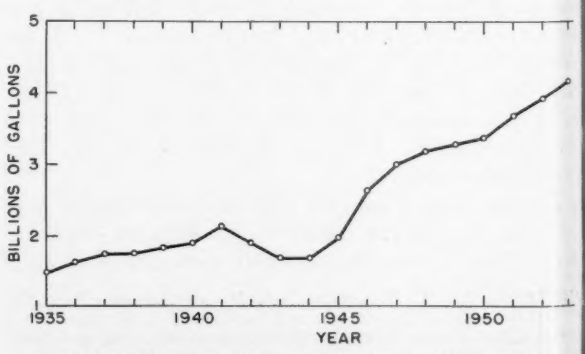

Fig. 5. Yearly consumption of gasoline, State of California.

Application of Infrared Spectroscopy to Exhaust Gas Analysis*

S. B. Twiss, D. M. Teague, J. W. Bozek, and M. V. Sink
Chrysler Corporation, Engineering Division
Detroit, Michigan

At the recent Third National Air Pollution Symposium in Pasadena, California, it was pointed out that smog and the related factors of plant damage and eye irritation are not exclusive products of Los Angeles County. Such symptoms have appeared around other large cities such as San Francisco, New York, Philadelphia, Baltimore, and London. Therefore, the problem of smog is of general interest.

Despite the parallel which has been pointed out between the appearance of plant damage and rising levels of gasoline consumption, the relation between automobile exhaust and smog has not been clearly defined. As stated by James C. Zeder at the Pasadena conference, members of the AMA Vehicle Combustion Products Subcommittee have been unable to establish to what extent, if any, reduction of hydrocarbon emissions from automobile exhaust would reduce smog. In spite of this, it was decided that a program for developing means of hydrocarbon reduction should be a main object of industry attention.

Reduction of exhaust gas hydrocarbons might be made in 2 ways: (1) by control of the engine variables which affect efficiency of operation, and (2) by mechanical improvements in present engines. The first item is concerned with the effect of fuel-air ratio, manifold pressure, spark timing, and good engine maintenance on hydrocarbon emission. Of course, in actual testing, the effect of these variables must be determined for the 4 representative operating conditions of acceleration, deceleration, road load and idle. With this knowledge, criteria could be set up for engine tune-ups, which should have a considerable effect in reducing hydrocarbon emission.

The second item above is concerned with devices to be incorporated in engines to improve combustion or reduce hydrocarbon loss. These might be devices for fuel cut-off during deceleration, air valves to maintain manifold vacuum below a specified maximum, or swirl devices to improve homogeneity of the charge. For all this type of work, an absolute necessity is a rapid, accurate method for analyzing exhaust gases, and in particular, the per cent of unburned fuel.

In addition to the vehicle manufacturers, several other groups are concerned with methods of exhaust gas analysis: the Air Pollution Control District in Los Angeles, the various research institutes who now have contracts to work on various phases of this air pollution problem, and the Field Survey Panel of the AMA Subcommittee on Vehicle Combustion Products. Most of these groups, as well as the vehicle manufacturers, desire portable, continuous-exhaust analyzers which are also rapid to operate and accurate.

Now, many methods of exhaust analysis have been developed, and a few are widely used. The traditional Orsat analysis, although lacking somewhat in accuracy, is fairly rapid, and the instrument is inexpensive. Various types of combustion methods have been evolved, specifically for analyzing hydrocarbons. A gravimetric method for trapping out condensible materials in exhaust, excluding water and carbon dioxide, has been developed. The method giving the greatest amount of information on exhaust gas composition is the mass spectrometer. This instrument is a miracle of modern science, but it is expensive and definitely not portable. The one method that appears to offer most promise, at this time, is infrared analysis. Infrared spectrometers are moderately priced, rapid and accurate. They do not give as much detailed information on specific hydrocarbons as the mass spectrometer. Certain types of infrared analyzers offer the possibility of continuous analysis on a portable instrument which could be mounted in an automobile. For these reasons, the technique developed for exhaust gas analysis at Chrysler Corporation has been infrared analysis.

Principles of Infrared Absorption

Infrared spectroscopy offers a direct identification of many common atomic groups which occur in chemical compounds. With the infrared spectrometer, qualitative and quantitative determinations may be be made that previously were possible only by involved chemical methods. Hence, it has achieved an established place in industrial chemistry and is a primary tool for analyzing organic compounds.

Chemical compounds exhibit selective absorption in the infrared region of the spectrum, since the atoms of each molecule are capable of vibrating only with definite, characteristic frequencies. If a thin layer of a solid or liquid or a thicker layer of a gaseous material is irradiated with infrared light of all wavelengths, those wavelengths which correspond to the vibrational frequencies of its molecules are absorbed; light of all other wavelengths is transmitted. Since no 2 compounds have identical structures or combinations of atomic groupings, the resulting transmission spectrum is characteristic of the material in

*Presented at the 48th Annual Meeting of the Air Pollution Control Association, Detroit, Michigan, May 22-26, 1955.

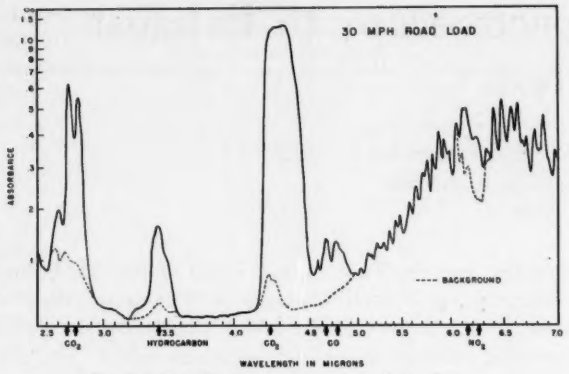

Fig. 1. Infrared spectrum of automotive exhaust.

question. Matching such a fingerprint of an unidentified material against that of a known material permits identification of the unknown.

Fig. 1 is a transmission spectrum of automotive exhaust under 30 mph. road load conditions. You will note that the absorption intensity is plotted on the ordinate and wavelength in microns on the abscissa. You will also note in this spectrum that 4 compounds are present, identified by the wavelengths of the absorption peaks: the carbon dioxide peaks around 2.7 and 4.3 μ, the hydrocarbon peaks at 3.42 μ, the carbon monoxide peaks at 4.6 and 4.7 μ and the nitrogen dioxide peaks at 6.2 μ.

Since infrared spectral characteristics are largely retained on admixture, the characteristic absorption bands obtained by the use of an infrared spectrometer offer wide possibilities for quantitative analysis. The concentration of one component of a mixture may be quickly determined by measuring the absorption intensity of its characteristic bands. Referring again to Fig. 1, we see that at least 4 compounds can be determined quantitatively, and with a different cell and method of operation a much larger number could be determined. The height of the absorbance peak is directly proportional to the concentration of that component in the exhaust gas mixture.

In Fig. 2 we see the spectrum of exhaust for the acceleration condition, which is very similar to the 30 mph. road load, except that the height of the carbon monoxide

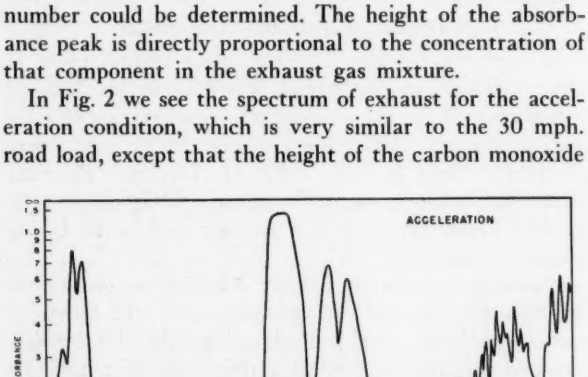

Fig. 2. Infrared spectrum of automotive exhaust.

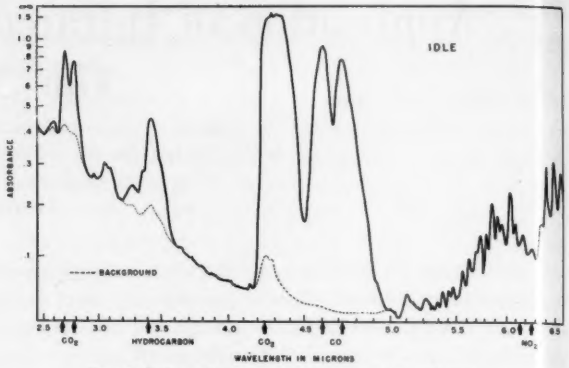

Fig. 3. Infrared spectrum of automotive exhaust.

peaks is increased, indicating a higher concentration of this component.

Fig. 3 shows the characteristic spectrum of the idle condition. Comparing this spectrum with the road load condition, it is apparent that the hydrocarbon and carbon monoxide peaks are increased, while the carbon dioxide peaks are slightly reduced. This indicates that under idle condition the combustion is less efficient, resulting in a higher content of carbon monoxide and unburned fuel in the exhaust.

Fig. 4 shows an infrared spectrum of the deceleration condition. It is very apparent here that the hydrocarbon reaches a much higher value than in any of the other conditions. The carbon monoxide concentration is about the same as at idle, while the carbon dioxide concentration is somewhat lower. It has been observed by several investigators that deceleration is the most serious condition from the viewpoint of hydrocarbon emission. We will show later a reason for this, and a method that appears to be effective in reducing the hydrocarbon emission during deceleration.

Dispersion-Type Infrared Spectrometers

In principle, the infrared method of analysis is quite simple, although in actual practice a precision instrument containing a number of components is required for successful operation. Fig. 5 is a diagram of the light path. The infrared rays from a globar source are reflected from

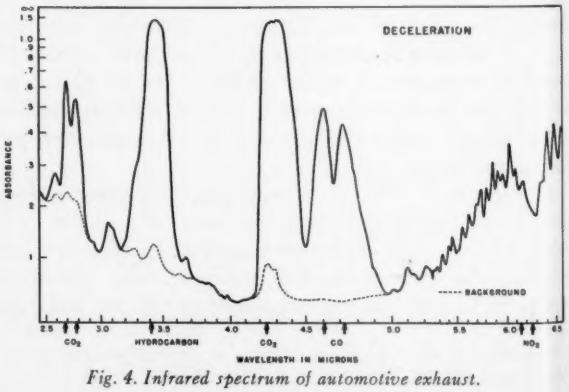

Fig. 4. Infrared spectrum of automotive exhaust.

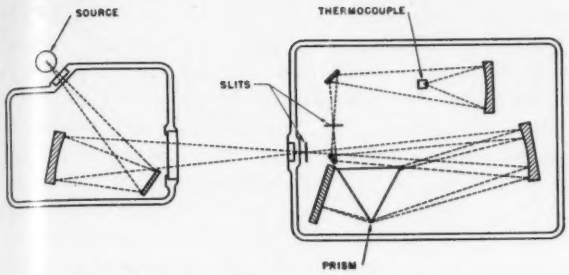

Fig. 5. Diagram of single beam infrared spectrometer.

2 mirrors and then passed through the sample. The radiation is focused on a slit, reflected from a mirror through the prism and then back-reflected from a rotating mirror. Use of the prism and rotating mirror makes it possible to split the infrared radiation into individual wavelengths and to progressively scan the wavelength region from 1 to 15 μ. The monochromatic radiation thus produced is finally converged by mirrors on a thermocouple detector. The amount of energy falling upon the thermocouple depends upon the degree of absorption of that particular wavelength by the compound being analyzed. When the absorption is low, the energy will be high, and vice versa. This energy is then amplified and recorded on a standard chart recorder giving a permanent record of the analysis. The spectra shown earlier were tracings of these chart recordings.

Fig. 6 shows the infrared spectrometer set up in our laboratory, including the one meter gas cell used for exhaust analysis in the sample holder. A second gas cell is being evacuated preparatory to taking a hydrocarbon sample for analysis. The total time involved in making an analysis of exhaust gas is about 15 min. An additional 15 min. is required for calculation of the concentration of the 4 components shown in the earlier spectra. The dispersion-type instrument is quite versatile and capable of analyzing any type of organic compound. Its chief disadvantage from the viewpoint of exhaust gas analysis lies in the fact that it is not easily portable.

Non-Dispersion Infrared Analyzer

A different type of infrared analyzer is the non-dispersion type of instrument, where the infrared radiation is not split up by a prism and rotating mirror into separate wavelengths. Rather, 2 infrared sources are involved and the instrument sensitized for absorption of a specific compound or atomic grouping so that quantitative analyses can be made. Fig. 7 shows a schematic diagram of the non-dispersive gas analyzer. The analysis is made by passing the exhaust gas through the right-hand cell. The compensating cell, in parallel with the sample cell, contains air and serves as a blank. Two sensitized cells (shown in the bottom of Fig. 7) are placed in series with the parallel sample and blank cells. These sensitized cells contain the compound which is being determined; in the present case, a representative hydrocarbon.

Infrared radiation passes down through both cells. Since there is no hydrocarbon in the blank cell, this infrared radiation is absorbed by the sensitized cell at the characteristic wavelength of hydrocarbons (chiefly 3.42 μ). This absorption of energy heats the gas in the left-hand portion of the sensitizing cell. Similar infrared radiation passes through the sample cell, but is partially absorbed by the gasoline-type hydrocarbons in the exhaust. The percentage of absorption depends on the concentration of hydrocarbons in the exhaust gas. The infrared radiation which is not absorbed by the hydrocarbons in the exhaust sample is subsequently absorbed by the hydrocarbon in the sensitizing cell. Since the amount of radiation remaining to be absorbed is less, the amount of heat produced in the sensitizing cell on the right is less. A diaphragm between the sensitizing cells forms one side of a condenser. Differential heating of the sensitizing gas produces a deflection of the diaphragm, changing the condenser capacity. After suitable amplification, the change is indicated on a meter or a strip chart recorder.

By this means, it is possible to make an integrated measurement of the hydrocarbons present in an exhaust gas sample. The saturated, isomeric hydrocarbons of C_3 and above have a very similar absorption per unit weight, irrespective of molecular structure. The instrument must, of course, be calibrated with a hydrocarbon or hydro-

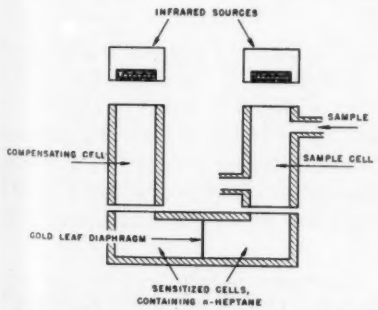

Fig. 7. Diagram of non-dispersive infrared analyzer.

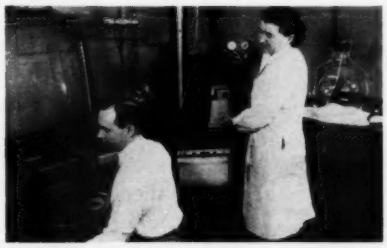

Fig. 6. Exhaust analyses using infrared spectrometer and gas cell.

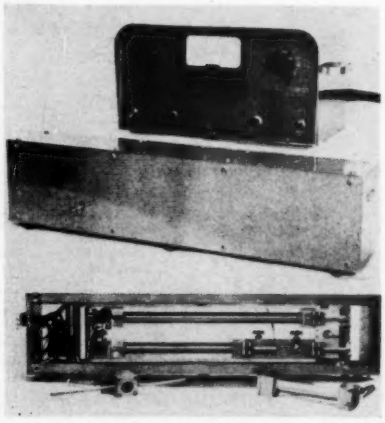

Fig. 8. Portable infrared analyzer. ➟

carbon mixture characteristic of hydrocarbons present in the exhaust gas sample. Although heptane or gasoline are used at present for calibration, future work involves the use of hydrocarbons extracted from exhaust.

The equipment proper is much simpler than the dispersion-type spectrophotometer, as shown in Fig. 8. The upper section of this figure shows the rectangular box, housing the infrared source, parallel sample cells and sensitizing cells, and the separate container housing the amplifier and meter. In the lower portion of this figure is shown the analyzer with the cells exposed. It is readily seen that this is portable equipment capable of being installed either in a dynamometer laboratory or in road test cars. Two additional units are required for portable operation in a test car: (1) a 110 v. power supply of fairly constant frequency and (2) a strip chart recorder, such as the Esterline-Angus clock-wound type. The recorder may be eliminated if desired, since the amplifier is provided with a meter which can be read and results manually recorded.

Infrared Determination of Hydrocarbon in Automotive Exhaust

Analysis of Gas Samples

This method is intended primarily for the measurement of unburned hydrocarbon in automotive exhaust, but is also suitable for the determination of carbon dioxide, carbon monoxide, and nitrogen dioxide. Only a fraction of the lowest hydrocarbons (methane and ethane) will be measured because of the reduced infrared response to these hydrocarbons. However, the content of C_3 and higher hydrocarbons should provide a satisfactory weight measurement of unburned fuel in the exhaust.

The sampling procedure involves drawing a sample of exhaust through a heated stainless steel sampling line and absorption tube containing Drierite into an evacuated infrared cell or sample container. The sample container is filled to approximately atmospheric pressure. Quantitative absorption measurements are obtained at 3.42 μ for the total hydrocarbon content.

The sampling line is shown in Fig. 9. This line should

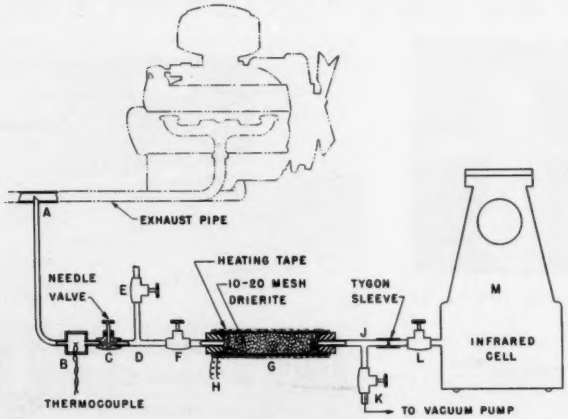

Fig. 9. Diagram of exhaust sample apparatus.

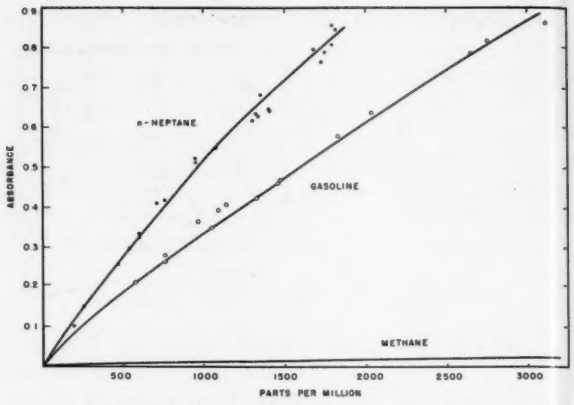

Fig. 10. Infrared calibration for hydrocarbons.

be as short as possible and heated to about 150° F. to prevent condensation of water and the higher hydrocarbons. The temperature of the exhaust gas is measured with a thermocouple located at *B* in the gas stream. The needle valve at *C* controls the exhaust sample flow. The sample line is connected to a drying tube containing Drierite for the absorption of water. The Drierite absorption bulb is also maintained at 150° F. to minimize hydrocarbon absorption. Measurements indicate that hydrocarbon absorption by Drierite is relatively small at such a temperature, averaging about 9.5%.

Prior to taking a sample, the exhaust gas is bled through the opening at *E* to the atmosphere while valve *F* is closed. The sampling cell, or bottle, and drying tube are evacuated through *K* to a pressure of about 1 mm. Hg. Valve *K* is closed. The valve to the atmosphere at *E* is closed and valve *F* opened. The exhaust gas sample flows through the drying tube into the sample cell, reaching equilibrium pressure in about 10 to 30 sec. Needle valve *L* has been previously adjusted to provide the proper rate of flow. Valve *L* is then closed and the cell disconnected from the sample line. When a one-meter-length infrared cell is used directly, ½ to 1 atmosphere pressure has been found adequate. If a sample bottle is used, the sample should always be obtained at full exhaust pressure and transferred by connecting to an evacuated infrared gas cell.

After the sample in the infrared gas cell has reached room temperature, its pressure is measured accurately with a manometer. Dry nitrogen is added to the cell to bring the final pressure up to 760 mm. Hg. The infrared spectrum in the wavelength region from 2.5 to 6.5 μ is then prepared. This should be completed within 15 to 30 min. from the time of sampling to minimize changes in the exhaust sample.

The hydrocarbon absorbance is measured at approximately 3.42 μ wavelength. This provides a value for C_3 and higher hydrocarbons, and is preferably based on a calibration with the original gasoline which is used as the fuel.

In Fig. 10 is shown an infrared calibration for the hydrocarbons, gasoline, n-heptane and methane. It should be noted that although the molecular weight of heptane corresponds very closely to the average molecular weight of gasoline, the infrared response of gasoline is lower than that of n-heptane. This is due to the presence of aromatic and unsaturated hydrocarbons in gasoline, whose molecular structures absorb at wavelengths other than 3.42 μ characteristic of paraffinic hydrocarbons. An exceptional case of reduced response is shown in the methane curve, whose absorbance is very much lower than that of gasoline or n-heptane. It would be desirable to obtain a calibration on hydrocarbons condensed from the exhaust, since this would correspond most closely with the desired products. It is believed, however, that at least under idle and deceleration conditions the composition of exhaust hydrocarbons is similar to that of the original gasoline used as fuel.

The calibration curve for gasoline, in Fig. 10, was obtained by assuming an average molecular weight of 100. This is the same molecular weight as heptane, and is on the low side of the average molecular weight of U.S. gasoline, which ranges from 100 to 110.

The carbon dioxide absorbance is measured at 2.67 μ, the carbon monoxide absorbance at 4.60 μ, and the nitrogen dioxide absorbance at 6.15 μ. With these light gases, such as carbon monoxide, carbon dioxide, nitrogen oxides, methane and ethane, it is particularly important that the total pressure in the infrared cell be constant, preferably atmospheric, during absorption measurement. The reason for this is shown in Fig. 11. This demonstrates "pressure broadening" in the carbon monoxide spectrum. Although the same partial pressure of carbon monoxide is present when the total pressure is low (2.4 cm. Hg.) the absorbance by carbon monoxide is much less than if the total pressure is brought to atmospheric by the addition of nitrogen. Such gases as nitrogen and oxygen have no absorption in the infrared region, so the effect here is one of increasing the response of carbon monoxide to infrared radiation simply by an increase in the total pressure.

For improved accuracy, a blank spectrum is obtained with nitrogen only in the cell. These blank values are subtracted from the observed sample values at each specified wavelength. The net absorbance for each compound is converted to mole per cent, or parts per million, using prepared calibration curves. These results are on the "dry gas" basis since moisture is removed from the sample. The hydrocarbon calibration curve is increased 9.5% to correct for this loss in the Drierite bulb.

$$AK\frac{760}{P} = \text{parts per million (ppm.)}$$

where A is the net absorbance of the compound analyzed
K is the factor relating absorbance to parts per million (read from calibration curve)
P is the original pressure of sample in the infrared cell, in mm. Hg.

To convert results to mole per cent, divide parts per million by 10,000.

Other Procedures for Sample Analysis

Instead of collecting the exhaust sample in the form of a gas and analyzing as a gas, other procedures may be used. Paul P. Mader and co-workers of the Los Angeles County Air Pollution Control District[1] have used a freezeout method for collecting hydrocarbons in the Los Angeles atmosphere. A similar method has been used for collecting exhaust samples. The method consists essentially in passing a measured volume of atmosphere or exhaust gas through a freeze-out assembly, such as a Shepherd trap immersed in a Dewar flask filled with liquid oxygen. A tube filled with Ascarite for the removal of water vapor, carbon dioxide, aldehydes, ketones, and organic acids is inserted in the sample line ahead of the freeze-out trap. The hydrocarbon components of the gas stream are reported not to be retained by the Ascarite trap.

The sample contained in the freeze-out assembly is then transferred to an evacuated infrared cell by warming the trap and allowing the vapors to flow from the sampler into the gas cell. After all condensate has vaporized, the sampler is repeatedly filled with nitrogen and emptied into the infrared cell until atmospheric pressure in the cell is reached. Finally, the gas cell containing the hydrocarbon sample is scanned in the 3.0-4.0 μ region of the spectra. The per cent transmittance of the sample is measured at the 3.45 μ absorption peak for hydrocarbons. n-heptane-air mixtures were used for a quantitative calibration.

Another method which might be used for infrared identification of hydrocarbons involves the selective adsorption of the hydrocarbons in exhaust on a suitable adsorbant. The hydrocarbons are transferred to the gas cell

(1) Mader, P. P., Heddon, M. W., Lofberg, R. T., and Koehler, R. H., "Determination of Small Amounts of Hydrocarbons in the Atmosphere," *Anal. Chem. 24*, 1899-1902 (1952).

TABLE I
Exhaust Composition at Various Car Operating Conditions
(Based on Dry Gas)
Commercial Premium Grade Fuel

Plymouth 6-Cylinder, 1954	Carbon Dioxide %	Carbon Monoxide %	Hydrocarbon ppm. (vol.)	% Fuel Unburned
30 mph. road load	9.03	.43	190	.94
Acceleration	6.32	1.25	171	.69
Idle	5.65	5.70	751	3.48
Deceleration	4.55	5.20	4420	16.9
	5.00	5.45	2510	9.7
Dodge V-8, 1955				
30 mph. road load	16.1	1.87	158	.80
Acceleration	16.0	3.77	163	0.79
Idle	8.9	10.9	785	3.24
Deceleration	7.43	4.32	5020	20.2

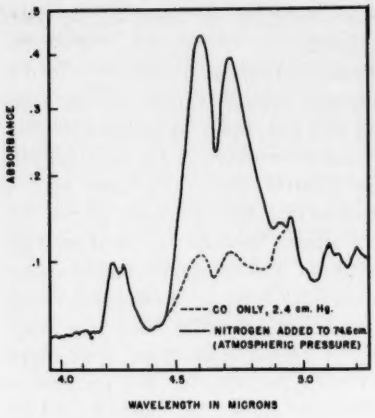

Fig. 11. Pressure broadening in carbon monoxide.

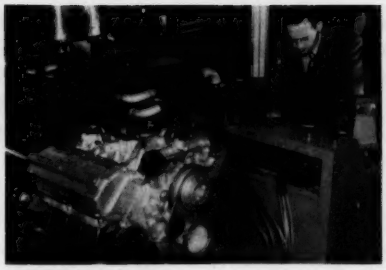

Fig. 12. Sampling on dynamometer for infrared analyses.

Fig. 14. Sampling in road test car for infrared analyses.

by heating the adsorbant to drive them off, starting with low temperatures and going to progressively higher temperatures.

Application of Dispersion Type Instrument

An extensive number of exhaust gas analyses have been made by the first method outlined in detail above, using one-meter gas cells and a Perkin-Elmer, Model 12-C, spectrometer. Each sample was analyzed for: C_3 and higher hydrocarbons, carbon dioxide, carbon monoxide, and nitrogen dioxide, for which the approximate level only was noted. The reproducibility of measurement on successive samples was good with respect to total hydrocarbon and carbon monoxide, the average deviation being about ± 3%. The deviation in carbon dioxide measurement was slightly greater.

Table I presents results for 4 representative car operating conditions, with 2 different engines. Exhaust hydrocarbon results are based on the infrared calibration with gasoline.

An examination of the data clearly indicates that both engines are quite efficient at road load and acceleration operation, burning about 99% of the fuel. At idling conditions, however, a somewhat larger percentage of fuel is unburned, while during deceleration 10 to 20% of the original fuel hydrocarbon is emitted. These 4 operating conditions were selected as being representative of normal city and highway driving, and show that the highest emission of hydrocarbon occurs during deceleration. Fuel loss through the exhaust can vary appreciably during deceleration, depending on the time of sampling, as evidenced by the values shown for the Plymouth engine. Nearly all of the above results were obtained on an engine dynamometer, where the operating conditions for normal driving were carefully simulated.

In order to gain a clearer idea of the reasons for the variations in composition, a more detailed study was made of the effect of engine manifold vacuum on exhaust gas composition, again using an engine dynamometer. Table II presents results on the relationship. In all of these tests, actual car operating conditions and a road speed of 30 mph. were simulated. Fig. 12 illustrates the engine dynamometer assembly for obtaining exhaust samples.

It is apparent from these results that the fuel is burned most completely at an intermediate manifold vacuum (intermediate engine load). With an engine properly adjusted for maximum efficiency, as in these tests, only about 1% of the fuel is lost. However, the amount of unburned fuel increases rapidly as the manifold vacuum rises above 22 in. Hg., characteristic of deceleration.

Similarly, carbon monoxide content is relatively high at maximum acceleration, falls to a minimum at inter-

TABLE II

Engine Manifold Vacuum vs. Exhaust Analysis—(Based on Dry Gas)
Dodge V-8 Engine, PowerFlite Transmission
Commercial Premium Grade Fuel

Operating Condition	Manifold Vacuum In. Hg.	Fuel-Air Ratio	Carbon Dioxide %	Carbon Monoxide %	Hydrocarbon, ppm. (vol.)	% Fuel Unburned
	0.95	.0829	.....	10.18	265	1.06
Acceleration	3.5	.0777	.....	6.69	167	.70
	9.1	.0575	16.7	1.24	159	.91
	14.2	.0651	15.9	1.50	160	.80
Road Load	17.2	.0653	17.3	2.37	155	.78
	19.2	.0692	16.3	4.09	213	1.00
	21.2	.0735	13.7	5.76	313	1.50
Deceleration	22.05(b)	.0800	11.7	6.28	1960	8.08
	22.95(b)	.0816	7.43	4.32	5020	20.2

(b) Engine misfiring.

mediate road load conditions, and rises again at deceleration. The carbon dioxide content rises correspondingly as carbon monoxide decreases; the relationship between the two is largely a function of the fuel-air ratio, carbon monoxide increasing with richer mixtures. At the highest manifold vacuum, where combustion is relatively incomplete, both carbon monoxide and carbon dioxide decrease.

According to the infrared spectra, nitrogen dioxide is present in relatively large amounts at intermediate engine manifold vacuums but decreases to zero at very low and very high vacuums.

The relationship between engine manifold vacuum and unburned fuel is shown graphically in Fig. 13. Here the results of infrared measurement of C_3 and higher hydrocarbons are compared with exhaust hydrocarbon analyses made with a mass spectrometer[2]. Both are calculated as per cent of fuel not burned; the correspondence of infrared values with the detailed mass spectrometer values is very good.

Poor combustion and a high percentage of unburned fuel in the exhaust is the direct consequence of a high manifold vacuum. The high manifold vacuum is produced during deceleration by the car inertia, driving the engine as a vacuum pump. More detailed observations have shown that there is a residue of burned gases remaining in the cylinder when each exhaust cycle is completed. When operating at a high manifold vacuum, the amount of fresh gasoline and air drawn in is less than normal. Its dilution by the unexhausted residue produces a mixture which burns more slowly and incompletely than normal. Because of this condition, a method is sought which will prevent engine manifold vacuum from exceeding the value (about 21 in. Hg.) at which the amount of unburned fuel increases rapidly. Various means of accomplishing this are now being studied and evaluated.

In addition to the detailed engine dynamometer studies, measurements were made of exhaust composition during the operation of test cars on the road. These results were obtained specifically in connection with the evaluation of engine devices, installed for the purpose of reducing the unburned fuel during deceleration. Since in driving, conditions of deceleration are relatively transient, it was necessary to sample at carefully timed periods of very short duration. This was accomplished as follows:

A heated sampling line was attached to the engine manifold and carried directly back into the front passenger compartment. Here a series of electrically actuated solenoid valves were attached which made it possible to bleed exhaust gas through the line to the atmosphere. At a specified time, the exhaust gas was shut off to the atmosphere and conducted to a previously evacuated sample cell. The arrangement for taking the sample in an infrared cell is illustrated in Fig. 14. The Drierite bulb and infrared cell may be seen; the sampling line is quite similar to the one previously described for engine dynamometer measurements.

In order to fill the 1-l. infrared cell, the deceleration cycle was repeated several times, always from an initial speed of 30 mph. Each cycle, the sample line was opened for exactly 1 sec. duration, beginning at a specified time interval after the driver's foot was lifted from the throttle. Fig. 15 illustrates a portion of the automatic timing apparatus installed in a test automobile. By taking samples representing various delay intervals after the start of deceleration, a complete picture was constructed of exhaust composition during the entire deceleration period.

Using this technique of "grab" sampling to study transient conditions, the effectiveness of a throttle control device was evaluated, as may be seen in Fig. 16. When no control device is present, the amount of hydrocarbon rises rapidly to a very high level after the onset of deceleration. The exhaust hydrocarbon concentration reaches 6000 ppm., corresponding to more than 20% unburned fuel, within 1½ sec. Simultaneous records of the engine manifold vacuum showed an identical steep rise and fall, after correcting for the 0.6 sec. lag required for the sample to flow from engine to infrared cell. The operation of a throttle control unit, however, reduces the amount of unburned fuel by 79.3%. This represents a marked improvement and is a promising possibility for further study.

Application of Non-Dispersion Instrument

Although considerable information concerning exhaust hydrocarbon can be obtained with grab samples analyzed on the dispersion-type infrared spectrometer, this technique is not suitable for extensive studies of road vehicle operation. Rapid variations in exhaust composition resulting from normal driving cannot be satisfactorily followed with individual samples, except with great labor and the imposition of somewhat artificial driving procedures. There is a need for an instrument which will continuously measure exhaust hydrocarbon under all conditions, and which can be readily attached to the automobiles of private owners. Such a monitoring instrument

(2) Rounds, F. G., Bennett, P. A., and Nebel, G. J., "Some Effects of Engine Fuel Variables on Exhaust-Gas Hydrocarbon Content," *J. Air Poll. Control Assoc., 5,* this issue (August 1955).

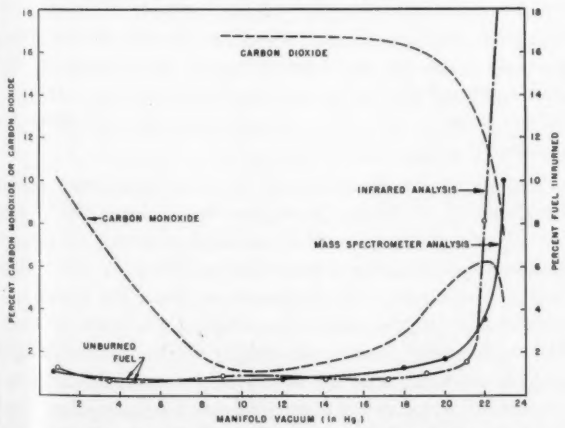

Fig. 13. Effect of manifold vacuum on exhaust analyses.

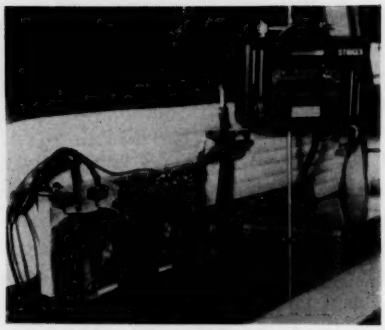

Fig. 15. Control equipment for road test sampling.

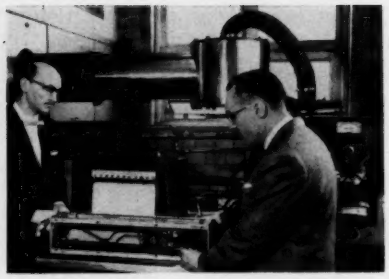

Fig. 17. Continuous analyses with portable infrared analyzer.

is essential to evaluate actual, on-the-spot conditions in critical areas, and the effectiveness of suggested car maintenance programs.

Since the standard dispersion-type infrared apparatus is moderately expensive, not portable, and not suited to continuous road measurements, another type of hydrocarbon-measuring apparatus is necessary. The non-dispersion infrared gas analyzer meets many of the requirements. As has been previously described, it is a relatively simple and portable instrument. Furthermore, an exhaust sample can be continuously passed through the sample cell, thus providing a continuous record of exhaust hydrocarbon while a car is operating.

The initial studies with a Liston-Becker Model 15 gas analyzer were made with an engine on a test dynamometer stand. The apparatus in use is pictured in Fig. 17. Different cell lengths and different amplifier settings provide a wide range of response, ranging from 1,000 ppm. to 30,000 ppm. for a full-scale reading.

After setting the instrument to zero with air in the sample cell, the exhaust sample is conducted through a heated line to a heated tube of Drierite. The dry exhaust gas is passed through the gas analyzer, which provides a continuous record of the C_3 and higher hydrocarbons. The effect of changing engine conditions can be directly observed.

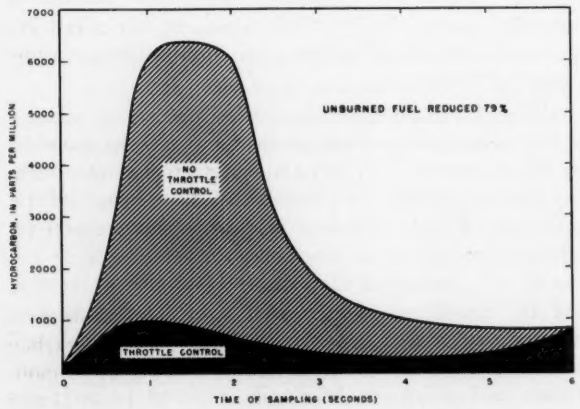

Fig. 16. Reduction in unburned fuel by throttle control device.

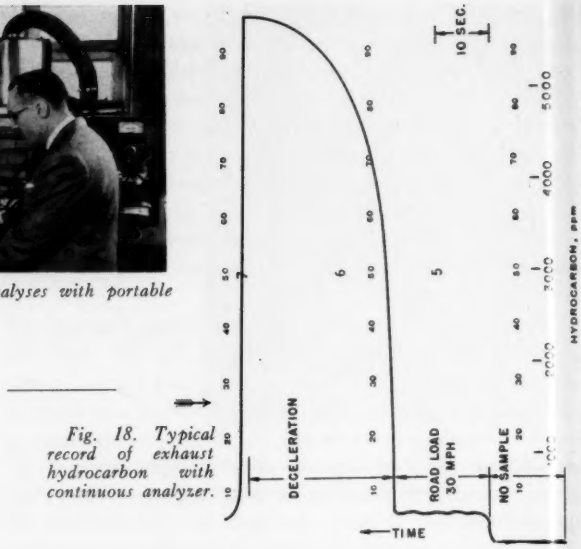

Fig. 18. Typical record of exhaust hydrocarbon with continuous analyzer.

A typical exhaust hydrocarbon record is shown in Fig. 18. Examination of the chart indicates that operating the engine at road load conditions produces an exhaust hydrocarbon output of about 360 ppm. As soon as the throttle is closed, simulating deceleration, the hydrocarbon rapidly increases to nearly 6,000 ppm. When the engine is again returned to road load, the hydrocarbon level falls abruptly.

To speed up the instrument response to changing engine conditions, the gas flow was increased by inserting a small diaphragm pump between drying tube and sample cell. Although the response is not as rapid as might be desired for very transient driving operation, results obtained with the non-dispersion gas analyzer are very promising. The instrument has been calibrated quantitatively by measuring the hydrocarbon with a laboratory dispersion-type infrared spectrometer, as outlined earlier in detail.

At present, the continuous gas analyzer has one serious deficiency: a drying tube must be inserted in the line to remove moisture from the exhaust sample. Although it had been anticipated that moisture would not interfere seriously with the total hydrocarbon measurement, the extremely high water content of exhaust gas not only produces condensation in the sample cells, but also provides a positive absorption error.

We are currently studying ways to eliminate water interference. A likely possibility is to heat the entire sample cell assembly so that no condensation can occur. This will prevent the serious loss of internal cell reflectivity. However, a blank correction must be applied to compensate for the relatively constant moisture content. Although water does not absorb at the same wavelength as hydrocarbons, Fig. 19 shows how the relatively huge amount of water in exhaust produces an absorption band which partially obscures the hydrocarbon peak.

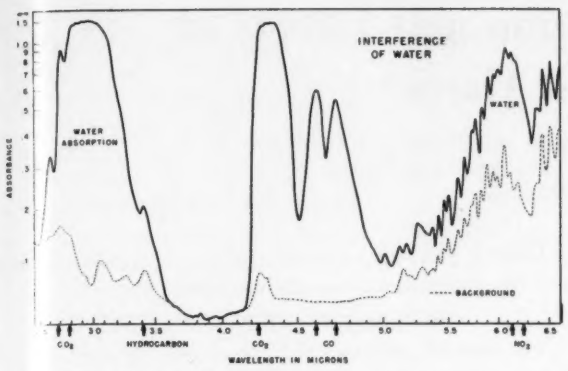

Fig. 19. Infrared spectrum of automotive exhaust.

The continuous infrared gas analyzer is currently being adapted for road test measurements. Although a satisfactory exhaust flow can be obtained on a test car by tapping into the exhaust pipe, this would not be acceptable for the monitoring of privately owned automobiles. A sampling line is therefore being devised which can be inserted into the tailpipe, yet will be adequately heated to prevent hydrocarbon loss. Rapid sample flow must be maintained in order to follow changing conditions. According to very preliminary results, the continuous analyzer yields hydrocarbon results which are quite similar to those obtained with individual samples, as analyzed with the laboratory infrared spectrometer. Work is actively proceeding on the continuous infrared gas analyzer because of its ease of operation, portability, moderate cost and continuous measurement.

Summary and Conclusions

1. An infrared spectroscopic method of exhaust analysis has been developed which is generally satisfactory. Some of the advantages of this technique are:
   a. Speed—a complete analysis for C_3 and higher hydrocarbons, carbon dioxide, carbon monoxide and nitrogen dioxide, requires about 30 min. for preparation of spectra and calculation of results.
   b. Wide range of response—low concentrations of exhaust components, characteristic of road load, to the high concentrations obtained during deceleration can be readily analyzed.
   c. Accuracy—reproducibility is about 3%.
   d. Specificity—the concentration of a specific atomic grouping is measured, e.g., the C-H group in hydrocarbons.
   e. Moderate cost of instrument—the cost of an infrared instrument ranges from about $2,000 for the non-dispersive gas analyzer to $15,000 for a double-beam dispersion instrument.
   f. Equipment and trained personnel are readily available.
2. In spite of its marked advantages, infrared spectroscopy does suffer from certain disadvantages, such as:
   a. Low value for hydrocarbons—only a fraction of methane and ethane, unsaturated hydrocarbons and aromatic hydrocarbons are measured.
   b. Interference of water in exhaust—water interferes with the hydrocarbon measurement and must be removed from sample before analysis.
   c. Less detailed analysis — individual hydrocarbon components and water are not readily measured.
3. A procedure has been developed for rapidly obtaining a gaseous exhaust sample from an engine operating either on the dynamometer or in a road test car. This procedure includes a technique for the absorption of water and correcting for the small amount of hydrocarbon inadvertently removed from the exhaust.
4. Using this infrared analysis technique, exhaust analyses are presented for representative operating conditions on 6-cylinder and V-8 engines. These conditions are: 30 mph. road load, idle, acceleration, and deceleration.
5. This infrared technique has been applied to a determination of the effect of manifold vacuum on hydrocarbon, carbon monoxide and carbon dioxide content of exhaust. The hydrocarbon results show excellent agreement with mass spectrometer analyses obtained with different makes of cars.
6. A technique for rapidly obtaining "grab" samples of 1-sec. duration has been developed for the study of transient conditions during deceleration, which is the most severe operating condition for hydrocarbon emission. The technique set up in a road test car was used to demonstrate the effectiveness of a throttle control device to reduce hydrocarbon during deceleration.
7. Techniques for the continuous analysis of exhaust are being developed by adapting a non-dispersive infrared analyzer to exhaust analysis. This instrument is portable, easy to operate, relatively inexpensive, but limited to measurement of hydrocarbon in exhaust.

Acknowledgment

The assistance of the Chrysler Research Dynamometer Group, under the direction of M. E. Noftz, in setting up and operating the engines for this study, and for installation of road test sampling equipment is gratefully acknowledged.

Note

Since the date of presentation, improved calibration curves have been obtained for hydrocarbon and carbon dioxide, and an improved cell correction for carbon monoxide. This has permitted revision of Tables I and II and Fig. 13.

Study of the Distribution and Effects of Auto Exhaust Gases*

GORDON P. LARSON, JOHN C. CHIPMAN, AND ERWIN K. KAUPFR
Air Pollution Control District of County of Los Angeles
Los Angeles, California

The complex mixture of air contaminants that exists in industrial communities may produce a variety of effects. Some of the resultant nuisances are associated with chemical reactions of one or more pollutants in the atmosphere. Under certain atmospheric conditions, the oxidation of sulfur dioxide to sulfur trioxide and the resulting sulfuric acid mist contributes to haze formation(1). When stable air conditions are such as to provide time for the oxidation of hydrocarbon vapors in the air, aerosols and irritating gases are formed. The particles produced in this photo-chemical reaction result from the polymerization of the oxidation products of certain unsaturated hydrocarbons(2). Haze and the consequent reduction in visibility result from these oxidation processes in the air, together with the direct emissions of dusts, fumes and mists from a large variety of sources. On the other hand, the contaminating gases cause damage to vegetation, irritation of the eyes, higher ozone content of the air and strong odors(3). Sulfur dioxide, fluorine, hydrocarbons, ammonia and hydrogen sulfide are prominent among the contaminating gases and vapors found in the atmosphere.

Effects other than haze formation have been shown in reactions of hydrocarbons in extreme dilution. Olefinic, branched-chain, and cyclic compounds present in gasoline vapor are readily oxidized in the presence of sunlight and oxides of nitrogen to produce gases which are highly irritating to the eyes and cause damage to vegetation(4-5). A by-product of this chemical reaction is ozone which, in spite of its known activity, leaves residual ozone concentrations sufficiently high to produce rubber cracking during smog attacks(6). Some of the organic acids, aldehydes and peroxides resulting from the oxidation of hydrocarbons can be measured in the atmosphere and in test chamber experiments.

Table I presents a classification of important sources and the potential air contaminants from each(7).

Hydrocarbons—A New Problem

The research studies which developed the role of gasoline vapor as a factor in the Los Angeles smog problem have been extensively reported. Essentially, the work consisted of test chamber experiments in which the reaction products of oxidized gasoline vapors produced eye irritation and a specific pattern of damage on certain vegetable plants. This type of damage is found extensively in the field on plants after smog attacks. Analyses revealed that the organic aerosol in the atmosphere compared favorably in its chemical and physical properties with the aerosol produced when gasoline vapors are oxidized.

Accompanying these studies was an inventory of the sources of gasoline vapor to estimate the losses of all types of hydrocarbons to the atmosphere. Sampling programs were conducted to determine the concentrations of hydrocarbons during smog attacks in close proximity to sources. Samples of air collected in the vicinity of refineries or similar sources of hydrocarbon vapors gave typical smog effects when exposed to sunlight. The extensive work done in connection with hydrocarbons led to studies of the internal combustion engine. While it could be expected that certain types of hydrocarbons would be found in the exhaust gases, no evidence existed that the mixture of combustion products at the temperatures found in the exhaust would give any of the effects which had been determined in the experiments with pure hydrocarbons or gasoline vapors. As a matter of fact, the exhaust gases do not produce crop damage typical for smog until photochemical reactions take place.

Test Procedure

Since the quantities of contaminants vary for each operating condition, an estimate of total emissions was based on the consumption of gasoline under average driving conditions. Consideration of traffic flow and traffic densities led to the selection of a 39 mile route throughout the community. This route was chosen as representative of average driving conditions in Los Angeles. It includes freeway driving, residential driving, congested city traffic, and industrial areas.

Accumulative stop watches were used to record the time

(1) Aitken, J., "The Sun as a Fog Producer," *Proceedings of the Royal Society of Edinburgh, 32,* 1911-1912.
(2) Mader, P. P., MacPhee, R. D., Lofberg, R. T., and Larson, G. P., "Composition of Organic Portion of Atmospheric Aerosols in the Los Angeles Area," *Ind. Eng. Chem., 44,* 1352 (June 1952).
(3) Larson, G. P., "Recent Identification of Atmospheric Contaminants in the Los Angeles Basin," 44th Annual Convention *Proceedings Air Pollution and Smoke Prevention Association of America, Inc.* Roanoke, Virginia, 1951.
(4) Haagen-Smit, A. J., "Chemistry and Physiology of Los Angeles Smog," *Ind. Eng. Chem., 44,* 1342-46 (1952).
(5) L. A. Co. Air Pollution Control District, *Second Technical and Administrative Report on Air Pollution Control in L. A. Co.,* 1950-1951.
(6) Haagen-Smit, A. J., "Photochemical Ozone Formation with Hydrocarbons and Automobile Exhaust," *Air Repair, 4,* 105-08, 36 (1954).
(7) Larson, G. P., "Smokes and Fumes" in "Encyclopedia of Chemical Technology," vol. *12,* pp. 558-73, The Interscience Encyclopedia, Inc., New York, N. Y., 1954.

*Presented at the Annual Meeting of the Society of Automotive Engineers at Detroit, Michigan, January 10-14, 1955.

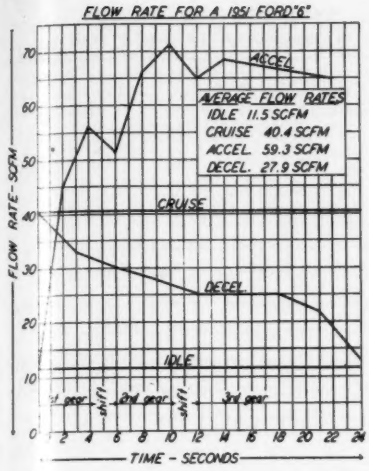

Fig. 1. Flow rate for a 1951 Ford "6."

spent in (1) idling, (2) acceleration, (3) cruising, and (4) deceleration, while driving the predetermined route. The cruising cycle recorded was in high gear between 25 and 35 mi./hr. at approximately 17 in. Hg. Deceleration was at closed throttle with a manifold vacuum of between 20 in. and 24 in. Hg. Data on acceleration were obtained between approximately 2 in. and 15 in. Hg., and results from idling were obtained under full stop with a manifold vacuum of about 18 in. Hg. The average operating time of the test was found to be as follows: idling, 18%; acceleration, 18%; cruising, 46%; and deceleration, 18%.

As an example of the procedure used, a test on a 1951 Ford Six is described. A stainless steel orifice meter using a 1¼ in. orifice plate was attached to the tail pipe. It was of sufficient size to minimize exhaust back pressure. Orifice pressure differentials were obtained by a standard self-compensating X gauge which indicated the pressure differentials in inches of water.

Idling exhaust flow was obtained with the engine idling at approximately 450 rpm. (Fig. 1). The acceleration cycle consists of accelerating on level terrain in first gear from 0 to 12 mph., then in second gear from 12 to 22 mph., and in high (third) gear from 22 to 35 mph. Orifice differential pressure readings were taken every 2 seconds through the 3 forward gears.

The average exhaust flow rate in first gear was determined by graphically integrating the area under the plotted curve for the first 5-second increment (to the midpoint of the first shift); the average for second gear operation was determined from the 5 to 11-second increment. The average exhaust flow for the entire acceleration cycle was obtained by graphically integrating the area under the plotted curve for the full 22-second period. The average exhaust flow rate for the entire deceleration cycle was obtained by averaging the area under the plotted curve for the entire 0 to 24-second interval. The average flow rates are shown in Fig. 1.

Reducing these figures to a ratio of exhaust gas volumes with idling as unity, they become for a 1951 Ford Six:

TABLE I
Sources and Air Contaminants

Source, Type, or Industry	Aerosol	Specific Gases and Vapors	Vapors
Combustion			
Coal	Dust, fume (smoke, fly ash)	NO_2, SO_2, CO, aldehydes, acids	
Fuel oil and gas	Dust, fume (smoke)	SO_2, NO_2	
Gasoline (motor fuel)	Fume (smoke)	Organic acids, aldehydes, NO_2, CO	Hydrocarbons(a)
Rubbish	Dust, fume (smoke, fly ash)	Organic acids, aldehydes, NO_2, CO	
Petroleum			
Production			Saturated hydrocarbons
Refining	Dust, mist	Mercaptans, SO_2, H_2S, NH_3, CO	Hydrocarbons(a)
Marketing			Hydrocarbons(a)
Chemical and allied products			
Chemicals	Dust, fume, mist	(Process-dependent)	(Process-dependent)
Soap and detergent	Dust	Odor	
Paints and varnish	Mist	Solvent, organic acids	Solvent, organic acids
Fertilizer	Dust	NH_3, odor	
Animal and vegetable oils	Mist	Odor	
Paper and plastics	Dust, mist	Odor, solvent, sulfide (process-dependent)	
Metallurgical and metal fabrication			
Smelters and mills	Dust, fume (smoke)	SO_2, fluorides, CO	
Foundries	Dust, fume (smoke)	Aldehydes	
Fabricators	Dust		
Mineral earth processing			
Ceramic	Dust	Fluorides	
Aggregate and cement	Dust		
Calcining	Dust		
Food products			
Feed and flour	Dust		
Fish and meat	Dust, mist	Odor	
Food processing	Dust, mist	Odor	

(a) Mixtures containing types of hydrocarbons that are readily oxidized in the atmosphere.

(1) Idling	1.00	(3) Cruising	3.50
(2) Acceleration	5.15	(4) Deceleratoin	2.42

Collection of Samples

Instantaneous samples for hydrocarbon and Orsat determinations were collected behind the muffler by drawing the exhaust gases into evacuated 300 ml. glass mine-sampling tubes. Two-liter evacuated flasks were used to collect samples for aldehyde, oxides of nitrogen, and acetylene determinations. The chemical methods that were employed are beyond the scope of this article. The references are listed separately in the Appendix.

During the acceleration cycle, samples were first collected while driving in each of the 3 forward gears at approximately 6, 17 and 28 mph., respectively. It has been found through experience that the sample taken in second gear at 17 mph. represents an average condition of the entire acceleration cycle. For this reason, samples are now taken only in second gear at approximately 17 mph.

During the deceleration cycle, samples were taken originally at 3-second intervals, corresponding to 0+3, 0+6, 0+9, etc. The zero time corresponds to the moment that the throttle was closed from a speed of 35 mph. Repeated tests have shown that the sample taken at 0+6 seconds represents a suitable average of the entire deceleration cycle. For this reason, only one sample (0+6 seconds) is now taken.

Instantaneous samples are also taken for idling (at approximately 450 rpm.) and cruising (level-road load at 35 mph.)

For the idling and cruising cycles another sampling technique is frequently substituted for the instantaneous sampling method. When this method is used, samples are drawn through a small orifice restriction into an evacuated 2-liter flask. This prolongs the sampling time and tends to give a better average for any fluctuations in the exhaust gas composition due to slight variations in engine operation. Checks made on the 2 methods, however, have shown no appreciable difference.

Estimated Emissions

Hydrocarbon Emissions From Automobile Exhausts

In 1940, there was a total of 1,160,110 automobiles and trucks in Los Angeles County. By 1954, the total had increased to 2,296,400. Calculations of the total amount of hydrocarbon vapors from automobile exhausts made by the District[8], and similar calculations by others[9] based on exhaust gas analyses, have shown that about 850 tons* of hydrocarbons enter the atmosphere in Los Angeles County each day from automobiles. This calculation is made from the exhaust analyses obtained while driving under moderate traffic conditions.

[8] Viets, F. H., Fischer, G. I., and Fudurich, A. P., "Atmospheric Pollution from Hydrocarbons in Automobile Exhaust Gases," L. A. Co. Air Pollution Control District, 1953.

[9] Magill, P. L., Hutchison, D. H., and Stormes, J. M., "Hydrocarbon Constituents of Automobile Exhaust Gases," *Proceedings of the Second National Air Pollution Symposium*, p. 71, 1952.

*4,500,000 gallons of gasoline, daily consumption in Los Angeles County, used in calculations.

TABLE II
Average Automobile Performance in Los Angeles Traffic

Operating Cycle	% Operation Time—Average Traffic	Exhaust Volume Ratio[a]	Gas Consumption Ratio[b]
Idle	18	1	1
Acceleration	18	4.5	7
Cruising	46	3	4
Deceleration	18	2	2

(a) Values are ratios of exhaust volume to idling exhaust volume of 14 scfm.

(b) Values are ratios of gasoline consumption to idling gasoline consumption of 0.4 gallon per hour.

Table II shows the per cent of time the vehicle was operating on the 4 cycles of the engine, the exhaust gas volumes, and gasoline consumption over a selected driving course through traffic. Using these values with the typical analytical results shown in Table III, the totals for various contaminants and other components can be estimated on the basis of current gasoline consumption.

Particulates from Automobile Exhausts[10]

In addition to the analyses for gases and vapors, preliminary data were collected under idling conditions for the solid and liquid aerosols. The weight of particulate matter collected on a filter and electrical precipitator was found to be 3.3 mg./scf. This value may be compared to the hydrocarbon measurements of 1275 ppm. or 139 mg./scf. for idling conditions. Theoretical calculations have been made on the quantities of lead and other additives to gasoline which might be emitted. If all of the lead and other compounds added to gasoline were exhausted to the atmosphere, the total for Los Angeles

[10] L. A. Co. Air Pollution Control District, *Third Technical and Administrative Report on Air Pollution Control in L. A. Co.*, 1953-1954.

TABLE III
Results of a Typical Analysis of Automobile Exhaust Gases[a]

Component	Idling	Acceleration	Cruising	Deceleration
Hydrocarbons (C_3-C_9) as hexane, p.p.m.	1275	410	354	5125
Acetylenic, as acetylene, p.p.m.	825	18	64	587
Oxides of Nitrogen, as NO_2, p.p.m.	8	4180	1606	18
Lower aldehydes, as formaldehyde, p.p.m.	88	1369	264	193
CO percentage	3.6	0.0	0.4	1.5
CO_2 percentage	10.0	13.7	12.9	6.1
O_2 percentage	1.4	1.3	1.1	9.5

(a) Automotive Exhaust Testing Procedures and Efficiency Studies in the Evaluation of Catalytic Muffler, Air Pollution Control District, Appendix II, 1954.

County would be 11 tons/day. The estimated oil consumption is 80 tons/day but only a small fraction of the oil burned would be emitted in particulate form.

The above values for smoke particles, or particulates, emitted in exhaust would lead to estimates ranging from 35 tons to 50 tons/day in the Los Angeles Basin. The material collected in tests is known to be extremely small and may be relatively unimportant in reducing the visibility. Air sampling studies are underway to obtain more data on this particular aspect of exhaust contributions.

Diesels

Only 120,000 gallons of Diesel fuel are burned per day by buses, trucks, and railroads in Los Angeles County for transportation as compared to 4,500,000 gallons of gasoline. From these figures, it is obvious that the quantity of material discharged from Diesel exhausts is insignificant from an over-all air pollution point of view, as compared to that of gasoline-driven vehicles.

Liquid Petroleum Gas

Preliminary tests on engines using liquefied petroleum products have been made. An insufficient number of tests have been completed to report any valuable data at this time. Analyses for aldehydes would appear to be less than found with the gasoline motor, which may account for the noticeable difference in odor. The analyses for the quantities and types of hydrocarbons must be extended further before conclusions can be reached.

Test Chamber Experiments on Exhaust Gases

In order to determine the effect of automobile exhausts, experiments and tests were run, exposing leafy vegetables, as indicators, to exhaust gases in fairly low concentration. The hydrocarbons were oxidized with ozone in a test chamber. The results of these tests demonstrated that automobile exhausts could cause typical smog damage to leafy vegetables.

A series of experiments were conducted to learn if constituents found in exhaust gas were capable of producing smog effects. Measured quantities of exhaust gases, mixed with air to dilute the hydrocarbon content, were introduced into the Plexiglas chamber. A controlled amount of ozone was introduced in each fumigation through a separate tube. The outlets of the hydrocarbon and ozone tubes in the chamber were located over a fan to aid the mixing in the atmosphere of the chamber. Earlier experiments in fumigating plants with single hydrocarbons or gasoline introduced the ozone directly into the hydrocarbon stream. Air [11-12] was then introduced to dilute the reaction products for the fumigation experiments.

Damage typical of that found in the field after smog attacks, was produced on all 5 indicator plants when the exhaust gases and ozone were introduced into the chamber at separate points. Results are shown in Table IV. A comparison was made of the quantities of equivalent weights of gasoline against hydrocarbons in automobile exhausts to give a minimal damage effect, with the results as shown in Table V. Borderline damage was obtained with 8.05 ppm. gasoline vapor and with 5.46 ppm. exhaust hydrocarbons. While it is recognized that the concentrations of hydrocarbons used in these experiments are above those found in the atmosphere, the experimental conditions imposed limitations which precluded using concentrations at the dilutions found in the atmosphere. The time for reaction in the chamber, because of its limited size, is only 17 minutes. The oxidation reaction in the atmosphere is continuous and is difficult to duplicate in an enclosure.

Eye Irritation and Aerosol Formation

During these and other experiments, observations were made for eye irritation and for formation of aerosols from the oxidation of the exhaust gases. Eye irritation was noted in some of the fumigation experiments. The presence of aldehydes in the exhaust gases may account for some of this effect. An experiment, using 4.3 ppm. of exhaust hydrocarbons, produced eye irritation when the

(11) Haagen-Smit, A. J., Bradley, C. E., and Fox, M. M., *Ind. Eng. Chem. 45*, 2086 (1953).

(12) Cann, G. R., Noble, W. M., and Larson, G. P., "Detection of Smog Forming Hydrocarbons in Automobile Exhaust Gases Using Plants as Indicators," *Air Repair, 4*, 31-34 (August 1954).

TABLE IV

Damage to Vegetation by Automobile Exhaust Gases

Hydrocarbons as Hexane[a] p.p.m.	Ozone[b] p.p.m.	Nitrogen Dioxide[a] p.p.m.	Formic Acid[a] p.p.m.	Aldehydes[a] p.p.m.	Exhaust Dilution	Temperature °F.	Relative Humidity %	Damage to Vegetation[a,c]				
								S	B	O	A	E
5.46	0.19	0.20	0.41	1.67	1:116	83	51	T	T	T	T	T
8.40	0.28	0.17	0.23	1.18	1:116	71	68	T	T	T	T	T
8.60	0.26	0.32	0.23	1.15	1:116	83	53	T	T	T	T	T
35.00	0.33	0.71	ND	1.04	1:29	80	64	T	T	T	T	T
38.50	0.33	1.81	ND	2.69	1:29	82	58	T	T	T	T	T
5.74	0.17	0.23	0.27	1.02	1:116	80	45	T	t	T	t	T
17.40	0.33	0.32	0.33	1.40	1:58	83	58	T	N	t	t	T
16.50	0.33	0.20	0.20	2.15	1:58	87	52	T	t	t	t	N
4.48	0.20	0.25	0.17	0.24	1:232	83	59	N	N	t	N	t
3.01	0.18	0.23	0.07	0.22	1:232	79	60	t	N	N	N	N

(a) As measured in the Plexiglas chamber during the fumigation.
(b) Consumed in the reactions; value obtained equals amounts introduced into the chamber minus amount measured in the chamber after reaction had occurred.
(c) S—spinach; B—sugar beet; O—oat; A—alfalfa; E—endive. T—typical smog damage; t—typical smog damage in a lesser degree; N—no damage.
ND Not determined.

TABLE V
Damage to Vegetation by Gasoline

Hydrocarbons as Hexane[a] p.p.m.	Ozone[b] p.p.m.	Nitrogen Dioxide[a] p.p.m.	Formic Acid p.p.m.	Aldehydes[a] p.p.m.	Temperature °F.	Relative Humidity %	Damage to Vegetation[c]				
							S	B	O	A	E
8.05	0.23	0.86	0.67	1.50	83	54	T	T	T	T	T
10.50	0.19	0.00	ND	1.85	87	53	T	T	t	t	t
12.20	0.21	0.41	0.45	1.64	83	56	T	t	T	T	T
3.08	0.05	0.33	0.25	0.96	92	41	t	t	N	N	N
4.00	0.04	0.36	0.13	0.51	86	45	t	N	t	N	t
15.80	0.25	0.00	ND	1.99	81	54	t	N	N	N	N
2.52	0.11	0.23	0.10	0.35	69	71	t	N	N	N	N
2.87	0.08	0.26	0.15	0.42	88	43	N	t	t	t	t

(a) As measured in the Plexiglas chamber during the fumigation.
(b) Consumed in the reactions; value obtained equals amount introduced into the chamber minus amount measured in the chamber after reactions had occurred.
(c) S—spinach; B—sugar beet; O—oat; A—alfalfa; E—endive. T—typical smog damage; t—typical smog damage in a lesser degree; N—no damage.
ND Not determined.

aldehyde concentration was below the eye irritating threshold known for fomaldehyde. No actual measurements were made of the quantities of aerosols formed from a given amount of hydrocarbons in the exhaust. Observations were made by introducing ozone into the exhaust stream and noting the visual increase of aerosols. Exhaust gases exposed to sunlight in a Plexiglas box showed increases in aerosol formation using a Tyndall beam. From these experiments, it was concluded that the exhaust gases from the gasoline internal combustion engine are as effective in producing smog effects as is gasoline vapor when both are oxidized in the presence of NO_2 and ozone.

Automobile Exhaust Distribution[13]

Upon completion of the analytical work for the quantities of hydrocarbons, studies were undertaken to determine the hydrocarbon concentrations in the atmosphere which might result from the emissions of automobile exhaust. This project involved a study of the distribution of traffic throughout the basin, measurements in the atmosphere of carbon monoxide, oxides of nitrogen, and hydrocarbons together with trajectory studies of wind flow patterns in the area. Since the peak periods of traffic obviously occur during the morning and late afternoon, atmospheric samples were taken prior to and during the period of early morning activity. Studies of air movement had already determined that the pollution would accumulate to the maximum during the early morning hours because of stagnation which occurs at night, followed by a period of low wind velocities.

(13) L. A. Co. Air Pollution Control District, *op. cit.*, ref. (10).

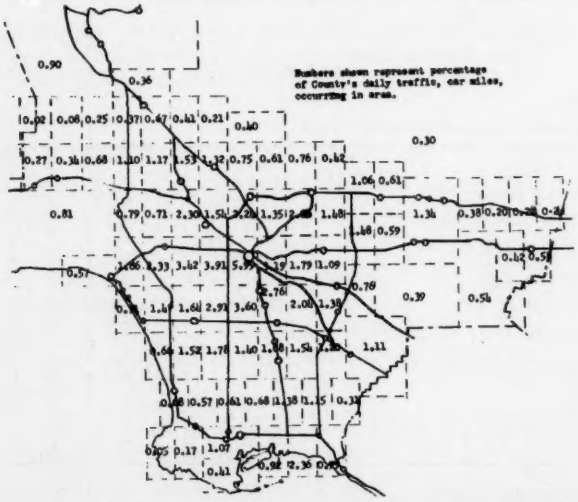

Fig. 2. Traffic Distribution in Los Angeles County. Numbers Represent Percentage of County's Daily Traffic (Car Miles) Occurring in Each Area.

Traffic Distribution

A study of the traffic flow indicates a distribution over the 24 hours on week days as follows:

Period	Per cent of 24-Hour Traffic
6:00 A.M.—10:00 A.M.	20—25
10:00 A.M.— 4:00 P.M.	30—35
4:00 P.M.— 7:00 P.M.	20—25
7:00 P.M.— 6:00 A.M.	20—25

Detailed traffic counts show the percentages of car miles/day in the populated sections of the county.

Fig. 2 shows the traffic distribution in unit areas of approximately 25 mi.^{2} each. This distribution indicates approximately 6% of the total traffic miles as being covered in the densely populated downtown Los Angeles section. It can, therefore, be estimated from the analysis of automobile exhausts that 60 to 75 tons/day of hydrocarbons could reach the air in this area from automobile exhaust.

Atmospheric samples measuring hydrocarbons, carbon monoxide, and nitrogen dioxide taken on several days in the central section of Los Angeles are plotted in Fig. 3 to show the average values obtained. The initial peak for hydrocarbons which occurs between 1:00 and 3:00 A.M. results from the residual pollution in the atmosphere which increases in concentration as the inversion lowers and the air becomes stagnant during the early morning hours. Following sunrise and the increased mixing, the concentration of pollution decreases, to be followed by another peak between 6:00 A.M. and 9:00 A.M. This peak

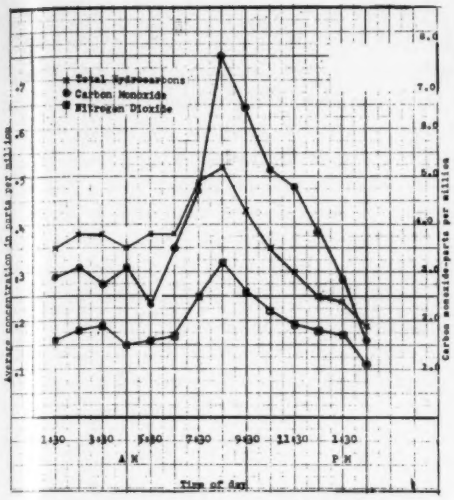

Fig. 3. Diurnal Curves for Hydrocarbons, Carbon Monoxide and Nitrogen Dioxide in Downtown Los Angeles During Days of Eye Irritation, 1953-1954.

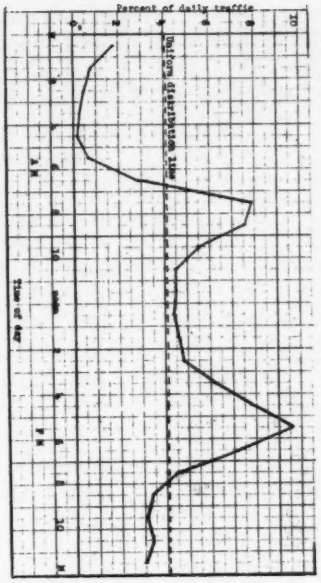

Fig. 4. Traffic Distribution on Hollywood Freeway at Cahuenga Pass. Weekday Traffic, 1950-1951.

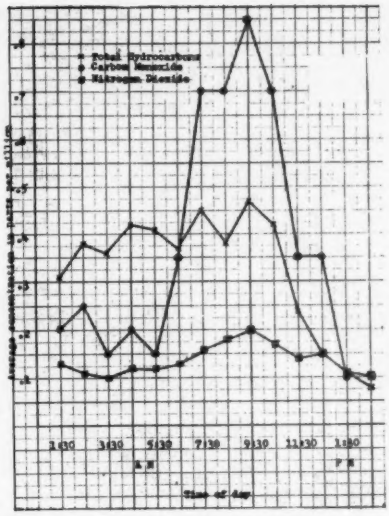

Fig. 5. Diurnal Curves for Hydrocarbons, Carbon Monoxide, and Nitrogen Dioxide in Dominguez Area, Carson St. Station, During Days of Eye Irritation, 1953-1954.

period corresponds well with the influx of traffic to this area. From the studies of the traffic flow in a 24-hour period, it is estimated that 25% of the total hydrocarbons emitted in this area for the day would be released during this peak period in the early morning hours. This quantity of hydrocarbons could account for the values measured in the air during the periods that measurements were being taken in this area. The values for carbon monoxide, and oxides of nitrogen as well, which would be released during a corresponding period, follow a similar pattern and are consistent with the total amount of material released for the period of time involved. A typical example of the traffic flow for a single freeway is shown in Fig. 4.

In order to determine whether or not another source of hydrocarbons would influence the concentrations measured in the downtown area, sampling was carried on in the refinery area, approximately 20 miles south of the Civic Center. At the time these studies were undertaken it was estimated that refinery sources were emitting approximately 300 tons/day of hydrocarbons. Carbon monoxide, and oxides of nitrogen as well, could be expected from sources in the refinery area. It will be observed from the values plotted in Fig. 5 that the carbon monoxide values in the Dominguez area are extremely low as compared to the downtown area. This marked difference in itself indicates a separate source as contributing this material to the Civic Center. While the peak concentrations for hydrocarbons in the refinery area between 3:00 and 4:00 A.M. might indicate a transfer of this material to influence the later peak in the downtown area between 6:00 and 9:00 A.M., studies of the wind currents on the days when samples were taken have indicated few occasions when this could occur. A series of studies on days of eye irritation in the Civic Center was made during July 1952 and January 1953[14]. For these periods a number of cases of surface wind flow were plotted for each day when eye irritation occurred.

Fig. 6 designates the nighttime stagnation area for the air which was polluted when it reached the Civic Center about 10:00 A.M. The symbols L, M and H indicate the degree of eye irritation as light, medium and heavy, respectively. The square symbols are for those cases where the trajectories passed over the refinery area before the air stagnated. The round symbols show the cases where the air could not have passed over the refinery area.

In the 37 cases of downtown eye-irritation studies, there were 3 instances of air arriving from the west traffic area without stagnating, 2 cases of air coming from the refinery area without stagnating, and 7 indeterminate cases where air passed over refinery and heavy traffic areas without stagnating. In addition, there were 25 cases where the air stagnated in heavy traffic areas (west 13, southwest 4, south 1, east 2, and northwest 5.) Studies of individual cases reveal several where winds both at the surface and aloft could not have brought air from the refinery area to downtown Los Angeles. The intense traffic activity was apparently sufficient in itself to produce the observed moderate to severe sieges of eye irritation.

Conclusions

The decision to control a source of pollution should be predicated upon studies which show a clear contribution

[14] *Special Report*, Meteorological Section, Air Pollution Control District of Los Angeles.

Fig. 6. Centers of Stagnation Areas for Air Arriving at Civic Center at 10:00 A.M.

of the source to the detrimental effects caused by polluted air. It could, of course, be conceded without extensive studies, that some of the contaminants in auto exhaust contribute to the pollution of the air. Since hydrocarbons or gasoline vapors were known to be an important factor in producing several of the deleterious effects of smog, one question to be answered is whether or not the removal of hydrocarbons from all other sources in the community would relieve the burden on the air sufficiently to avoid any control measures on auto exhaust.

The studies which show that hydrocarbons are present in the exhaust gases and that under irradiation or oxidation with ozone, smog-type damage can be produced on plants, represent only a part of the necessary information to determine whether control measures are necessary. The studies by Dr. A. J. Haagen-Smit at the California Institute of Technology concerning the formation of ozone from hydrocarbons and particularly from auto exhaust constitute another step in showing the effects which can be expected under certain conditions. Only when all of these facts are considered along with the measurements of hydrocarbons in the atmosphere and a study of the wind currents, can one conclude that the impact of traffic is significant.

Studies now closely show that the removal of all other sources of hydrocarbons from refineries and from the distribution of gasoline will not lower the concentration of hydrocarbons in the downtown area and the north-central section of the county sufficiently to relieve the eye irritation, crop damage effects, and high ozone content of the air in those areas. The marked influence of traffic in the early morning hours increases the concentration of hydrocarbons to levels which cannot be tolerated in the Los Angeles atmosphere. On the basis of the total studies, it has been concluded that the hydrocarbons must be removed from the exhaust gases of automobiles. Furthermore, the efficiency of removal must be extremely high. It is anticipated that the Los Angeles basin will ultimately serve 10,000,000 persons. Because of the topography and the limited atmosphere, it can be anticipated that other areas will be influenced by a dense traffic pattern in the future. Freeway improvement provides easy access to outlying areas and traffic density can be expected to increase. The Air Pollution Control District recommends that engineering studies seeking to remove hydrocarbon vapors from exhaust gases should strive for a 90% over-all removal under conditions of operation experienced in heavy traffic.

APPENDIX

Analytical Methods Used to Evaluate Auto Exhaust Emissions

Hydrocarbons

Beckman IR-2 Infrared Spectrophotometer with a specially constructed 100 cm gas cell. Concentrations are expressed as hexane.

Mader, P. P., Heddon, M. W., Lofberg, R. T., and Koeher, R. H., *Analytical Chem., 24,* 1899 (December 1952).

Oxides of Nitrogen

Phenoldisulfonic Acid Procedure
(Acid absorbing solution)

Jacobs, M. B., "The Analytical Chemistry of Industrial Poisons, Hazards and Solvents," p. 354, Interscience Publishing Company, New York, N. Y., 1949.

Acetylene and Its Homologs

Copper acetylide method. This method measures acetylene and all mono substituted acetylenes of the type RC ≡ CH in the form of copper acetylide.

Jacobs, M. B., *Ibid,* p. 516.

Aldehydes

Sodium bisulfite addition method (Ripper's Method). Concentrations are expressed in terms of formaldehyde.

Goldman and Yagoda, *Ind. Eng. Chem., Anal. Ed., 15,* 377 (1943).

Carbon Dioxide, Oxygen and Carbon Monoxide

Orsat method. Results expressed in percentages. For carbon monoxide concentrations less than 0.2%, a Mine Safety Appliance (MSA) sampler is used.

Mine Safety Appliance Company, Pittsburgh, Pennsylvania.

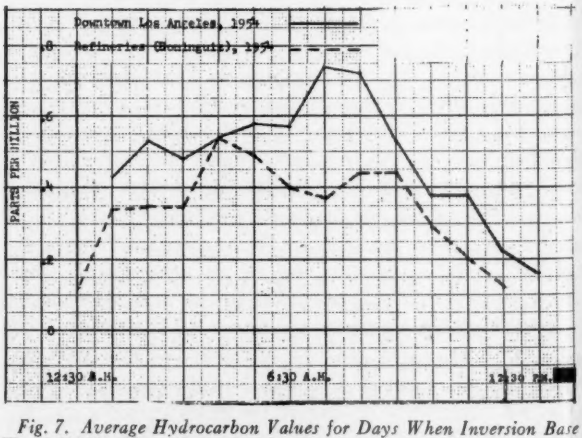

Fig. 7. Average Hydrocarbon Values for Days When Inversion Base Was 1,000 Ft. Above Ground or Lower.

Flame Photographs of Light Load Combustion Point the Way to Reduction of Hydrocarbons in Exhaust Gas*

J. T. WENTWORTH and W. A. DANIEL
Research Laboratories Division
General Motors Corporation

The unburned hydrocarbon content of exhaust gas from engines is of interest for two reasons: (1) the unburned hydrocarbons represent a loss in combustion efficiency, and (2) the unburned hydrocarbons contribute to air pollution. Work published by Viets, Fischer, and Fudurich[1] and also by Magill, Hutchison, and Stormes[2] in 1952 indicated that the largest concentration of unburned hydrocarbons in the exhaust gas of automobiles was found under decelerating conditions. The second largest concentration was found under idling conditions.

In certain important respects engine operation during deceleration and idle differ from engine operation at full throttle. During deceleration and idle operation the intake manifold vacuum is high, the residual exhaust gas dilution is high, and the resulting density of reactants in the combustion chamber is lower than during full throttle operation.

An abrupt increase in the concentration of unburned hydrocarbons in the exhaust gas with an increase in intake manifold vacuum above about 21 in. of mercury has been reported by Rounds, Bennett, and Nebel[3]. The present investigation was undertaken to determine the fundamental reasons for this abrupt increase in hydrocarbon concentration.

Also, in the present investigation, efforts were made to eliminate the high concentration of hydrocarbons in the exhaust gas of automobiles during deceleration. Two types of carburetor devices designed to reduce the concentration of hydrocarbons in the exhaust gas when an automobile decelerates were tested, and their effectiveness in reducing the concentration of unburned hydrocarbons in the exhaust gas during a closed throttle deceleration is reported in the present paper.

Combustion Studies Using a Single Cylinder, Quartz Window Engine

Equipment

In order to make visual observations and to obtain high-speed motion pictures of the flame, a quartz-window cylinder head was mounted on a CFR crankcase and L-head conversion block assembly as shown in Fig. 1. Also in Fig. 1 can be seen the intake surge tank, carburetor, rotameters, exhaust analysis apparatus, and other equipment grouped around the engine. Fig. 2 is a view through the quartz window showing the location of the piston, valves, and the spark electrodes located directly over the intake valve. The quartz, which forms the top of the combustion chamber, is a 1 in.-thick flat slab and is sloped upwards over the valves. The combustion chamber, therefore, is wedge-shaped.

The engine was coupled to a dynamometer capable of holding the speed within 10 rpm. for all conditions used. Engine operating conditions are listed in Table I.

A speed of 500 rpm. was chosen to facilitate the visual observation of the flame. Isooctane was used as the fuel since it was desirable to use an unleaded fuel to keep the window clean. Furthermore, others[2-3] have shown that there is little or no effect of fuel type on the per cent unburned hydrocarbons in the exhaust gas (weight per cent of input fuel, hereafter referred to as per cent hydrocar-

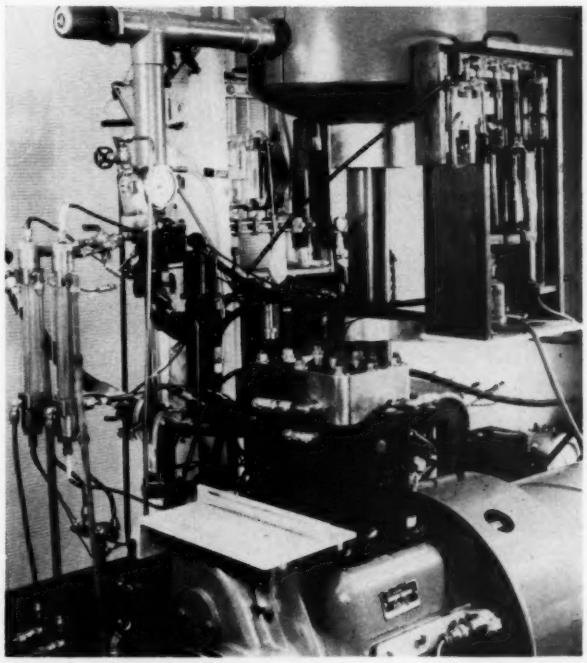

Fig. 1. Single Cylinder Engine and Equipment.

(1) Viets, F. H. Fischer, G. I., and Fudurich, A. P., "Hydrocarbon Pollution from Automobile Exhaust Gases," *Report of Test 668*, Air Pollution Control District, County of Los Angeles.

(2) Magill, P. L., Hutchison, D. H., and Stormes, J. M., "Hydrocarbon Constituents of Automobile Exhaust Gases," *Proceedings, Second National Air Pollution Symposium*, May 1952.

(3) Rounds, F. G., Bennett, P. A., and Nebel, G. J., "Some Effects of Engine-Fuel Variables on Exhaust Gas Hydrocarbon Content," *J. Air Poll. Control Assoc., 5*, this issue (August, 1955).

*Presented at the Annual Meeting of the Society of Automotive Engineers at Detroit, Michigan, January 10-14, 1955.

TABLE I
Engine Operating Conditions

Speed	500 ± 5 rpm.
Fuel	Isooctane
Compression ratio	6.7
Spark timing	TDC
A/F	Varied from 5 to 17 in. Hg.
Mixture temperature[a]	Varied from 16 to 25 in. Hg.
Mixture temperature	67° to 130°F.
Oil sump temperature	102 ± 5°F.
Block coolant temperature	160 ± 3°F.

[a] No heat was added to the mixture. Temperature varied with air-fuel ratio and manifold vacuum.

bons in exhaust gas). The compression ratio of the engine was 6.7 and a spark timing of TDC was arbitrarily chosen.

The air-fuel ratio was determined from air flow rate and fuel flow rate measurements. The air flow to the engine was controlled and metered by critical-flow nozzles described by Cornelius and Caplan[4]. Fuel flow rate was measured with a calibrated rotameter.

The intake vacuum was adjusted by regulating the rate at which air was added to the surge tank, and the throttle was always fully open. The large surge tank near the engine served to smooth out pressure fluctuations in the intake system.

Correlation between Per Cent Hydrocarbon in the Exhaust and Complete Flame Propagation.

The procedure used to obtain the data was to wait until the engine had stabilized at a given set of conditions and then to observe whether or not the engine misfired. This was done for many air-fuel ratio and manifold-vacuum combinations until a "misfire limit" was determined. By definition, a misfire limit condition was taken as approximately one misfire in 50 cycles. The misfire limit thus determined is shown in Fig. 3 as a function of air-fuel ratio and manifold vacuum.

[4] Cornelius, W., and Caplan, J. D., "An Improved System for Control and Measurement of Air Consumption of a Single Cylinder Engine, *Transactions, Society of Automotive Engineers*, **6**, 106-08 (July, 1952).

Also shown in Fig. 3 is the range of air-fuel ratios and manifold vacuums within which the flame was observed to burn throughout the combustion chamber. The boundary of the region within which the flame apparently burned throughout the chamber included the range of air-fuel ratios and manifold vacuums within which the flame was observed to burn more than nine-tenths of the mixture.

At the rich boundary of the region within which the flame burned throughout, the flame burned so slowly that it had not completed its travel when the exhaust valve opened at 140°ATC. With the flame burning out the exhaust port, it could not be determined whether the flame burned throughout the mixture, since some burning took place in the exhaust port. The conditions where the flame burned out the exhaust port are indicated in Fig. 3 by a dashed line.

At a constant manifold vacuum, the per cent combustion space traversed by flame decreased as the air-fuel ratio decreased from the rich limit of complete inflammation, and at the rich misfire limit less than half of the combustion space was traversed by flame. At lean air-fuel ratios, the misfire limit and the boundary of the region within which the flame burned throughout coincided; thus, more than nine-tenths of the combustion space was traversed by flame at the lean misfire limit.

Although most of the observations of the flame were made visually while the tests were being run, a few high speed motion pictures (400 to 800 frames/sec.) were taken at the conditions enumerated in Fig. 4. Flame photographs from the motion picture sequences are reproduced in Fig. 5 through 8. To obtain these photographs, an Eastman High Speed Camera was used with Kodak Linagraph Pan film. The film was developed in Kodak SD-19a. In addition, it was found necessary to add powdered sodium chloride to the air-fuel mixture to get a good exposure from the flame. The addition of sodium made the flame a bright yellow, but did not change the power output of the engine, the exhaust temperature, or the apparent flame speed as determined by observation of the flame through

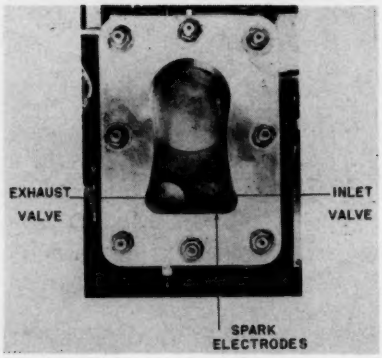

Fig. 2. Top view of cylinder head.

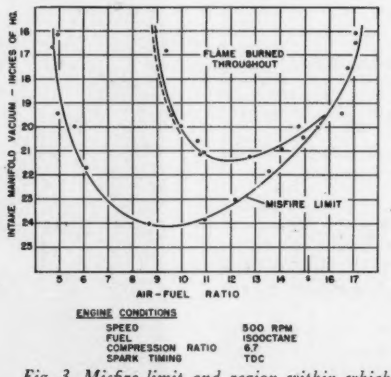

Fig. 3. Misfire limit and region within which the flame apparently burned throughout the chamber.

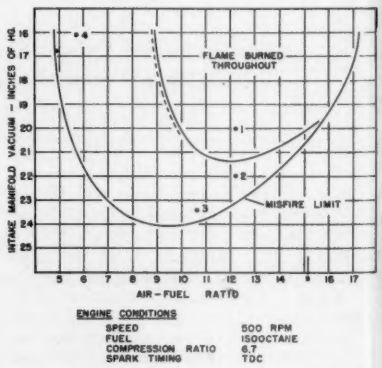

Fig. 4. Engine conditions at which motion pictures were obtained.

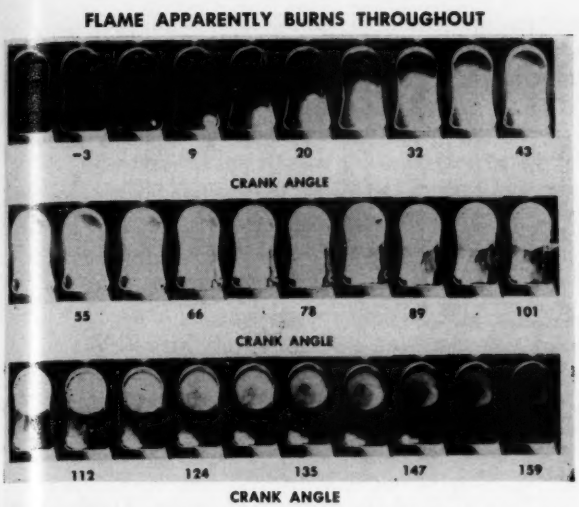

INTAKE MANIFOLD VACUUM 20" OF Hg., AIR-FUEL RATIO 12.2, SPARK TIMING TDC.

Fig. 5. Flame photographs for engine conditions of point 1 in Fig. 4.

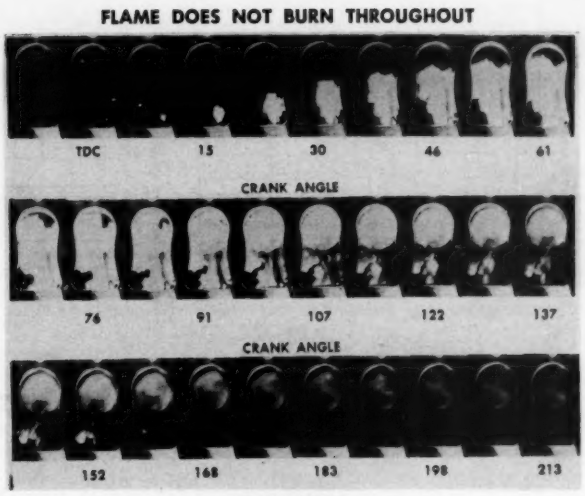

INTAKE MANIFOLD VACUUM 21.8" OF Hg., AIR-FUEL RATIO 12.2, SPARK TIMING TDC.

Fig. 6. Flame photographs for engine conditions of point 2 in Fig. 4.

a stroboscopic disk. Thus, it is believed that the flame with sodium added is representative of the flame without sodium.

In Fig. 5 are shown the flame photographs obtained at engine conditions indicated by point 1 in Fig. 4. Although the accuracy of the crank angles given in the flame photographs was only about ± 2° near TDC and about ± 5° at 140° ATC, the lack of accuracy in determining the crank angle for a given frame does not affect the conclusions drawn from the flame photographs. As can be seen from the location of point 1 in Fig. 4, the manifold vacuum and the air-fuel ratio were so adjusted that the flame was expected to burn throughout the combustion chamber. This was verified by the flame photographs shown in Fig. 5.

In Fig. 6 are shown flame photographs which illustrate the effect of increasing the intake vacuum to a point outside the region within which the flame burned throughout. As can be seen in Fig. 6, the flame failed to burn in the exhaust valve corner. In general, when engine conditions were changed so that the boundary of the region within which the flame burned throughout was crossed, the failure to burn occurred first in the exhaust valve corner.

The flame photographs shown in Fig. 7 were obtained at

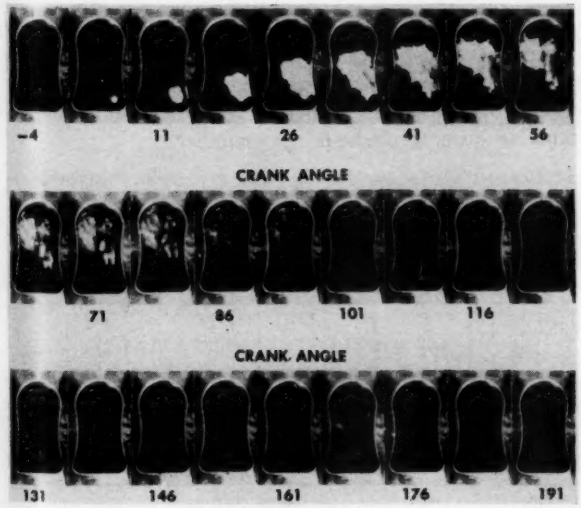

INTAKE MANIFOLD VACUUM 23.4" OF Hg., AIR-FUEL RATIO 10.6, SPARK TIMING TDC.

Fig. 7. Flame photographs for engine conditions of point 3 in Fig. 4.

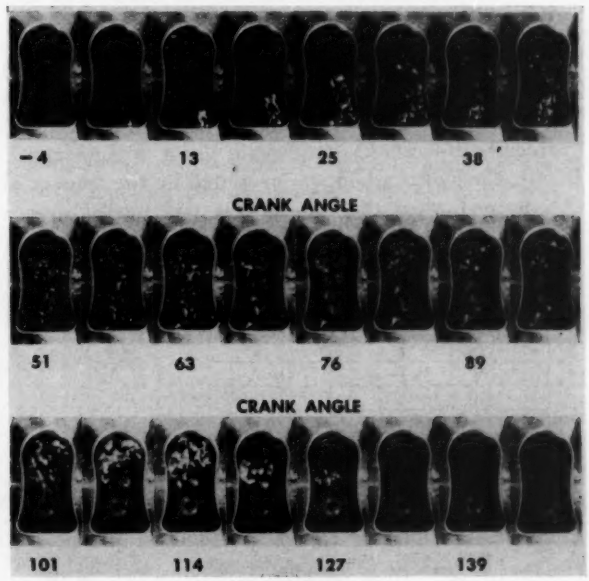

INTAKE MANIFOLD VACUUM 16.1" OF Hg., AIR-FUEL RATIO 5.7, SPARK TIMING TDC.

Fig. 8. Flame photographs for engine conditions of point 4 in Fig. 4.

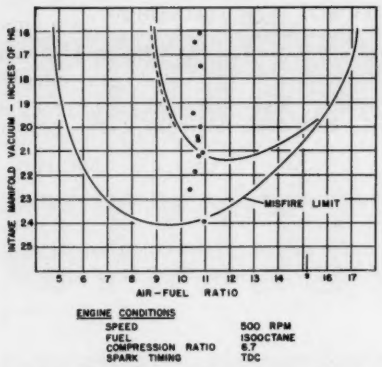

Fig. 9. Engine conditions used to show effect of intake manifold on % hydrocarbons in exhaust.

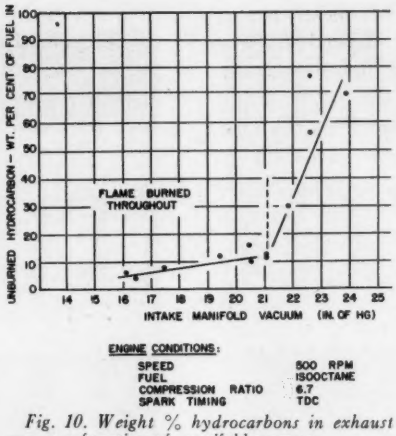

Fig. 10. Weight % hydrocarbons in exhaust gas as a function of manifold vacuum.

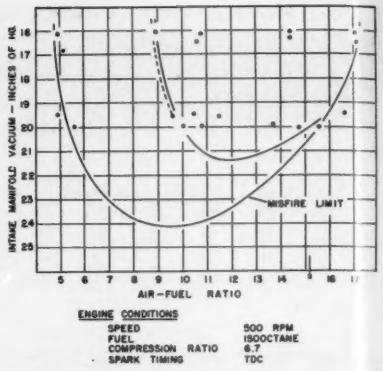

Fig. 11. Engine conditions used to show effect of air-fuel ratio on % hydrocarbons in exhaust.

the air-fuel ratio and manifold vacuum denoted by point 3 in Fig. 4. These conditions are farther from the boundary of the region within which the flame burned throughout, and the proportion of the combustion space traversed by flame was considerably reduced from that in Fig. 6.

Flame photographs were also taken at the manifold vacuum and air-fuel ratio represented by point 4 in Fig. 4. This sequence is shown in Fig. 8. These engine conditions were near the rich misfire limit and the flame was green in color. The flame burned in isolated patches, but the patches spread through the chamber in a more or less normal manner. The energy released by the green flame of Fig. 8 was low as evidenced by the facts that the indicated power was nearly zero, and there was approximately 20% oxygen in the exhaust. It is evident that at these conditions the per cent of hydrocarbons in the exhaust would be very high.

The per cent of hydrocarbons in the exhaust gas was determined at a number of different air-fuel ratios and manifold vacuums by means of a combustion Orsat. A description of the method for determining per cent of hydrocarbons in the exhaust gas is given in Appendix I. Briefly, the hydrocarbon was measured by the amount of CO_2 formed when the exhaust gas was passed over a heated catalyst in the presence of excess oxygen. Allowance was made for any CO_2 formed from combustion of CO.

The per cent unburned hydrocarbon values for the points shown in Fig. 9 with air-fuel ratios between 10.4 and 11.0 are plotted in Fig. 10. The curve of Fig. 10 shows the per cent of unburned hydrocarbons as a function of manifold vacuum at an approximately constant air-fuel ratio. The sharp increase in the per cent of unburned hydrocarbons occurring at about 21 in. of mercury vacuum coincides with the failure of the flame to burn throughout the mixture. As the manifold vacuum was increased above 21 in. of mercury, the per cent of combustion space traversed by flame decreased, and the per cent of hydrocarbons in the exhaust increased.

The values of the per cent hydrocarbon in the exhaust gas for points shown in Fig. 11 for the two manifold vacuum regions of 16.0 to 16.8 in. of mercury and 19.4 to 20.0 in. of mercury are plotted in Fig. 12. The two curves of Fig. 12 show the per cent of unburned hydrocarbons as a function of air-fuel ratio for two approximately constant manifold vacuums. Again the sharp increase in the per cent of hydrocarbons coincides with the failure of the flame to burn throughout the chamber.

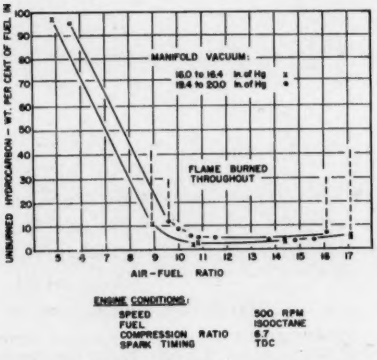

Fig. 12. Weight % hydrocarbons in exhaust gas as a function of air-fuel ratio.

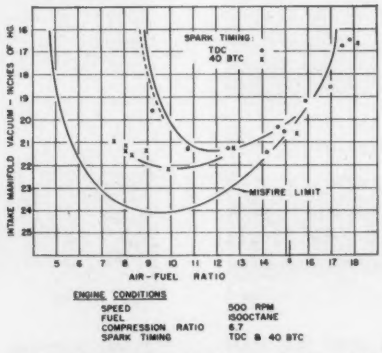

Fig. 13. Engine conditions at which residual fractions were determined.

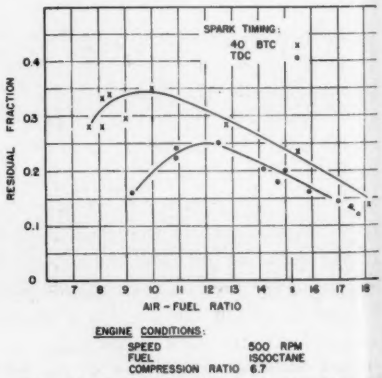

Fig. 14. Residual gas weight fraction for points shown in Fig. 13.

From the data of Fig. 10 and 12 it is concluded that when the visual inspection of the flame showed that the flame apparently burned throughout the mixture, the per cent of hydrocarbons found in the exhaust was relatively low. When the flame failed to burn throughout the mixture, whether due to the exhaust valve opening before the combustion was complete or to too high a manifold vacuum, the per cent of hydrocarbons in the exhaust gas increased.

Effect of Dilution on Flame Propagation and Misfire Limit

At this point an obvious question is: Why does the flame fail to burn throughout the combustion chamber at some engine conditions? It is known[5] that sufficient dilution of a gasoline-air mixture by an inert gas will prevent inflammation of the mixture. It is also known that the residual gas dilution of the charge in an engine increases with increasing intake manifold vacuum. Accordingly, experiments were conducted to determine whether residual gas dilution was the cause for the failure of the flame to burn throughout at the higher manifold vacuums.

It has already been noted that when engine conditions were such that a small portion of the mixture was not burned, the unburned portion would be in the exhaust valve corner. If exhaust gas dilution were the cause of the failure to burn in this corner, then a determination of the exhaust gas dilution in the exhaust valve corner should give the limiting exhaust gas dilution that would permit combustion.

To determine the residual gas dilution in the engine, a Cox Sampling Valve was placed so that the mixture in the exhaust valve corner could be sampled. The mixture sample was obtained by opening the valve for 130 crank angle degrees on the compression-expansion strokes. The valve open time was centered about TDC, and the spark was interrupted on the cycle sampled. Since more than one cycle (3 to 8) had to be sampled to fill a 100 ml. burette, a pause was made between the sampled cycles to allow the engine to recover from the effects of the unfired cycle.

The residual gas weight fraction was determined from the per cent CO_2 in the exhaust and the per cent CO_2 in the mixture sample as outlined in Appendix II.

The particular engine conditions at which the residual fractions were determined are shown in Fig. 13. Each engine condition was chosen to give a small unburned area in the exhaust valve corner; thus the points would follow the boundary of the region within which the flame burned throughout. At the rich air-fuel ratios and a spark timing of TDC the flame burned so slowly that the exhaust valve opened before the flame passage was complete. At an advanced spark timing, 40°BTC, the flame no longer burned out the exhaust port and the engine conditions which gave an unburned area in the exhaust valve corner are shown by the crosses in Fig. 13. The residual fraction was determined for both spark timings.

In Fig. 14 are shown the residual fractions as a function of air-fuel ratio for the points shown in Fig. 13. It can be seen that, for the range of air-fuel ratios commonly used in spark ignition engines, the richer mixtures tolerated more dilution than the leaner mixtures.

A comparison between the results shown in Fig. 14 and the results of experiments by Jones and Gilliland are shown in Fig. 15. Jones and Gilliland reported the limiting percentages of exhaust gas for inflammability of gasoline-air mixtures of controlled composition in a tube. The data were obtained with the test gases at a reduced pressure and with a spark for ignition. Jones' and Gilliland's data were reported on a volume basis. By assuming an average molecular weight of the gasoline to be 98, their data were changed to a weight basis and plotted in Fig. 15. For air-fuel ratios richer than about 8 the data of Jones and Gilliland show an abrupt boundary between diluted gasoline-air mixtures that will and will not burn; however, at leaner air-fuel ratios the data indicate a spread between the per cent dilution that will burn and the per cent dilution that will not burn. This probably means that within the spread the mixture would burn sometimes and at other times would not.

For air-fuel ratios between 12.5 and 18 and a spark timing of TDC it would appear that the reason the flame does not burn the mixture in the exhaust valve corner of the engine is because the dilution has reached the upper limit that will permit combustion. Dilution is probably not the cause for the unburned portion of mixture for the air-fuel ratios richer than 12.5 since the measured dilution appears to be well in the range of dilution that should permit combustion. High speed motion pictures at these conditions have shown that unburned mixture is swept out the exhaust valve when it opens at 140°ATC. The failure to burn, therefore, has a simple physical explanation—the unburned mixture was swept out the exhaust valve before it had a chance to burn. The advanced spark provides a longer burning time and a good correlation was obtained between the engine results and Jones' and Gilliland's results for air-fuel ratios as rich as 9.

The fact that the limiting value of the exhaust gas dilution for a given air-fuel ratio is nearly the same in the tube and in the engine would indicate that residual gas dilution is a major factor limiting complete inflammation of the mixture in the quartz window engine operated at high intake vacuums.

Many differences exist between the conditions used in the tube and those present in the engine. One difference is the fuel used. In the engine the fuel was isooctane, and in the tube work the fuel was gasoline. Jones and Gilliland[5] found no effect on the ignition limits when using 3 different gasolines of widely different octane number and volatility. Pressures were also different in the two cases. The pressures present in the engine ranged from a maximum of 4.7 atmospheres to a minimum of about .25 atmospheres, while the tube experiments were con-

[5] Jones, G. W., and Gilliland, W. R., "Extinction of Gasoline Flames by Inert Gases," *U. S. Bureau of Mines, R. I. 3871,* April, 1946.

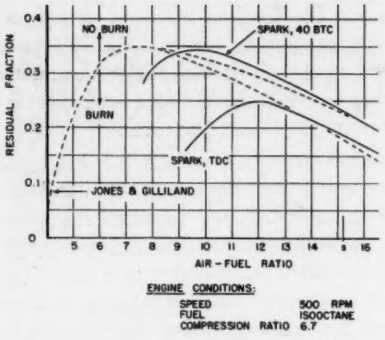

Fig. 15. Comparison of exhaust gas dilution in exhaust valve corner with limiting exhaust gas dilution in a tube.

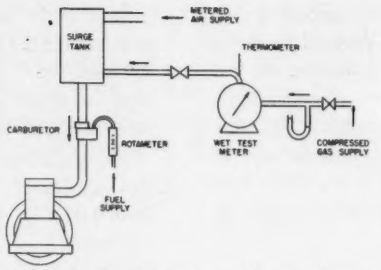

Fig. 16. Apparatus for adding oxygen or nitrogen to intake air.

Fig. 17. Misfire limit and region within which flame burned throughout with extra oxygen added to intake air. (Oxygen-nitrogen weight ratio = 0.44).

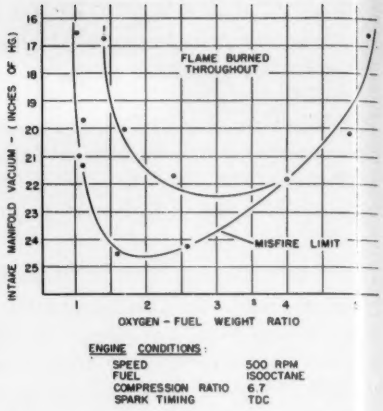

ducted at "reduced pressure." Jones and Kennedy[6] investigated the effect of pressure on the inflammability limits of natural gas-air mixtures with no dilution. The results of this work showed little effect of pressure within the range of pressures used in the engine and in the tube work. Another difference in the two cases is the diluting exhaust gas. In the tube work the exhaust gas was apparently a dry mixture of 85% nitrogen, 15% CO_2 for all air-fuel ratios; while the exhaust gas diluent in the engine is a mixture containing N_2, H_2O, CO, CO_2, and H_2, depending on the air-fuel ratio. The effect of the differences in exhaust gas in the two cases has not been evaluated, and in particular the effect of the difference in the amount of H_2O present could be significant.

If the boundary of the region within which the flame burned throughout is mainly determined by the limiting dilution that will permit burning, a change in the dilution would cause a corresponding change in the position of the boundary of the region within which the flame burned throughout. The "over-all dilution" of the oxygen-fuel mixture in the combustion chamber comes from two sources: (1) the nitrogen which accompanies the oxygen-fuel mixture fed to the engine, and (2) the residual exhaust gas. One way to change the over-all dilution of the oxygen-fuel mixture, therefore, would be to change the per cent nitrogen in the intake "air". This was done by adding nitrogen or oxygen to the intake surge tank.

As indicated in Fig. 16 the added gas passed from a gas cylinder through a needle valve to the wet test meter. From the wet test meter it passed through a second needle valve into the surge tank of the air system. By adjusting the two needle valves it was possible to obtain the desired rate of flow and to maintain the pressure between the valves at approximately atmospheric.

The procedure followed was to adjust the air flow and added gas flow to obtain a given oxygen-nitrogen ratio in the inlet charge and also to obtain a given manifold vacuum. The fuel flow was then changed to obtain a range of oxygen-fuel ratios to determine the misfire limit and the range of oxygen-fuel ratios within which the flame apparently burned throughout the chamber. By repeating this procedure for several different manifold vacuums, a plot of the misfire limit and the region within which the flame burned throughout was obtained. A plot for an oxygen-nitrogen weight ratio of 0.44 (oxygen-nitrogen ratio of air is 0.30) is shown in Fig. 17. A plot for an oxygen-nitrogen ratio of 0.26 is shown in Fig. 18. The plots shown in Figs. 3, 17, and 18 are shown superimposed in Fig. 19. It was necessary to change the abscissa of Fig. 3 from air-fuel ratio to oxygen-fuel ratio for Fig. 19.

In Fig. 19 it can be seen that a decrease in the over-all dilution of the charge from that given by air, by increasing the oxygen-nitrogen ratio to 0.44, widened and lowered

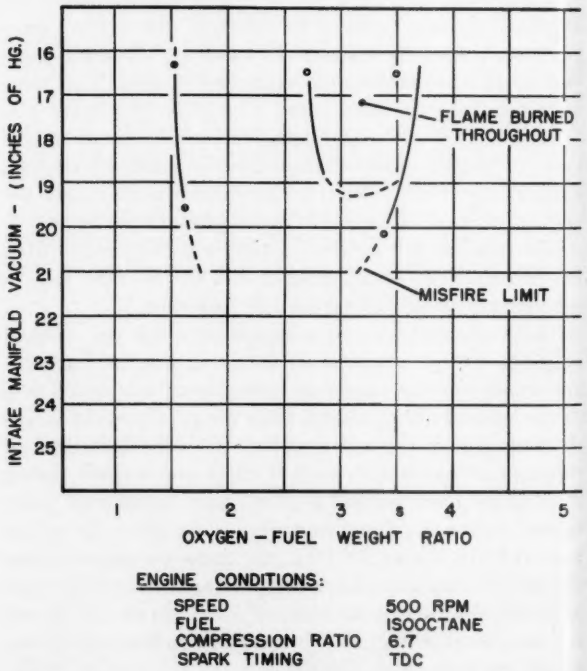

Fig. 18. Misfire limit and region within which flame burned throughout with extra nitrogen added to intake air. (Oxygen-nitrogen weight ratio = 0.26).

[6] Jones, G. W., and Kennedy, R. E., "Inflammability of Natural Gas; Effect of Pressure upon the Limits," *U. S. Bureau of Mines, R. I. 3798,* February, 1945.

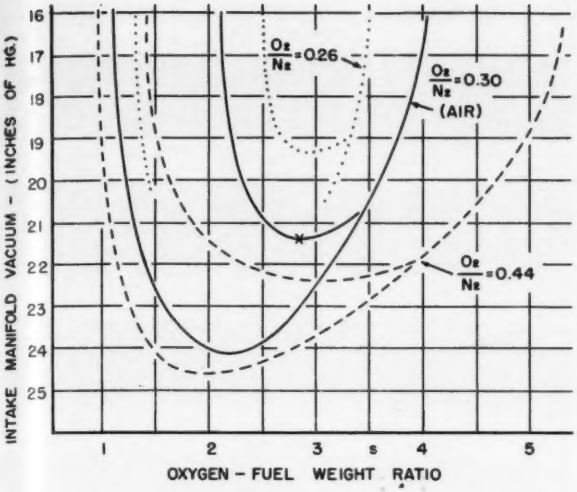

Fig. 19. The effect of a change in the overall dilution on the misfire limit and on the region within which the flame burned throughout.

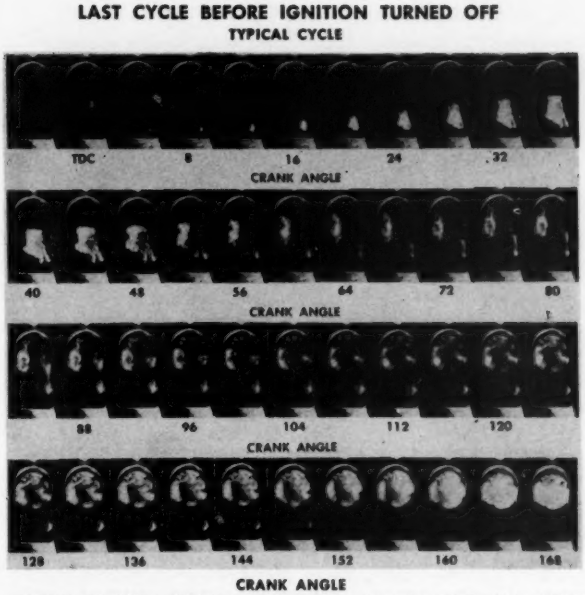

INTAKE MANIFOLD VACUUM 23.4" OF Hg., AIR-FUEL RATIO 10.6, SPARK TIMING TDC.

Fig. 20. Sequence showing effect of interrupted ignition on flame propagation (Fig. 20-22).

the range of air-fuel ratios and manifold vacuums within which the flame burned throughout. An increase in the over-all dilution of the charge by decreasing the oxygen-nitrogen ratio below that of air, narrowed and raised the range of air-fuel ratios and manifold vacuums within which the flame burned throughout. Thus, these results appear to confirm qualitatively the hypothesis that the boundary of the region within which the flame burned throughout was primarily determined by the dilution of the mixture.

Reviewing the results of Fig. 19 in more detail, however, yields the following argument: Consider a point on the plot; for example, the bottom point of the boundary for complete burning at an oxygen-nitrogen weight ratio of 0.30 designated by an "X" on the plot. If the oxygen-nitrogen ratio of the charge is changed to 0.26 by replacing some of the oxygen-fuel mixture by nitrogen, it is apparent that at point X the nitrogen is now a larger proportion of the charge, but also the concentration of fuel and oxygen (moles/unit volume) has been decreased. Thus, the failure to burn may be due either to the increased dilution or to the lower concentration of reactants. Similarly at point X, but with an oxygen-nitrogen ratio of 0.44, the over-all dilution is lower and the concentration of reactants is higher. Whether the failure to burn then is due to the dilution effect or to the change in the concentration of reactants cannot be determined from the data shown in Fig. 19; although the correspondence between the residual dilution values obtained in the engine and the values of "exhaust gas" dilution that prevent inflammation in a tube would indicate that the dilution effect is the limiting factor.

In Fig. 19 it may be seen that the misfire limit was affected by a change in the over-all dilution in the same manner as the boundary of the region within which the flame apparently burned throughout. Evidently the ignition of the mixture is determined by the same variable(s) that control complete inflammation.

Perhaps the most striking evidence of the role of dilution is given in Fig. 20, 21, and 22. The flame photographs shown in these figures were obtained with a manifold vacuum of 23.4 in. of mercury and an air-fuel ratio of 10.6. These engine conditions, incidentally, are the same as those for point 3 in Fig. 4. At these engine conditions the flame did not normally burn throughout the combustion chamber. Flame photographs of a typical cycle are shown in Fig. 20. The ignition was turned off for 4 cycles to allow the engine to purge itself of exhaust gas. The ignition was then turned on and the flame photographs shown in Fig. 21 were obtained from the first cycle after the ignition was turned on. For this cycle the exhaust gas dilution was low and the flame burned throughout the combustion chamber. It can be noted by comparing Fig. 20 and 21 that the flame was brighter and the apparent flame speed was greater with the low dilution. Flame photographs of the second cycle after the ignition was turned on are shown in Fig. 22. The exhaust gas dilution in this second cycle is relatively high due to the complete combustion of the preceding cycle. With this high dilution the flame burned only a small portion of the mixture as may be seen in Fig. 22.

Again this experiment did not separate the effects of a change in dilution and a change in concentration of reactants, since the manifold pressure was maintained con-

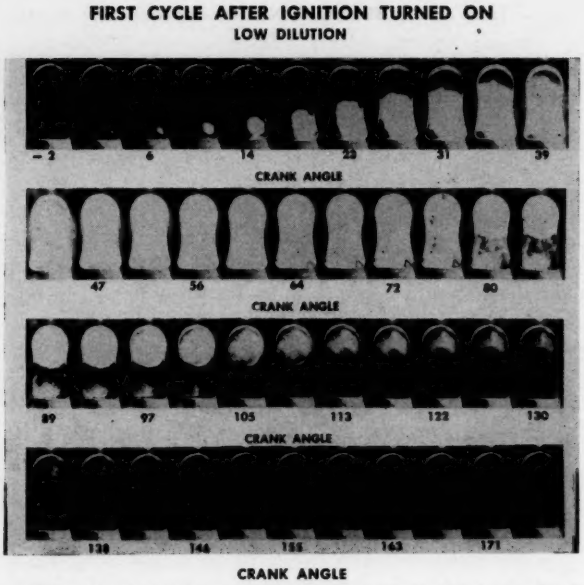

INTAKE MANIFOLD VACUUM 23.4" OF Hg., AIR-FUEL RATIO 10.6, SPARK TIMING TDC.

Fig. 21

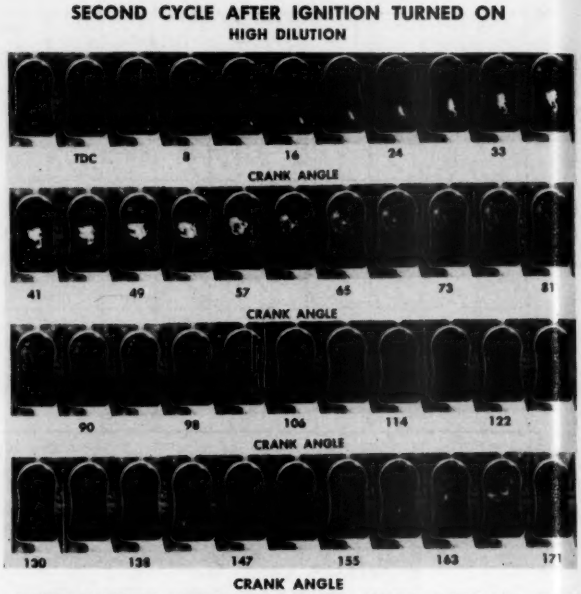

INTAKE MANIFOLD VACUUM 23.4" OF Hg., AIR-FUEL RATIO 10.6, SPARK TIMING TDC.

Fig. 22

Sequence showing effect of interrupted ignition on flame propagation (Fig. 20-22).

stant while the proportion of reactants and residual in the chamber was varied. Similar to the argument outlined previously, the inflammability of the mixture may have been determined by the concentration of the reactants.

Another experiment was made to determine if a concentration of reactants lower than the concentration of reactants at engine conditions near the bottom of the boundary of the region within which the flame burned throughout could be made to burn. A point at the bottom of the boundary was selected because it would have the lowest concentration of reactants of any point on the boundary and would provide the most critical test. If a mixture with a concentration of reactants lower than the concentration of reactants for the point just mentioned could be made to burn throughout, the possibility that complete inflammation of the mixture in the engine was limited by a critical concentration of reactants could be rejected.

Operating the engine at the highest possible vacuum with no burned product dilution appeared to afford the best possibility of accomplishing this. Accordingly, the interrupted ignition experiment described above was extended. It was found that when the engine was operated with an intake manifold vacuum of 26.2 in. of mercury (the highest manifold vacuum which the engine could pull) the flame would burn throughout the chamber for one cycle only; thereafter, the engine would not fire for a considerable length of time. The reason for this was that the residual fraction was close to one, and the burned products of the fired cycle oscillated back and forth in the engine and manifolds. If the burned products were cleared from the system, the engine would again fire for one cycle. To aid in clearing the burned products, the exhaust manifold was removed at the block and the intake manifold was closed about a foot from the block. Fuel was metered through a needle valve into this short section of intake manifold. Upon turning the engine over, the intake vacuum rose immediately to 26.2 in. of mercury (1.7 psia). The spark ignition was then turned on and the fuel flow was adjusted until the engine fired. At an optimum fuel rate the engine would fire every second or third cycle, burning the mixture completely. After a cycle in which the flame burned throughout it took about one cycle to replace the residual burned products with sufficient air for combustion, since all the air for combustion entered through the exhaust port. Thus it was found that the flame would burn throughout the chamber when the intake manifold pressure and the pressure at the beginning of compression was 1.7 psia.

At an intake vacuum of 21.3 in. of mercury (3.9 psia) and an air-fuel ratio of 12.5, the flame did not burn throughout the chamber when the engine was operated normally as may be seen in Fig. 13. The residual fraction for these engine conditions was 0.24 (from Fig. 14). Therefore, the partial pressure of the reactants at the beginning of compression was about 3 psia.

Making the simplifying assumption that the concentration of the reactants is proportional to the partial pressure of the reactants, it is apparent that the concentration of reactants is less in the case where the partial pressure of reactants was, at most, 1.7 psia than in the case where the partial pressure of the reactants at the beginning of compression was 3.0 psia. Since the flame burned throughout the chamber when the partial pressure of the reactants

was 1.7 psia, the failure of the flame to burn throughout when the partial pressure of the reactants was 3.0 cannot be attributed to too low a concentration of reactants.

Similarly, if the partial pressures of the reactants for the conditions considered in Fig. 19 were known, it could be determined whether the effect of the added nitrogen was due to the increased dilution or to the decreased concentration of reactants. Unfortunately, the residual gas fraction was not determined for these conditions, and therefore the partial pressures of reactants were not known. However, the lowering of the limits when oxygen was added cannot be due to a concentration effect, since it has been shown that the concentration of reactants for the "air" curve (oxygen-nitrogen ratio = 0.30) was not a threshold concentration, and with oxygen added (oxygen-nitrogen ratio = 0.44) the concentration of reactants at a given point, X, is greater than that for air.

The experiments described above indicate that dilution is an important factor in preventing the complete inflammation of the mixture; however, the possibility that the incomplete inflammation may be partly due to pressure and/or other unknown factors has not been entirely eliminated.

Two Devices to Reduce Hydrocarbons in Automobile Exhaust Gas

Assuming that the plot of the misfire limit and the region within which the flame burned throughout is applicable to present day automobile engines, the single-cylinder engine investigation indicates that in most cases idle operation is probably within the region in which the flame burns throughout. Idle vacuum is usually between 18 to 20 in. of mercury, so it is necessary only to maintain the air-fuel ratio between 10 and 16. In most instances the idle air-fuel ratio is undoubtedly within this range. One would expect, therefore, that the concentration of unburned hydrocarbons in the exhaust at idle would be relatively low.

In addition the single cylinder investigations confirmed the findings of previous investigators[1-2-3] who found that the high concentrations of unburned hydrocarbons in the exhaust gas of engines occur when the engine is operated at high intake vacuums (greater than about 21 in. mercury vacuum). Usually, intake manifold vacuums above 21 in. of mercury can be attained only by deceleration and may be as high as 25 in. of mercury.

Since the highest concentration of hydrocarbons in the exhaust occurs during deceleration, an attempt was made to reduce the concentration during deceleration. There are at least two ways to modify a carburetor in order to reduce the high concentration of unburned hydrocarbons found in the exhaust of an engine during deceleration:

1. The fuel flow may be shut off when the intake manifold vacuum exceeds about 21 in. of mercury.
2. The vacuum may be prevented from reaching the values which give high concentrations of unburned fuel in the exhaust.

Two devices, one operating on each principle, were tested. The device operating on the fuel flow shut-off principle was installed on the family car of one of the authors. The car was of 1947 vintage and was equipped with a synchromesh transmission. The mechanical condition of the engine was good, having had an overhaul 10,000 miles or one year before the test. It was found that with the throttle closed (closed to idle position), all of the fuel going into the engine passed through the idle circuit of the carburetor. Therefore, to shut off the fuel, it was only necessary to close the idle circuit. It was realized that at higher speeds, deceleration with the throttle held partly open might result in fuel passage through the high speed circuit, but in view of the facts that the high speed circuit was more inaccessible and that the contribution to fuel wasted from this source was probably small, it was decided to neglect it.

The second device limited the vacuum attained during deceleration by admitting additional air-fuel mixture to the manifold when the vacuum tended to rise above 21 in. of mercury. This device was installed on a 1954 model car equipped with a torque converter type of transmission.

The effectiveness of the two devices was checked by taking exhaust gas samples in evacuated bottles. A steel line, 3 ft. in length, was connected to the exhaust manifold near the exhaust pipe flange and extended through the fire wall to the sample bottles. For the tests, each car was decelerated with the throttle closed to idle position from 50 mi/hr., and samples were obtained at 5-sec. intervals after the start of the deceleration. Two such runs were made for each car, one with the particular device oper-

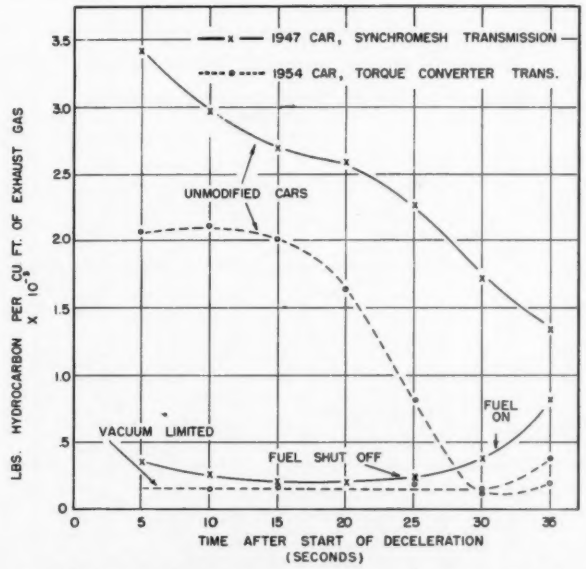

Fig. 23. Effect of carburetor devices on concentration of hydrocarbon in exhaust during deceleration.

(1) See footnote 1, page 91.
(2) See footnote 2, page 91.
(3) See footnote 3, page 91.

ative and one with the device inoperative. In every case the samples were analyzed (by the method outlined in Appendix I) on the same day that they were taken.

In Fig. 23 are shown plots of concentration of unburned hydrocarbons in the exhaust gas (lbs./ft.^{3}) as functions of elapsed time after the start of deceleration for the two cars with the devices operative and inoperative. Both devices reduced the concentration of hydrocarbons in the exhaust gas to a low value but did not eliminate it. With the devices inoperative the car which was equipped with the synchromesh transmission had the largest concentration of hydrocarbons in the exhaust gas. This car also had a higher intake vacuum at a given car speed than the car with the torque converter transmission. The difference in the concentration of unburned hydrocarbons in the exhaust of the two cars with the devices inoperative is probably largely due to the difference in intake vacuum. Thus, Fig. 23 shows a marked reduction in the concentration of unburned hydrocarbons when either type of device is used and in addition shows an effect of transmission type on the concentration of hydrocarbons in the exhaust of standard cars.

The *rate* of unburned hydrocarbon emission to the atmosphere may be more significant to the air-pollution problem than the *concentration* of hydrocarbon emission from a given source. Therefore, in Fig. 24 are shown the curves of rate of hydrocarbon emission (lbs./min.) against time after the start of a deceleration from 50 mph. The relative positions of the curves obtained with the devices inoperative are the same as in Fig. 23; but the relative position of the two curves obtained with the two devices operative is reversed. This reversal in the relative positions of the two curves might be expected since the exhaust gas flow rate was greater in the car with the vacuum limiting device than in the car with the fuel shut-off device. The exhaust gas flow rate was somewhat greater since the engine in the car on which the vacuum limiting device was installed had a 38 per cent greater displacement than the engine in the car on which the fuel shut-off device was installed; however, the larger displacement of the one engine did not alone produce the difference in flow rate required to give the observed reversal of the relative positions of the two curves. The reversal of the relative positions of the two curves may be mainly attributed to the action of the vacuum-limiting device in permitting more air-fuel mixture to pass through the engine. The area under each curve in Fig. 24 is proportional to the total amount of unburned hydrocarbons emitted during the 30 sec. period from 5 to 35 sec. after the start of the deceleration. The amount of hydrocarbon emitted during the deceleration in each case and the per cent reduction obtained with each device is given in Table II.

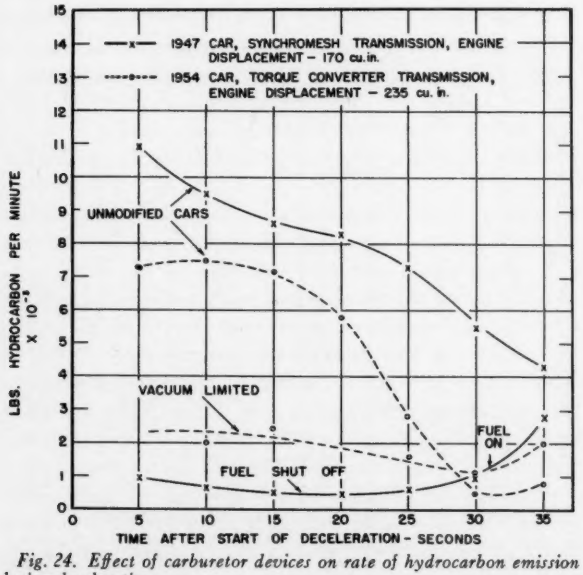

Fig. 24. Effect of carburetor devices on rate of hydrocarbon emission during deceleration.

TABLE II

Total Amount of Hydrocarbon Emitted During a Thirty Second Interval of a Closed Throttle Deceleration

Device	Weight Emitted (lbs.) Operative	Inoperative	% Reduction
Idle Circuit Shut-Off	0.4×10^{-3}	3.9×10^{-3}	90
Vacuum Limited	0.9×10^{-3}	2.3×10^{-3}	61

The per cent reduction of hydrocarbon emitted with the idle circuit shut-off device is greater than the per cent reduction with the vacuum limiting device, partly because the idle circuit shut-off was installed on the car that was emitting hydrocarbons at the highest rate and therefore subject to the greatest improvement. In spite of this fact, the total amount of hydrocarbon emitted by this car was reduced to less than one-half that obtained with the vacuum limiting device. Unfortunately, all aspects of the operation of the devices were not entirely satisfactory, and further development work is indicated.

Another consideration that has no bearing on the air-pollution problem but would be important to potential owners of automobiles equipped with these devices is the effect of the devices on fuel economy. The device which shuts off the idle circuit during deceleration has been found in preliminary tests to give 2.9% more fuel economy in all-around family driving. The vacuum limiting device has not been checked for fuel economy, but it is probably lower with the device in operation because more fuel is used during deceleration with the device in use than without it.

The two devices just described were made for experimental purposes in the hope that they would point the way to a practical means of reducing hydrocarbon emission in the exhaust of a decelerating automobile. However,

many problems remain to be solved before a device which is effective and economical can appear on automobiles.

Summary

1. It was found that the abrupt increase in the concentration of unburned hydrocarbons in the exhaust gas with an increase in intake manifold vacuum above about 21 in. of mercury corresponded to the initial failure of the flame to propagate throughout the mixture. As the proportion of the combustion space traversed by flame decreased, the per cent of hydrocarbons in the exhaust gas increased.

2. The value of residual exhaust gas dilution existing in the engine when the mixture was just failing to burn throughout the chamber was found to correlate well with limiting values of dilution obtained from the literature.

3 Changes in the "over-all dilution" of the oxygen-fuel mixture affected the limit of complete inflammation in the same manner that would be predicted if dilution were a factor determining the limit.

4 It was found that the failure of the flame to burn throughout the combustion chamber at the boundary of the region within which the flame burned throughout was not due to too low a concentration of reactants.

5 Therefore, it was concluded that residual gas dilution was a major factor limiting the complete inflammation of the mixture at engine conditions near the boundary of the region within which the flame burned throughout.

6 The concentration and amount of unburned hydrocarbon emitted in the exhaust gas of automobiles during deceleration were substantially reduced by modifying the carburetor in either of two ways, (1) by admitting additional air and fuel to the intake manifold during deceleration, and (2) by shutting off the fuel during deceleration. The problem of eliminating all the unburned hydrocarbon emission during all driving conditions remains a challenge.

Acknowledgments

The authors wish to thank J. B. Bidwell of Research Laboratories Division, General Motors Corporation, for making his vacuum limiting device available for tests. Also we are indebted to Dr. F. W. Bowditch for his aid in obtaining the flame photographs presented.

Appendix I

Method for Determining Per Cent Unburned Hydrocarbon in Exhaust Gas

Conventional Orsat equipment was used to determine the per cent unburned hydrocarbons (weight per cent of input fuel) in the exhaust gas. Exhaust samples were obtained simultaneously in the burettes of two Orsats. Sample I was analyzed in the usual manner for CO_2, O_2, and CO. Sample 2 was also first analyzed for CO_2. Oxygen was then added to Sample 2 and the sample was passed through a catalytic furnace to burn all the combustibles to CO_2 and water. The CO_2 and the remaining O_2 were then absorbed, leaving nitrogen. The total amount of CO_2 formed when all of the fuel fed to the engine was completely burned, even though the fuel was burned partly in the engine and partly in the catalytic furnace, was thus determined from the analysis of Sample 2. The portion of the fuel burned in the engine was determined from the volume per cent CO and CO_2 from the analysis of Sample 1, and the per cent hydrocarbon was determined by means of the following equation:

$$\text{weight \% unburned hydrocarbon} = \frac{CO_2'' - CO' - CO_2'}{CO_2''} \times 100$$

in which CO_2'' = the total volume per cent CO_2 obtained from the analysis of Sample 2

CO' = the volume per cent CO obtained from the analysis of Sample 1

CO_2' = the volume per cent CO_2 obtained from the analysis of Sample 1

This method of analysis of the exhaust gas does not differentiate between hydrocarbons and partially oxidized hydrocarbons. The weight per cent unburned "hydrocarbon" thus obtained includes all carbon containing compounds, except CO, which burn to form CO_2. The assumptions necessary for this type of analysis are:

1. All of the carbon in the fuel entering the engine leaves the engine in the exhaust gas as some gaseous product.
2. No oil is burned in the engine.
3. The average hydrogen-carbon ratio of the carbon containing compounds which burned to form CO_2 in the catalytic furnace is equal to the average hydrogen-carbon ratio of the input fuel.

Appendix II

Method for Determining Residual Gas Weight Fraction From Orsat Gas Analyses

The experimental data required to determine the residual gas weight fraction were the Orsat analysis of the mixture which existed in the combustion chamber after the valves were closed and before ignition, and the Orsat analysis of the exhaust gas. In addition, air-fuel ratio charts similar to those of D'Alleva and Lovell [7] were used to determine the average molecular weight of the exhaust gas and to determine the volume per cent water in the exhaust gas. The air-fuel ratio of the input charge was determined by measuring the air flow and fuel flow. The sample of the mixture was obtained with a sampling valve on the compression-expansion strokes of a cycle in which the spark was not fired. The mixture sampling was repeated enough times to obtain 100 milliliters of unburned mixture in an Orsat burette. Next, a sample of exhaust gas was pulled into a second Orsat burette while the engine was firing steadily. Both samples were analyzed for CO_2, O_2, and CO.

The residual gas fraction, "f", is defined as the proportion of residual gas in the mixture of fuel, air and residual exhaust gas:

$$f = \frac{\text{weight of residual}}{\text{weight of mixture}} \qquad (1)$$

Note that the weight of residual includes water formed due to combustion and will be referred to hereafter as "wet residual." The mixture may be divided into two parts, wet residual and charge, so Equation (1) may also be written:

$$f = \frac{\text{weight wet residual}}{\text{weight wet residual} + \text{weight charge}} \qquad (2)$$

Air in the charge was assumed to be dry and the CO_2 in air was considered negligible.

To express "f" as a function of the CO_2 in the exhaust and the CO_2 in the mixture, assume that the proportion of CO_2 in the residual is the same as the proportion of CO_2 in the exhaust:

$$\frac{\text{wt. } CO_2 \text{ in residual}}{\text{wt. wet residual}} = \frac{\text{wt. } CO_2 \text{ in exhaust}}{\text{wt. wet exhaust}}$$

$$\text{or, } \frac{\text{wt. } CO_2 \text{ in residual}}{\text{wt. wet residual}} = \text{wt. fraction of } CO_2 \text{ in wet exhaust} \qquad (3)$$

$$\text{Also, wt. fraction } CO_2 \text{ in wet mixture} = \frac{\text{wt. } CO_2 \text{ in wet residual}}{\text{wt. wet mixture}} \qquad (4)$$

Divide (4) by (3):

$$\frac{\text{wt. fraction } CO_2 \text{ in wet mixture}}{\text{wt. fraction } CO_2 \text{ in wet exhaust}} = \frac{\dfrac{\text{wt. } CO_2 \text{ in wet residual}}{\text{wt. wet mixture}}}{\dfrac{\text{wt. } CO_2 \text{ in wet residual}}{\text{wt. wet residual}}}$$

$$\text{or, } \frac{\text{wt. fraction } CO_2 \text{ in wet mixture}}{\text{wt. fraction } CO_2 \text{ in wet exhaust}} = \frac{\text{wt. wet residual}}{\text{wt. wet mixture}} \qquad (5)$$

Therefore, from (5) and (1):

$$f = \frac{\text{wt. fraction } CO_2 \text{ in wet mixture}}{\text{wt. fraction } CO_2 \text{ in wet exhaust}} \qquad (6)$$

[7] D'Alleva, B. A., and Lovell, W. G., "Relation of Exhaust Gas Composition to Air-Fuel Ratio," *Journal Society of Automotive Engineers*, **38**, 90 (March, 1936).

The numerator of Equation (6) may be written:

$$\text{wt. fraction } CO_2 \text{ wet mixture} = \frac{\text{volume } CO_2 \text{ in mixture} \times 44}{(\text{vol. wet residual})\,mw_e + (\text{vol. charge})\,mw_c} \quad (7)$$

in which mw_e = average molecular weight of exhaust
mw_c = average molecular weight of charge

Similarly, the denominator of Equation (6) may be written:

$$\text{wt. fraction } CO_2 \text{ wet exhaust} = \frac{\text{volume } CO_2 \text{ in exhaust} \times 44}{(\text{volume wet exhaust})\,mw_e} \quad (8)$$

Substituting (7) and (8) into (6):

$$f = \frac{\dfrac{(\text{vol. } CO_2 \text{ mixture}) \times 44}{(\text{vol. wet residual})\,mw_e + (\text{vol. charge})\,mw_c}}{\dfrac{(\text{vol. } CO_2 \text{ in exhaust}) \times 44}{(\text{vol. wet exhaust})\,mw_e}} \quad (9)$$

To express the volume of wet residual and the volume of charge in terms of the volume of wet mixture and to further simplify Equation (9), assume that the volume percentage of CO_2 in the residual equals the volume percentage of CO_2 in the exhaust:

$$\frac{\text{vol. } CO_2 \text{ residual}}{\text{vol. wet residual}} = \frac{\text{vol. } CO_2 \text{ exhaust}}{\text{vol. wet exhaust}}$$

$$\text{or, } \frac{\text{vol. } CO_2 \text{ residual}}{\text{vol. wet residual}} = \text{vol. fraction of } CO_2 \text{ in wet exhaust} \quad (10)$$

$$\text{Also, vol. fraction } CO_2 \text{ in wet mixture} = \frac{\text{vol. } CO_2 \text{ in mixture}}{\text{vol. wet mixture}} \quad (11)$$

Define "M" as,

$$M = \frac{\text{vol. fraction } CO_2 \text{ in wet mixture}}{\text{vol. fraction } CO_2 \text{ in wet exhaust}} \quad (12)$$

Substituting (10) and (11) into (12):

$$M = \frac{\dfrac{\text{vol. } CO_2 \text{ in mixture}}{\text{vol. wet mixture}}}{\dfrac{\text{vol. } CO_2 \text{ in residual}}{\text{vol. wet residual}}} \quad (13)$$

Since vol. CO_2 in mixture = vol. CO_2 in residual, Equation (13) may be simplified:

$$M = \frac{\text{vol. wet residual}}{\text{vol. wet mixture}} = \frac{\text{vol. wet residual}}{\text{vol. wet residual} + \text{vol. charge}} \quad (14)$$

Therefore,

$$\text{volume wet residual} = M(\text{volume wet mixture}) \quad (15)$$

$$\text{and, volume of charge} = (1\text{-}M)(\text{volume wet mixture}) \quad (16)$$

Substituting (15) and (16) into (9),

$$f = \frac{\dfrac{(\text{vol. } CO_2 \text{ in mixture})\,44}{M(\text{vol. of wet mix.})\,mw_e + (1\text{-}M)(\text{vol. wet mix.})\,mw_c}}{\dfrac{(\text{vol. } CO_2 \text{ in exhaust})\,44}{(\text{vol wet exhaust})\,mw_e}} \quad (17)$$

$$\text{or, } f = \left[\frac{\dfrac{\text{vol. } CO_2 \text{ in mixture}}{\text{vol. wet mixture}}}{\dfrac{\text{vol. } CO_2 \text{ in exhaust}}{\text{vol. wet exhaust}}}\right]\left[\frac{44}{\dfrac{M(mw_e) + (1\text{-}M)mw_c}{mw_e}}\right] \quad (18)$$

The first term in Equation (18) is M, therefore:

$$f = \frac{M(mw_e)}{M(mw_e) + (1\text{-}M)mw_c} \quad (19)$$

"M" may be expressed in terms of dry, volume percentages obtained with the Orsat as follows:

$$\text{By definition, } M = \frac{\dfrac{\text{vol. } CO_2 \text{ in dry mixture sample}}{\text{volume wet mixture sample}}}{\dfrac{\text{vol. } CO_2 \text{ in dry exhaust sample}}{\text{volume wet exhaust sample}}} \quad (20)$$

Considering first the denominator of Equation (20), volume wet exhaust sample = volume dry exhaust sample + volume of water vapor, and the volume of water may be determined from the volume per cent of water in the burned products "Z".

$$\text{volume of water} = \frac{100Z}{100 - Z}, \quad (21)$$

if a 100 ml. dry exhaust sample is assumed. Then the denominator of Equation (20) may be written as:

$$\frac{\text{vol. } CO_2 \text{ in dry exhaust sample}}{100 + \dfrac{100Z}{100 - Z}}$$

$$\text{or, } \frac{(100 - Z)\ (\text{vol. } CO_2 \text{ in dry exhaust sample})}{(100)^2} \quad (22)$$

To simplify the numerator of Equation (20) the volume of the wet mixture sample may be expressed in terms of the volume of the dry mixture sample, M, and Z:

volume wet mixture sample = vol. dry charge + vol. dry residual + vol. water, and assume vol. dry charge + vol. dry residual = 100

Equation (14) may be written:

$$M = \frac{\text{volume dry residual} + \text{volume water}}{100 + \text{volume water}} \quad (23)$$

By definition,

$$Z = \frac{(\text{volume water})100}{\text{volume dry residual} + \text{volume water}} \quad (24)$$

Combine Equations (23) and (24) to obtain

$$\text{volume water} = \frac{100\,MZ}{100 - MZ} \quad (25)$$

and the numerator of Equation (20) becomes

$$\frac{\text{volume } CO_2 \text{ in dry mixture sample}}{100 + \dfrac{100\,MZ}{100 - MZ}}$$

$$\text{or, } \frac{(100 - MZ)\ (\text{volume } CO_2 \text{ in dry mixture sample})}{(100)^2} \quad (26)$$

Thus, putting Equations (26) and (22) into Equation (20):

$$M = \frac{(100 - MZ)\ (\text{vol. } CO_2 \text{ in dry mixture sample})}{(100 - Z)\ (\text{vol. } CO_2 \text{ in dry exhaust sample})} \quad (27)$$

Solving (27) for M:

$$M = \frac{100\ (\text{vol. } CO_2 \text{ in dry mixture sample})}{100\ (\text{vol. } CO_2 \text{ in dry exhaust}) + Z\ (\text{vol. } CO_2 \text{ dry mixture} - \text{vol. } CO_2 \text{ dry exhaust})} \quad (28)$$

Substituting Equation (28) into (19) and simplifying:

$$f = \frac{[CO_2]_m\ (mw_e)}{[CO_2]_m\ (mw_e) + ([CO_2]_m - [CO_2]_e)\left(\frac{1\text{-}Z}{100}\right)\ (mw_c)}$$

where $[CO_2]_m$ = volume CO_2 in mixture sample
$[CO_2]_e$ = volume CO_2 in exhaust sample
mw_e = average molecular weight of exhaust
mw_c = average molecular weight of charge
Z = volume per cent water vapor in burned products

The Composition of Exhaust Gases from Diesel, Gasoline and Propane Powered Motor Coaches*

MARTIN A. ELLIOTT, GERGE J. NEBEL AND FRED G. ROUNDS
General Motors Research Laboratories
Detroit, Michigan

Air-pollution studies have shown that certain constituents in exhaust gases from automotive vehicles may react in the atmosphere to form smog-type pollutants. As a result, considerable effort has been made to determine the composition of these exhaust gases with particular emphasis on trace constituents, such as hydrocarbons and oxides of nitrogen. Most of this experimental work has been conducted on passenger cars with little similar work being done on motor coaches. However, there is considerable interest in the composition of motor coach exhaust gases on the part of manufacturers and operators. Their interest is caused by a desire to manufacture and operate equipment which contributes least to air pollution.

This report compares motor coaches powered by 2-cycle Diesel, gasoline, and propane engines with respect to their emission of objectionable exhaust gas constituents. The tests were made under road operating conditions typical of normal coach operation.

Constituents of Exhaust Gases From Internal Combustion Engines

The exhaust gases from internal combustion engines are complex mixtures consisting principally of the products of complete combustion, small amounts of the oxidation products of sulfur and nitrogen, and compounds derived from the fuel and lubricant. The major and minor constituents are listed in Table I.

In relation to air pollution, exhaust gas constituents may be divided into 3 classifications:

1. Harmful to health
2. Objectionable
3. Potentially objectionable

Certain constituents may be placed in more than one of the above classifications.

Some typical harmful exhaust gas constituents and their permissible concentration for a continuous 8-hour exposure are shown in Table II.

The objectionable constituents are either odorous or irritating, and include aldehydes and other compounds resulting from the partial oxidation or reaction of the fuel. The latter compounds may appear as smoke.

The potentially objectionable constituents are those materials which may react directly or indirectly to form irritating and lachrymating pollutants. Since it has been shown that certain hydrocarbons may react in the presence of oxides of nitrogen and ozone to form eye and nose irritants, hydrocarbons must be considered in this classification.

The subsequent discussion is limited to carbon monoxide, oxides of nitrogen, formaldehyde, and hydrocarbons since these compounds are believed to be of greatest importance to air pollution.

TABLE I
Constituents of Internal Combustion Engine Exhaust Gases

Major Constituents (greater than 1%)	Minor Constituents (less than 1%)
Water, H_2O	Oxides of sulfur, SO_2, SO_3
Carbon dioxide, CO_2	Oxides of nitrogen, NO, NO_2
Nitrogen, N_2	Aldehydes, HCHO, etc.
Oxygen, O_2	Organic acids, HCOOH, etc.
Carbon monoxide, CO[a]	Alcohols, CH_3OH, etc.
Hydrogen, H_2[a]	Hydrocarbons C_nH_m
	Carbon monoxide, CO[b]
	Hydrogen, H_2[b]
	Smoke

(a) Spark ignition engine
(b) Diesel engine

Experimental Procedure

Selection of Coaches

Three coaches of each engine type, 2-cycle Diesel, gasoline, and propane, were selected from the Chicago Transit Authority's operating fleet. The physical size and passenger capacity of the different model coaches were about the same. The selection of the individual coaches was made on the basis of the fuel and lubricating oil consumption being close to the average for their type. No engine adjustments were made prior to the tests. De-

TABLE II
Threshold Limits for Continuous 8-Hour Exposure[a]

Constitutent	Per Cent by Volume	Parts Per Million by Volume
Carbon dioxide	0.5	5000
Carbon monoxide	.010	100
Sulfur oxides (SO_2)	.0010	10
Formaldehyde	.0005	5
Nitrogen oxides	.0005	5

(a) Adopted by the American Conference of Governmental Industrial Hygienists, April 24, 1954.

*Presented at the 48th Annual Meeting of the Air Pollution Control Association, Detroit, Michigan, May 22-26, 1955.

TABLE III
Description of Coaches Tested

Coach Designation	Passenger Capacity	Engine Type	Compression Ratio of Engine	Engine Displacement, In^3	Range of Miles Since Last Major Overhaul
A, B, C,	45	Diesel (2-cycle)	16.0	426	126,000 to 217,000
D, E, F,	44	Gasoline	6.0	707	208,000 to 217,000
G, H, I	50	Propane	9.5	477	(a)

(a) These coaches were new and had operated 21,000 to 27,000 miles without overhaul.

scriptive information on the 3 types of coaches is shown in Table III.

Operating Conditions

Each coach was tested under idling conditions and while operating on city streets under accelerating, cruising, and decelerating conditions. The acceleration test was made at full throttle up a slight grade at speeds less than 15 mi./hr. The cruising test was made with the coach operating in direct drive on a level street at 30 mi./hr. The decelerating test was made with the coach operating in direct drive on a slight down grade at 25-30 mi./hr.

Sampling Procedures

Two samples of the exhaust gases were collected in evacuated 250 ml. sampling tubes for analysis by mass spectrometer and by Orsat apparatus. Duplicate samples for determination of the concentration of total oxides of nitrogen and formaldehyde were collected in evacuated 500 ml. bottles containing suitable absorbing solutions.

The exhaust gas was sampled upstream from the muffler and as near the exhaust manifold as possible. The exhaust gas flowed from the sampling point through copper tubing to the sampling manifold. (See Fig. 1.) The sampling line to the manifold was continuously purged by the normal flow of exhaust gas resulting from the back pressure in the exhaust system. When samples were taken, the discharge end of the manifold was closed to prevent contamination of the samples with air.

Samples were taken when the coach reached the desired operating condition. Approximately 2 to 5 sec. were required to fill the evacuated bottles.

Analytical Procedures

Samples were analyzed by the mass spectrometer primarily to determine the concentration of hydrocarbons, although the concentrations of the major constituents were also reported. Carbon dioxide, oxygen, and carbon monoxide were also determined by Orsat analysis. It is believed that the Orsat determinations of these 3 constituents, particularly carbon monoxide, are the more reliable and consequently were used in calculations.

Formaldehyde was determined by a modification of the phenylhydrazine-ferricyanide method described by Kersey, Maddock, and Johnson[1]. The total oxides of nitrogen (except N_2O) were determined by the phenol disulfonic acid method described by Beatty, Berger, and Schrenk[2]. Both are relatively sensitive colorimetric tests.

Exhaust-Gas Flow-Rate Measurement

In order to calculate the total quality of any exhaust-gas constituent discharged per unit time, it is necessary to know the exhaust gas flow rate as well as the concentration of the constituent. The direct measurement of the exhaust-gas flow rate of a moving vehicle is difficult. Accordingly, it seemed advisable to use a dilution metering technique. Helium was admitted to the air intake of the engine through a rotameter at a known rate just prior to and during the sampling period (Fig. 1.) The concentration of helium in the exhaust was determined by mass spectrometric analysis. Thus it was possible to calculate the exhaust-gas flow rate. Previous laboratory studies indicated that the addition of as much as 3% of helium had little or no effect on engine performance.

Experimental Results

The experimental results for the 3 coaches of each type have been averaged and, for simplicity, only these averages will be considered in the following discussion. Complete experimental data for each coach are presented at the end of the report in Tables VI, VII, VIII and IX.

For each of the 4 constituents, both the concentration in the exhaust gas and the total rate of emission are presented. Exhaust gas composition is useful for comparing the concentration of the harmful constituents with the permissible toxic limits. However, in relation to air pollution, the total quantity of an exhaust gas constituent discharged per unit time is most significant. If the total quantities of an exhaust gas constituent are known, comparisons of emission from vehicles in comparable service but powered by different types of engines can be made.

Carbon Monoxide

The concentration of carbon monoxide observed in the various tests is shown in Fig. 2. Under all driving condi-

(1) Kersey, R. W., Maddocks, J. R., and Johnson, T. E., "The Determination of Small Amounts of Formaldehyde in Air," *The Analyst, 65,* 203-06 (1940).

(2) Beatty, R. L., Berger, L. B., and Schrenk, H. H., "Determination of the Oxides of Nitrogen by the Phenoldisulfonic Acid Methods," Bureau of Mines, Report of Investigations No. *3687,* (1943).

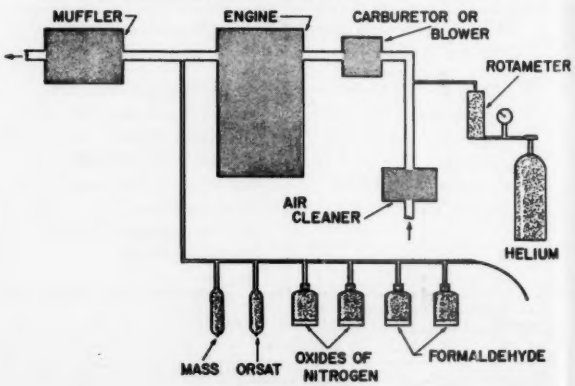

Fig. 1

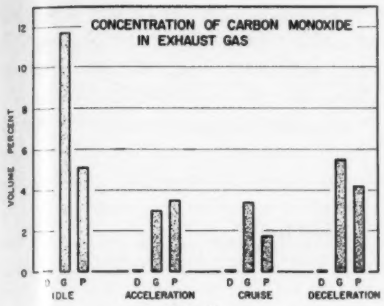

Fig. 2

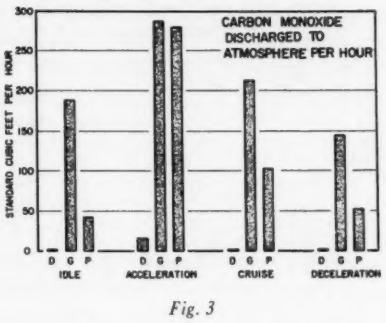

Fig. 3

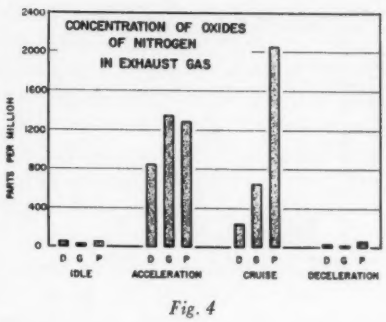

Fig. 4

tion the exhaust gases from Diesel engines contained less than 0.1% carbon monoxide, whereas the carbon monoxide concentrations in the exhausts of the carbureted engines ranged from 1.5 to 12%. The reason for this difference is the well-known fact that carbureted engines generally operate with a deficiency of air whereas Diesel engines always operate with a substantial excess of air. In these tests the concentration of carbon monoxide in the exhaust from the propane coaches was generally less than that from the gasoline coaches. Since the vehicles were tested with the carburetor adjustments "as received," no generalizations should be made from these tests concerning the relative merits of the gasoline and propane coaches.

The concentration of an exhaust-gas constituent alone is not indicative of the contribution of the constituent to the over-all air-pollution problem because of the wide variations in exhaust-gas flow rate with different engine types and different operating conditions. What is important is the amount of the constituent discharged per unit time. Fig. 3 shows the carbon monoxide emission expressed in standard cubic feet, at 60°F. and 1 atmosphere, per hour (scfh.) The average emission of carbon monoxide for the Diesel coaches was less than 15 scfh. under all driving conditions whereas the amount discharged by the carbureted engines ranged from about 40 to 290 scfh.

Oxides of Nitrogen

The concentrations of oxides of nitrogen observed in these tests for the various types of coaches and driving conditions are illustrated in Fig. 4. During cruise and acceleration, average oxides of nitrogen concentrations ranged from about 200 to 2000 ppm. but at idle and deceleration the concentrations were below 60 ppm. These observations are consistent with thermodynamic predictions that higher combustion chamber temperatures favor the formation of oxides of nitrogen.

Fig. 5 shows the emission of oxides of nitrogen. From 4 to 24 scfh. were discharged to the atmosphere during cruise and acceleration, whereas during idle and deceleration the amount discharged was less than 0.5 scfh. In these tests no one engine type consistently discharged more or less oxides of nitrogen than the other two types.

Formaldehyde

The concentration of formaldehyde shown in Fig. 6 is an indication of the amount of partially oxidized hydrocarbon in the exhaust. The average formaldehyde concentrations were less than 30 ppm. with the exception of the carbureted engines during deceleration. At that condition, the formaldehyde concentrations were appreciably higher, up to 300 ppm.

The amount of formaldehyde discharged to the atmosphere, illustrated in Fig. 7, ranged from 0.025 to 0.75 scfh. The deceleration driving condition was the most critical for the carbureted engines, whereas for the Diesel engines high emission rates were observed at both acceleration and deceleration.

Aldehydes have been used as a measure of the odor intensity of exhaust gases from a particular type of engine. It should not be inferred from this that aldehydes, especially formaldehyde, can be used as a criterion for the odor intensity of exhaust gases from different types of engines burning different fuels. A discussion of this subject is beyond the scope of this paper but this problem is being actively investigated in this laboratory.

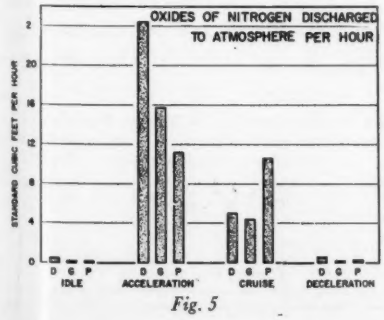

Fig. 5

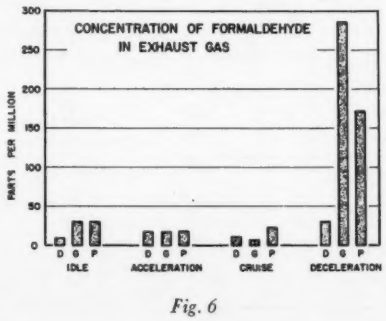

Fig. 6

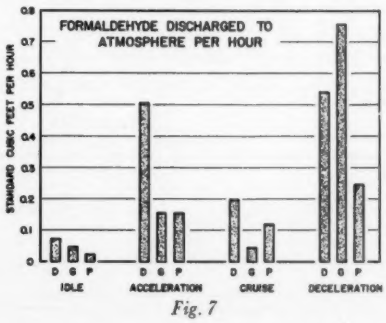

Fig. 7

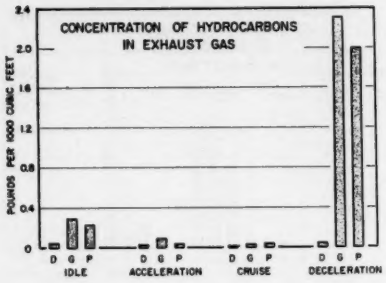

Fig. 8

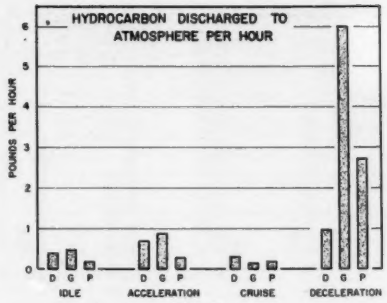

Fig. 9

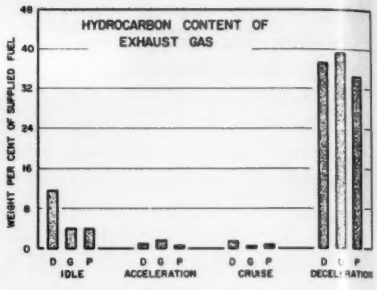

Fig. 10

Hydrocarbons

In the previous discussion, the concentration of the exhaust gas constituents has been expressed as per cent or ppm. by volume. For hydrocarbons, such a method of expressing concentration is not satisfactory for comparative purposes because the average molecular weight of the hydrocarbons in exhaust gas is not constant. A more satisfactory basis is to express the hydrocarbon concentration in terms of weight per unit volume of exhaust. Such data are illustrated in Fig. 8. The observed hydrocarbon concentrations ranged from less than 0.04 lb./Mft.^{3} of exhaust during cruise to more than 2.3 lb./Mft.^{3} of exhaust during deceleration. The similarity of the data for the carbureted engines in Fig. 6 and 8 suggests that the engine conditions giving rise to high hydrocarbon concentrations also favor the formation of formaldehyde.

Of more importance to the over-all air-pollution problem is the total amount of hydrocarbon discharged to the atmosphere per unit time. A comparison of the 3 different engine types at each driving condition is shown in Fig. 9. At deceleration, the carbureted engines discharged from 2.7 to 6 lb./hr. compared to 1 lb./hr. for the Diesel engines. For the other driving conditions there was little difference among the various engine types with emission rates ranging from 0.2 to 0.9 lb./hr.

The weight per cent of the supplied fuel present in the exhaust gases as C_1 to C_8 hydrocarbons is one indication of the combustion efficiency of the engine. The data in Fig. 10 show that for all types of engines less than 2% of the supplied fuel is wasted during cruise or acceleration, whereas more than 34% of the supplied fuel is wasted during deceleration. With the exception of the Diesel at idle, the various types of engines appear quite similar on this basis. However, the data in Fig. 9 show that the amount of hydrocarbons found in the exhaust of Diesel engines under decelerating conditions was smaller than that in carbureted engines and comparable at idle.

TABLE IV
Typical Motor Coach Driving Patterns

City	Per Cent of Time Spent at				
	Idle	Accel.	Cruise	Decel.	Stop
A	35	15	30	15	5
B	25	20	30	25	
C	30	15	40	15	

Discussion

Driving condition has a marked effect on the emission rate of all constituents. Furthermore, the relative order of the coaches was not the same at all driving conditions, except for carbon monoxide emission. Therefore, for the other constituents, it is necessary to take into account the time spent at each driving condition when comparing the coaches.

An indication of the importance of driving condition may be obtained from the following example. Consider two identical gasoline coaches operating either (a) at constant speed corresponding to the 30 mph. cruise condition, or (b) alternately accelerating and decelerating. While the carbon monoxide emission for the two coaches would be about the same, the emission of oxides of nitrogen from the cycling coach would be double, the formaldehyde emission 9 times, and the hydrocarbon emission 20 times that from the coach operating at constant speed.

Some typical city driving patterns for motor coaches are given in Table IV.

These driving patterns are based on rush-hour and off-hour operation in both downtown and residential areas. Their similarity suggests that comparisons of the different engine types based on one driving pattern are applicable to most city operation.

The total emission per hour of each constituent based on the City A driving pattern is shown in Table V.

These data show that the Diesel coaches produced substantially less carbon monoxide than either the propane or gasoline coaches. With respect to the other constituents, no such large differences were observed, and the relative rank of the different coaches was not consistent. For example, the gasoline coaches produced the least quantity of oxides of nitrogen; the propane coaches, the least formaldehyde; and the Diesel and propane coaches, the least hydrocarbons. At the other extreme, the pro-

TABLE V
Total Hourly Emission Based on City A Driving Pattern

	Carbon Monoxide SCFH	Oxides of Nitrogen SCFH	Formaldehyde SCFH	Hydrocarbons lb./hr.
Diesel	2	5.4	0.24	0.47
Gasoline	194	3.8	0.17	1.24
Propane	96	4.9	0.11	0.57

pane and Diesel coaches produced the greatest quantity of oxides of nitrogen; the Diesel coaches, the most formaldehyde; and the gasoline coaches, the most hydrocarbons.

The Diesel coaches were markedly superior with respect to carbon monoxide emission. There was comparatively little difference between coach types in the overall emission of the other constituents.

Summary

Exhaust-gas samples were obtained from Diesel, gasoline, and propane-powered motor coaches of similar passenger capacity under idling, accelerating, cruising, and decelerating driving conditions. The samples were analyzed for carbon monoxide, oxides of nitrogen, formaldehyde, and hydrocarbons. In addition, the exhaust-gas flow rates were measured to permit calculation of the emission rate for each constituent at each driving condition. Based on a typical city driving pattern, it was concluded that:

1. The carbon monoxide emission from the Diesel coaches was only a small fraction of that from the gasoline and propane coaches.
2. The differences observed in the emission of oxides of nitrogen, formaldehyde, and hydrocarbons by the 3 coach types were relatively small. No one coach type discharged either the greatest or least amounts of all of these 3 constituents.

Acknowledgments

The authors wish to express their appreciation to:

1. The Chicago Transit Authority of Chicago, Illinois, for their cooperation in conducting the tests.
2. Mr. D. V. Kniebes and co-workers of the Institute of Gas Technology for conducting the mass spectrometer analyses.
3. Messrs. J. T. Wentworth and W. A. Daniel for their assistance in running the tests.
4. The members of the Fuels and Lubricants Department, General Motors Research Laboratories, for their suggestions and criticisms during the preparation of the manuscript.

TABLE VI
Summary of Experimental Results at Idle

Vehicle	Engine Type	Exhaust Flow SCFM	Carbon Monoxide		Hydrocarbons				Oxides of Nitrogen		Formaldehyde	
			vol %	SCFH	vol %	lbs/SCF-10^6	% UBF	lbs/hr	P.P.M.	SCFH	P.P.M.	SCFH
A	Diesel	98	0.0	0	0.047	61.6	14.4	0.363	60	0.353	6	0.035
B	(2-cycle)	95	0.0	0	0.017	23.1	5.4	0.132	50	0.285	4	0.023
C		159	0.0	0	0.053	66.4	15.4	0.633	68	0.648	17	0.162
	Average		0.0	0	0.039	50.4	11.7	0.376	59	0.429	9	0.073
D	Gasoline	27	13.85	225	0.983	602	7.7	0.975	45	0.074	72	0.117
E		25	11.15	167	0.304	152	2.2	0.228	15	0.023	12	0.018
F		29	10.1	176	0.163	124	1.8	0.215	38	0.066	5	0.009
	Average		11.7	189	0.483	293	3.9	0.473	33	0.054	30	0.048
G	Propane	15	3.65	32.8	0.176	183	3.5	0.164	90	0.081	24	0.022
H		13	8.0	62.3	0.359	281	4.6	0.219	25	0.019	35	0.027
I		15	3.75	33.7	0.189	205	3.7	0.184	27	0.024	30	0.027
	Average		5.1	43.0	0.241	223	3.9	0.189	47	0.041	30	0.025

TABLE VII
Summary of Experimental Results at Acceleration

Vehicle	Engine Type	Exhaust Flow SCFM	Carbon Monoxide		Hydrocarbons				Oxides of Nitrogen		Formaldehyde	
			vol %	SCFH	vol %	lbs/SCF-10^6	% UBF	lbs/hr	P.P.M.	SCFH	P.P.M.	SCFH
A	Diesel	447	0.0	0	0.018	20.5	0.8	0.550	827	22.2	7	0.188
B	(2-cycle)	461	0.1	27.7	0.023	30.1	1.2	0.833	863	23.9	6	0.166
C		529	0.05	15.9	0.021	21.3	0.9	0.677	856	27.2	37	1.173
	Average		0.05	14.5	0.021	24.0	1.0	0.683	849	24.4	17	0.509
D	Gasoline	129[a]	2.8	217	0.202	174	3.0	1.345	1430	11.1	28	0.217
E		271	2.2	357	0.051	66.2	1.2	1.08	1940	31.5	13	0.211
F		123[a]	3.9	288	0.036	32.5	0.6	0.240	670	4.9	6	0.044
	Average		3.0	287	0.096	90.9	1.6	0.888	1347	15.8	16	0.157
G	Propane	165	2.7	267	0.024	21.0	0.4	0.208	2215	21.9	25	0.247
H		112	3.05	205	0.040	38.6	0.7	0.260	1130	7.6	13	0.087
I		127	4.8	369	0.052	48.1	0.8	0.369	524	4.0	17	0.138
	Average		3.5	280	0.039	35.9	0.6	0.279	1290	11.2	18	0.157

[a] Not full throttle acceleration.

TABLE VIII
Summary of Experimental Results at Cruise

Vehicle	Engine Type	Exhaust Flow SCFM	Carbon Monoxide		Hydrocarbons				Oxides of Nitrogen		Formaldehyde	
			vol %	SCFH	vol %	lbs/SCF-10[6]	% UBF	lbs/hr	P.P.M.	SCFH	P.P.M.	SCFH
A	Diesel	395	0.0	0	0.013	20.2	1.3	0.478	310	7.35	4	0.095
B	(2-cycle)	279	0.0	0	0.000	0	0.0	0.000	224	3.73	19	0.318
C		360	0.0	0	0.015	19.6	2.2	0.423	178	3.85	9	0.195
	Average		0.0	0	0.009	13.3	1.2	0.300	237	4.98	11	0.203
D	Gasoline	93	5.1	285	0.045	36.1	0.6	0.202	314	1.76	1	0.005
E		114	2.35	161	.....	.....	....	.....	740	5.06	15	0.096
F		117	2.7	189	0.018	12.5	0.2	0.088	906	6.36	6	0.042
	Average		3.4	212	0.032	24.3	0.4	0.145	653	4.39	7	0.048
G	Propane	85	0.85	43.3	0.037	51.9	1.0	0.264	3050	15.5	39	0.198
H		85	1.0	51.0	0.026	25.3	0.5	0.129	2150	10.4	15	0.077
I		105	3.4	214	0.037	30.5	0.5	0.192	956	6.0	14	0.094
	Average		1.75	103	0.033	35.9	0.7	0.195	2052	10.6	23	0.123

TABLE IX
Summary of Experimental Results at Deceleration

Vehicle	Engine Type	Exhaust Flow SCFM	Carbon Monoxide		Hydrocarbons				Oxides of Nitrogen		Formaldehyde	
			vol %	SCFH	vol %	lbs/SCF-10[6]	% UBF	lbs/hr	P.P.M.	SCFH	P.P.M.	SCFH
A	Diesel	350	0.0	0	0.061	95.2	72.7	2.00	40	0.840	7	0.147
B	(2-cycle)	238	0.0	0	0.000	0	0.0	0	42	0.600	10	0.143
C		318	0.0	0	0.038	45.7	38.7	0.87	9	0.171	70	1.335
	Average		0.0	0	0.033	43.6	37.1	0.96	30	0.537	29	0.541
D	Gasoline	46	4.8	132	2.641	4170	60.7	11.52	12	0.033	244	0.675
E		36	6.25	135	1.844	2110	39.7	4.51	12	0.026	303	0.658
F		50	5.5	165	0.541	637	17.4	1.92	30	0.090	312	0.936
	Average		5.5	144	1.675	2306	39.3	5.98	18	0.050	286	0.756
G	Propane	18	3.2	34.6	1.734	1895	34.6	2.05	77	0.083	154	0.167
H		18	5.3	57.2	2.475	2560	41.3	2.77	15	0.016	193	0.208
I		36	3.0	64.7	1.500	1530	27.1	3.31	77	0.166	169	0.365
	Average		4.2	52.2	1.903	1995	34.3	2.71	56	0.095	172	0.247

(Continued from page 70)

Engine Variables and Their Effects

paper resulted from testing and analytical procedures still in the development stage, and are thus subject to larger-than-normal degrees of error. In addition, the substantial reductions in hydrocarbon emission during deceleration were achieved with experimental devices which must yet be thoroughly developed and proved before they can be considered ready for production release.

Acknowledgment

The authors would like to express their gratitude to Messrs. F. E. Carr and R. R. Crandall for their assistance in the preparation of this paper.

Some Effects of Engine-Fuel Variables on Exhaust Gas Hydrocarbon Content*

F. G. Rounds, P. A. Bennett, and G. J. Nebel
Research Laboratories Division
General Motors Corporation
Detroit, Michigan

Since the twenties it has been known that automotive engine exhaust gases contain hydrocarbons[1-2], but the amount has been generally considered too small to be of practical concern. However, recent reports[3-4-5] indicate that the amount of hydrocarbons present in exhaust gases under some driving conditions may be significant.

The presence of hydrocarbons in engine exhaust is of interest to the automotive industry for two reasons. The first is air pollution, and particularly the type known as smog encountered in the Los Angeles area. Although no one knows exactly what smog is or how it is formed, some investigators[6-7-8] agree that hydrocarbons (particularly olefins), nitrogen oxides, and ozone are important in the mechanism of smog formation.

The second reason for this interest is fuel conservation. The miles per gallon to be gained by utilizing the chemical energy of exhaust gas hydrocarbons would be small and difficult for the average motorist to detect. However, the nation's gasoline consumption is approaching 3,500,000 barrels each day, and even a small percentage loss of hydrocarbons in the exhaust gases represents a tremendous waste of fuel.

The present investigation was undertaken to obtain a better understanding of the factors influencing the concentration of hydrocarbons in engine exhaust. Initially, tests were made to determine the fraction of the total fuel supplied to the engine which appeared as hydrocarbons in the exhaust at different driving conditions. Later, more exhaustive tests were made to determine the effect of common engine-fuel variables at each driving condition.

The data presented in this paper are based on mass spectrometer and/or Orsat analyses of exhaust gas samples obtained from 163 passenger cars and 8 public transit buses. The test results suggest some practical methods of reducing hydrocarbon losses from motor vehicles.

Test Equipment and Procedure

All 5 makes of General Motors passenger cars, predominantly 1953 models, were tested. The cars were equipped with V-8, 6 cylinder, or line 8 engines, and either standard or automatic transmissions. Of the 163 passenger cars used in this investigation, 11 were test cars and the remainder customer-owned. All the customer-owned cars were tested in the "as received" condition. Exhaust gas samples were also collected from 8 motor coaches used in public transit service. These commercial vehicles were equipped with either Diesel, gasoline, or LPG engines.

Previous investigators have usually divided vehicle operation into 4 driving conditions: idle, acceleration, cruising, and deceleration. Idle and cruising are essentially steady state conditions whereas acceleration and deceleration are not. Since it is very difficult to make quantitative determinations during unsteady state operation, special test procedures were adopted in the passenger car studies to simulate normal acceleration and deceleration. These operating conditions are described below:

1. *Idle*
   Idle is operation of the engine at no load with the vehicle stationary. The idle speed of 6 test cars was arbitrarily held constant at 400 rpm. A total of 152 customer-owned cars were tested.
2. *Part Throttle*
   This condition includes all engine operation at power output equal to or greater than road load. Thus both normal cruising and acceleration are included in this "part throttle" condition. To eliminate transient effects, all tests were run at constant engine speeds of 1000 rpm. or greater. For this phase of the investigation, 7 test cars were used.
3. *Simulated Deceleration*
   Deceleration is characterized by high intake-manifold

(1) Fieldner, A. C., and Jones, G. W., "The Sampling and Analysis of Automobile Exhaust Gas," *Franklin Inst. Journal, 194* (No. 5), 613-44 (1922).
(2) D'Alleva, B. A., and Lovell, W. G., "Relation of Exhaust Gas Composition to Air-Fuel Ratio," *SAE Journal Transactions, 38* (No. 3) 90-96T (1936).
(3) Magill, P. L., Hutchison, D. H., and Stormes, J. H., "Hydrocarbon Constituents of Automobile Exhaust Gases," *Second National Air Pollution Symposium,* 1952, p. 71.
(4) Viets, F. H., Fischer, G. I., and Fudurich, A. P., "Hydrocarbon Pollution From Automobile Exhaust Gas, a Report of Test 668 and Associated Work," Air Pollution Control District, County of Los Angeles, September 12, 1952.
(5) "Automotive Exhaust Testing Procedures and Efficiency Studies in the Evaluation of a Catalytic Muffler," *Los Angeles County Air Pollution Control District Publication No. 51,* July 30, 1954.
(6) Haagen-Smit, A. J., "Chemistry and Physiology of Los Angeles Smog," *Ind. Eng. Chem., 44,* 1342-46 (1952).
(7) Magill, P. L., and Benoliel, R. W., "Air Pollution Studies in Los Angeles County," *Ind. Eng. Chem., 44,* 1347-51 (1952).
(8) Mader, P. P., McPhee, R. D. Loftberg, R. T., and Larson, G. P., "Composition of Organic Portion of Atmospheric Aerosols in the Los Angeles Area," *Ind. Eng. Chem. 44,* 1352-55 (1952).

*Presented at the Annual Meeting of the Society of Automotive Engineers at Detroit, Michigan, January 10-14, 1955.

vacuums and decreasing engine speeds. Simulated deceleration data were obtained at constant engine conditions corresponding to those existing momentarily during normal deceleration. These conditions were established by allowing the vehicle to coast downhill at constant speed with closed throttle. It is believed that the data obtained under these simulated conditions are representative of those occurring during normal deceleration, where engine conditions are continually changing. In this work 5 test cars were operated at constant engine speeds of 1000 and 2000 rpm., whereas 33 customer-owned cars were operated in "drive" or highest gear at a fixed car speed of 30 mi./hr.

The test procedures for the commercial vehicles were somewhat different from those described above. The usual driving conditions of idle, cruising, acceleration, and deceleration were studied. The cruising tests were carried out at 25 mph. in high gear, the acceleration tests between 10 and 15 mph. in low gear at full throttle, and the deceleration tests beginning at 20 mph.

During this investigation, exhaust gas samples were collected in evacuated 250 or 500 ml. Pyrex bottles from a copper sampling line. In test cars, this sampling line was tapped into the exhaust system just ahead of the muffler. In customer-owned vehicles, the sampling line was pushed up the tailpipe as far as possible. Regardless of the sampling point, the exhaust gas flow rate was maintained great enough to prevent condensation in the sampling line. The containers were thoroughly cleaned prior to each use to prevent contamination. Stopcocks and rubber tubing were eliminated from the sampling system to prevent possible loss of hydrocarbons by adsorption.

The exhaust gas samples were analyzed on a Consolidated Engineering Corporation analytical mass spectrometer. The analyses were performed under contract by the Institute of Gas Technology in Chicago, Illinois. This method of analysis was selected since the mass spectrometer is capable of measuring the concentration of a large number of individual hydrocarbons. However, the mass spectrometer does have limitations that should be recognized. These are discussed in Appendix A. As a result of these limitations, the accuracy of the mass spectrometer exhaust gas analyses remains somewhat in doubt. The reported percentages of unburned hydrocarbons are believed to be no more accurate than ± 1% by weight of the supplied fuel. In spite of this, the trends shown in this paper are believed to be valid.

TABLE I
Exhaust Gas
Hydrocarbon Content Ranges

Test Condition	Hydrocarbon Content Weight Per Cent of Supplied Fuel
Idle	1 to 28
Part Throttle	1 to 5
Simulated Deceleration	1 to 63

Passenger Car Tests

The ranges of exhaust gas hydrocarbon contents observed at idle, part throttle, and simulated deceleration for the 5 makes of passenger cars investigated are shown in Table I. The hydrocarbon content is expressed as the weight per cent of the fuel supplied to the engine, a convention that will be used throughout this paper. The detected hydrocarbons included paraffins, olefins, aromatics, and naphthenes ranging from C_1 to C_9. No oxygenated products were reported. The weight per cent values were calculated from mass spectrometer analyses using a carbon balance. A typical calculation is shown in Appendix B.

There are two features in Table I of particular interest to the automotive engineer. First, the hydrocarbon content is markedly affected by driving conditions. Secondly, at any one driving condition, the hydrocarbon content may vary considerably. This latter observation points out the need for testing a large number of vehicles if significant "averages" are to be obtained. It also suggests that a reduction in the hydrocarbon losses may be possible once the factors responsible for this variation are known.

Idle

Fuel Type: Since the resistance of individual hydro-

TABLE II
Effect of Fuel Type on Exhaust Gas Hydrocarbon Content at Idle
Mixture Ratio — 80% of Theoretical Air

Fuel	Type	Critical Comp. Ratio	Hydrocarbon Content Weight Per Cent of Supplied Fuel	
			Total Hydrocarbons	Unreacted Fuel
n-Pentane	Paraffin	4.0	5.4	1.1
Premium Gasoline	Mixed	6.4	5.3	....
Isooctane	Paraffin	7.3	5.1	1.3
100 O.N. Gasoline	Mixed	.....	5.7	....
Diisobutylene	Olefin	12.0	6.1	0.8
Cyclopentane	Naphthene	12.4	5.9	1.7
Triptane	Paraffin	14.4	5.0	1.3
Benzene	Aromatic	14.0+	2.7	1.2

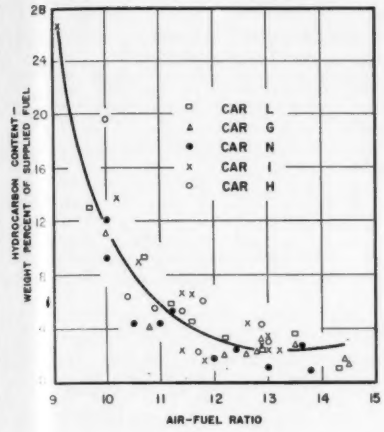

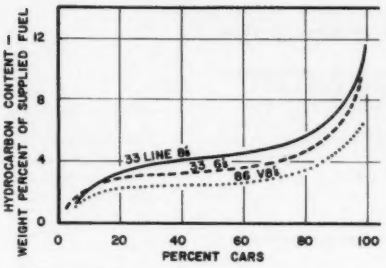

Fig. 2. Effect of engine type on exhaust gas hydrocarbon content at idle.

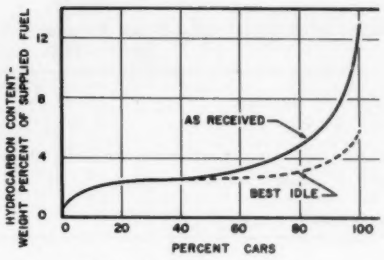

Fig. 3. Effect of idle mixture adjustment on hydrocarbon content.

Fig. 1. Effect of air-fuel ratio on exhaust gas hydrocarbon content at idle.

carbons to oxidaiton varies with molecular structure, it has been suggested that fuel type might influence the hydrocarbon content of exhaust gas. This is a very important consideration from the petroleum refiners' standpoint because higher octane fuels are inherently more resistant to oxidation and thus might be expected to burn less completely. To determine the importance of fuel type, a 1953 model car was operated at idle with several pure hydrocarbons and two gasolines. The results are shown in Table II where the fuels are listed in order of increasing critical compression ratio.

For 7 of the 8 fuels tested, fuel type had little or no effect either on the total hydrocarbon content in the exhaust or on the amount of unreacted fuel. For benzene, however, the total hydrocarbon content was about half that observed with the other fuels even though the amount of unreacted fuel was about the same. These results suggest that the exhaust gas hydrocarbon content at idle does not correlate with the oxidation resistance of the fuel as measured by the critical compression ratio.

Air-Fuel Ratio: Fig. 1 shows the results of idle tests in which the mixture ratio of test cars was varied over the range for miss-free operation. Additional data from 26 customer-owned cars in the "as received" condition are also included. The idle speed of each test car was set at 400 rpm., whereas the idle speeds of the customer-owned cars were found to vary from 280 to 680 rpm. Manifold vacuums varied from 16 to 20 in. of mercury. Although manifold vacuum and engine speed were not comparable in all tests, it appears that the most important variable causing the large effect on exhaust gas hydrocarbon content at idle was air-fuel ratio.

It has been observed that the mixture ratio range for miss-free idle operation varied with engine design. Since the mixture ratio range for the best idle operation generally corresponds to the "maximum power" air-fuel ratio, the data illustrated in Fig. 1 indicate that the lowest exhaust gas hydrocarbon content would also occur at the best idle mixture ratios. To determine how many cars in service are actually operating in the best idle range for the particular engine design, idle air-fuel ratios of 152 customer-owned cars were measured "as received." The hydrocarbon content for each customer car was estimated from Fig. 1. Cumulative distribution curves showing these estimates for 3 basic engine designs are plotted in Fig. 2. These data indicate that the exhaust gas hydrocarbon content of the compact V-8 engines was less than that for either the line 6's or the line 8's. This results from the fact that the V-8 engines will idle acceptably at leaner air-fuel ratios. In addition, it has been observed that L-head engines require somewhat richer mixtures for satisfactory idle than comparable overhead valve engines. These observations indicate that the current trend in automotive design towards overhead valve V-8 engines should result in a reduction in the total hydrocarbon lost during idle operation.

Weighting the data for the 152 customer-owned cars on the basis of 1953 production figures, a single cumulative distribution curve was obtained. The result is shown in Fig. 3 by the solid curve labeled "as received." Assuming equal idle fuel rates for all cars, the average exhaust gas hydrocarbon content at idle was calculated to be 4% by weight of the fuel supplied to the engine.

The idle mixture ratios of a few of the customer cars were found to be as rich as 10 to 1, whereas other cars of the same make and model were found to be set as lean as 14 to 1. Since the exhaust gases from the cars running on the rich mixtures contain appreciably higher hydrocarbon contents than those operating on mixtures in the "best idle" range, it would appear that an appreciable reduction in hydrocarbon emission could be achieved by proper maintenance. If the mixture ratio for each car were adjusted to the best idle range, the distribution curve in Fig. 3 would be changed to that shown by the dashed curve. Assuming equal idle fuel consumption rates for all cars, these adjustments would result in a calculated 30% reduction in the total idle hydrocarbon emission. Thus the motorist himself can help to reduce hydrocarbon emission by keeping his motor properly tuned. At the same time he will benefit from improved engine operation.

TABLE III
Effect of Engine Load On the Exhaust Gas Hydrocarbon Content
Car I — 1000 rpm.

Manifold Vacuum, In. Hg.	Hydrocarbon Content Weight Per Cent of Supplied Fuel
0.2 (Full Throttle)	1.4
8.0	1.6
18.0 (Road Load)	1.5

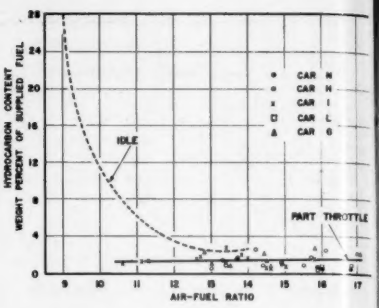

Fig. 4. Effect of air-fuel ratio on exhaust gas hydrocarbon content at part throttle.

Part Throttle

Engine Load: The "part throttle" operating condition has been defined as all engine operation at power output equal to or greater than road load. Thus all engine loads from road load to full throttle are included. To determine the effect of engine load, data such as that listed in Table III were obtained. The results of these and other tests indicate little or no effect of engine load on exhaust gas hydrocarbon content.

Fuel Type: To determine the effect of fuel type upon the exhaust gas hydrocarbon content at part throttle, a 1952 model car and a laboratory single cylinder engine were operated on several pure hydrocarbons, two leaded isooctane blends, and a commercial gasoline. The results are tabulated in Table IV where the fuels are arranged in order of increasing critical compression ratio.

The data in Table IV indicate that neither fuel type nor the presence of tetraethyllead has any significant effect on the exhaust gas hydrocarbon content.

Air-Fuel Ratio: Since air-fuel ratio was found to influence the hydrocarbon content at idle, the effect of this variable was investigated at part throttle. The results of 40 tests of 5 different makes of cars are shown in Fig. 4. The range of air-fuel ratios investigated corresponds roughly to those occurring in normal passenger car operation. For comparison, the effect of air-fuel ratio at idle previously shown in Fig. 1 has been reproduced in Fig. 4 as the dashed curve. Contrary to the experience at idle, air-fuel ratio has no significant effect on the exhaust gas hydrocarbon content at part throttle. Included in these tests were cars with engines of all types which suggests the engine design has little effect on hydrocarbon content under these test conditions.

Engine Speed: To study the effect of engine speed, tests were made employing 3 different makes of cars as well as a single-cylinder laboratory engine. The results of these tests covering the speed range from 1000 to 3000 rpm. are shown in Fig. 5. Although there are some minor variations among different engines and duplicate tests on the same engine, it is apparent that a three-fold increase in engine speed has essentially no effect on the exhaust gas hydrocarbon content at speeds above 1000 rpm.

Compression Ratio: It is well known that the thermal efficiency of an engine increases as the compression ratio is raised. Although this gain is usually explained on the basis of thermodynamic considerations, it was speculated that part of the increased efficiency might result from more complete combustion at higher compression ratios. To check this possibility tests were conducted on a variable compression ratio single-cylinder engine. The results are given in Table V.

These data indicate that compression ratio has little or no effect on the exhaust gas hydrocarbon content.

TABLE IV
Effect of Fuel Type on the Exhaust Gas Hydrocarbon Content at Part Throttle
Maximum Power Mixture Ratio

Fuel	Type	Critical Comp. Ratio	Hydrocarbon Content Weight Per Cent of Supplied Fuel	
			Car I 1000 rpm. Road Load	Laboratory Engine 1000 rpm. Full Throttle
n-Pentane	Paraffin	4.0	2.4	
Cyclohexane	Naphthene	4.9	1.9	
Premium Gasoline	Mixed	6.4	1.8	2.8
Isooctane	Paraffin	7.3	2.8	2.5
Isooctane plus 1 cc. TEL	Paraffin	9.6		2.8
Isooctane plus 2.5 cc. TEL	Paraffin	11.0	2.6	
Diisobutylene	Olefin	12.0	2.3	2.5
Cyclopentane	Naphthene	12.4	2.4	3.0
Triptane	Paraffin	14.4	1.7	2.3
Benzene	Aromatic	14.0+	1.9	2.1

TABLE V

Effect of Compression Ratio On The Exhaust Gas Hydrocarbon Content 1000 rpm. — Maximum Power Mixture Ratio

Compression Ratio	Hydrocarbon Content Weight Per Cent of Supplied Fuel
4.0	2.2
8.0	2.3
12.0	1.9

The fuel used in these tests, triptane, was selected to permit knock-free operation over the range of compression ratios investigated. Subsequent tests have shown, however, that neither heavy knock nor objectionable preignition influence the hydrocarbon content.

Coolant Temperature: It has been theorized that hydrocarbons are present in exhaust gases because the fuel-air mixture immediately adjacent to the combustion chamber walls is either too cool to burn or that the wall destroys certain active radicals necessary for flame propagation. If this were a temperature effect, one would expect the thickness of this layer of unburned gases and, thus, the hydrocarbon content of the exhaust, to depend upon the wall temperature and indirectly on the coolant temperature. This theory was investigated both in road tests and in single-cylinder laboratory engine tests. In the road tests, exhaust gas samples were collected from a car soon after starting and again after thorough warm-up. In the laboratory engine tests, the coolant temperature was regulated by suitable refrigeration. The results of these tests are shown in Table VI.

The car data show somewhat higher hydrocarbon contents immediately after starting than after warm-up. The single-cylinder engine tests, on the other hand, which were conducted under more carefully controlled conditions indicated little or no effect on the hydrocarbon content as the coolant temperature was reduced. Data shown previously would seem to indicate that the difference between the car and the single-cylinder engine results

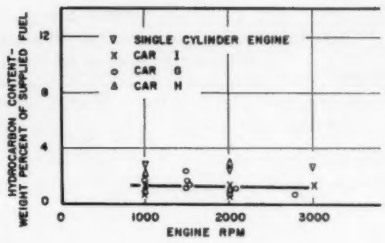

Fig. 5. Effect of engine speed on exhaust gas hydrocarbon content at part throttle.

is not due to a difference in either the fuel or the mixture ratios employed. However, the high values observed in the car tests may have been caused by rich mixtures exceeding the inflammability limit in some cylinders of the multi-cylinder engine.

None of the engine-fuel variables investigated had any significant effect on the exhaust gas hydrocarbon content at part throttle. Thus, on the basis of present knowledge, there seems very little that the engine designer can do to reduce the hydrocarbon emission at this driving condition. The average hydrocarbon content observed at part throttle was about 1.5% by weight of the fuel supplied to the engine.

Simulated Deceleration

Manifold Vacuum: Simulated deceleration tests were carried out by coasting downhill at various constant engine speeds at closed throttle. The results of these tests as well as some part throttle tests are illustrated in Fig. 6 for the 5 makes of cars investigated. The hydrocarbon content was found to be independent of manifold vacuum below 21 in. of mercury. However, at higher vacuums, the hydrocarbon content increased very rapidly. There was no abrupt change in the observed air-fuel ratios corresponding to this rapid increase in hydrocarbon content. Flame photography studies by Wentworth and Daniel[9] have shown that these high hydrocarbon contents at high manifold vacuums are due to the failure of the flame to propagate throughout the combustion chamber.

[9] Wentworth, J. T., and Daniel, W. A., "Flame Photographs of Light-Load Combustion Point the Way to Reduction of Hydrocarbons in Exhaust Gas," J. Air Poll. Control Assoc., *5*, (1955).

TABLE VI

Effect of Coolant Temperature On The Exhaust Gas Hydrocarbon Content Engine Speed — 1000 rpm.

Engine	Manifold Vacuum In. Hg.	Air-Fuel Ratio	Fuel	Temp. °F. Coolant	Oil	Hydrocarbon Content, Wt. Per Cent of Supplied Fuel
Car I	13	10.5	Premium Gas.	70	50	5.2
Car I	17.5	13.8	Premium Gas.	215	190	2.1
Car I	0.7	11.0	Premium Gas.	80	112	3.9
Car I	0.2	12.7	Premium Gas.	204	190	1.8
Single-Cylinder	10.1	9.3	Isooctane	9	86	2.3
Single-Cylinder	9.9	10.6	Isooctane	16	93	1.6
Single-Cylinder	9.9	14.2	Isooctane	49	94	1.4
Single-Cylinder	9.6	14.1	Isooctane	103	185	1.2
Single-Cylinder	10.0	16.0	Isooctane	149	182	1.1

TABLE VII
Effect Of Engine Speed On The Manifold Vacuum During Simulated Deceleration at Closed Throttle

Test Car Make	Manifold Vacuum, In. Hg.	
	1000 rpm.	2000 rpm.
L	22.1	24.0
G	22.3	23.8
N	21.8	23.8
I	23.2	24.2
H	24.0	25.0

The test car data shown in Fig. 6 were obtained at intake manifold vacuums from 19 to 24 in. of mercury at both 1000 and 2000 rpm. The engine speed and manifold vacuums of the customer-owned cars were those corresponding to 30 mph., closed throttle. The data seem to indicate that neither engine speed nor car make had any effect on hydrocarbon content at any given manifold vacuum. Fig. 6 is very useful because it permits a reasonable estimation of the exhaust gas hydrocarbon content to be made for any make or model of car if the manifold vacuum is known.

Engine Speed: The manifold vacuum at closed throttle is dependent upon the engine speed as shown in Table VII.

Since the manifold vacuum at 2000 rpm. was 1 to 2 in. of mercury greater than at 1000 rpm. for all cars, and since all the observed manifold vacuums were greater than 21 in. of mercury, much higher hydrocarbon contents were observed at the higher engine speed. Thus, engine speed affects the exhaust gas hydrocarbon content as a result of its effect on manifold vacuum.

The manifold vacuum at a fixed engine speed varied from one car to another. Although the cars listed in Table VII were each of a different make, similar variations have been observed among cars of the same make. These differences are believed to be the result of variations in the idle speed adjustment and the general mechanical condition of the engine.

Customer Car Survey: The manifold vacuums of a group of 33 customer-owned cars were measured at a constant speed of 30 mph. coasting down hill with closed throttle. With the aid of Fig. 6, the exhaust gas hydrocarbon content of each vehicle was estimated. Grouping the results on the basis of transmission type, or vehicle-

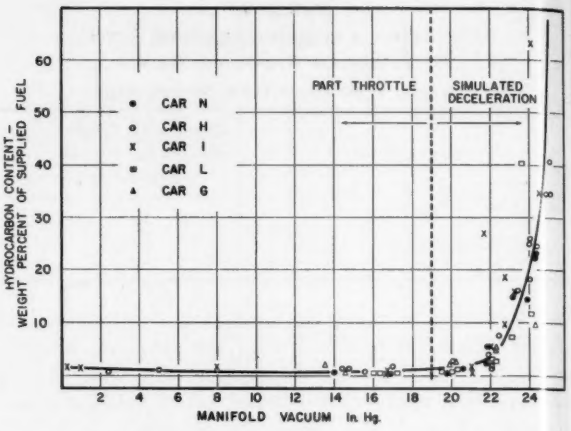

Fig. 6. Effect of intake manifold vacuum on exhaust gas hydrocarbon content.

model-year, shows some interesting effects of recent automotive design trends.

The effect of the transmission type used in the vehicle on the engine speed and thus the manifold vacuum and exhaust gas hydrocarbon content during deceleration is shown by the data in Table VIII.

The average engine speed and thus the average manifold vacuum of the cars equipped with standard transmissions was higher than that of the cars equipped with automatic transmissions. This was due primarily to differences in axle ratios and to the occurrence of some slip in the automatic transmissions. Thus the use of automatic transmissions, which are becoming increasingly popular with the motorist, should result in lower exhaust gas hydrocarbon contents during deceleration.

To point out the effect of other recent design changes, a comparison between 1950-51 and 1953-54 cars is shown in Table IX. For each car in the "old" group, which included 3 makes of cars and 3 transmission types, there was a corresponding car (same make and transmission type) in the "new" group.

At a constant car speed, lower engine speeds and lower manifold vacuums were generally observed with the newer cars. As a result, the average hydrocarbon content was also lower. Although only a limited number of cars were included in this comparison, the data suggest that the improvement shown was made possible largely because

TABLE VIII
Effect of Transmission Type on Estimated Exhaust Gas Hydrocarbon Content During Simulated Deceleration
Car Speed — 30 mph.

Transmission Type	Number of Cars Tested	Average Engine Speed, rpm.	Average Manifold Vacuum In. Hg.	Estimated Hydrocarbon Content, Weight Per Cent of Supplied Fuel
Standard	10	1405	24.0	22
Automatic:				
4 Speed Gear Type	15	1130	23.5	17
Torque Converter Type	8	1075	22.2	7

TABLE IX
Effect of Model Change on Hydrocarbon Content During Simulated Deceleration
Car Speed — 30 mph.

	1950-1951 Models	1953-1954 Models
Number of Cars Tested	7	7
Average Axle Ratio	3.82	3.54
Average Engine Speed, rpm.	1335	1225
Average Manifold Vacuum, In. Hg.	24	23
Estimated Hydrocarbon Content, Weight Per Cent of Supplied Fuel	20.6	13.3

modern high-output engines and improved transmissions permitted the use of lower rear axle ratios.

Since engine speed and manifold vacuum decrease during normal deceleration, the hydrocarbon content of the exhaust gases changes continuously. Therefore, it is impossible to determine a significant "average" hydrocarbon content unless all the exhaust products are collected or a continuous sampling procedure is used. The practical application of these methods is very difficult, particularly since many cars should be tested under many different conditions if a truly significant deceleration average is to be obtained. However, an approximate figure is easily obtained from the present simulated deceleration tests since the tests were carried out under steady state conditions. The speed, 30 mph., was selected because it is typical of city traffic conditions. The average so obtained, weighted for 1953 car and transmission production figures, was 12.5% by weight of the supplied fuel.

Comparison With Other Work

A comparison of the results of the present work with similar data obtained by other investigators is made in Table X. All the hydrocarbon contents have been expressed as weight per cent of the supplied fuel and were calculated from the data of the various investigators.

Each investigator reported the highest hydrocarbon contents at deceleration, the next highest at idle, and the lowest at cruising and acceleration. However, the actual values reported by each differed considerably in some cases. This is not surprising since different cars, different numbers of cars, different test procedures, and different analytical techniques were employed. The lowest hydrocarbon contents during deceleration and idle were reported in the present work. This may be due in part to the fact that the majority of the cars used in this investigation were 1953 or 1954 models rather than the older models used by the other investigators.

Commercial Vehicles

Even though gasoline-powered cars, trucks, and buses by far outnumber all other types, the use of Diesel and LPG powered vehicles in commercial service has grown considerably in recent years. Since there has been considerable discussion of the relative merits of the different engine types in air-pollution-conscious communities, information showing the hydrocarbon content from Diesel, LPG, and gasoline engines is of interest to both fleet operators and vehicle manufacturers.

A group of public transit coaches, consisting of 2 Diesel, 2 gasoline, and 4 LPG powered vehicles, were used for this investigation. However, instead of the steady state part throttle and simulated deceleration tests employed in the passenger car work, unsteady state acceleration and deceleration as well as cruising conditions typical of bus service were used. The results of the idle, cruising, and acceleration tests are shown in Table XI. It should be pointed out that Diesel fuels contain hydrocarbons in the C_{10} to C_{20} range whereas the mass spectrometer used for the analyses could not detect hydrocarbons heavier than about C_9. For this reason the results for the Diesel vehicles may be somewhat low.

The effect of driving conditions was similar to that observed in the passenger car tests. That is, higher hydrocarbon contents were observed during idle than at cruising and acceleration. Also, the similarity of the data for both cruising and acceleration indicates that all engine operation at power output equal to or greater than road load may be combined as was done with the passenger car tests. In general, the hydrocarbon contents listed in Table XI for each driving condition fall within the ranges observed during the passenger car tests.

The exhaust gas hydrocarbon content during deceleration for the 8 coaches is shown in Table XII. The hydro-

TABLE X
Average Exhaust Gas Hydrocarbon Content in Weight Per Cent of Supplied Fuel

Driving Condition	McGill, Hutchison, and Stormes[3]	Viets, Fischer, and Fudurich[4]	Los Angeles County Report No. 51[5]	Present Work
Idle	10.7	11.6(a)	5.7(b)	4.0
Acceleration	6.0	1.1(a)	1.8(b)	
Cruising	5.7	1.1(a)	1.7(b)	1.5(c)
Deceleration	19.2	16.3(a)	29.7(b)	12.5(c)
Cars Tested	10	1	1	7 to 152(d)

(a) Observed values, estimated by Viets, et.al., to be 25% low.
(b) All hydrocarbons assumed to be hexane or acetylene.
(c) Simulated deceleration and part throttle tests.
(d) Based on mass spectrometer and/or Orsat analyses as follows: idle, 152 cars; part throttle, 7 cars; and simulated deceleration, 33 cars.

TABLE XI
Comparison of Exhaust Gas Hydrocarbon Content of Diesel, Gasoline, and LPG Powered Vehicles

Vehicle Type	Hydrocarbon Content — Weight Per Cent of Supplied Fuel							
	Diesel Coaches		Gasoline Coaches		LPG Coaches			
Number	1	2	3	4	5	6	7	8
Driving Condition								
Idle	6.8	15.9	2.0	1.5	1.8	2.9	5.1	3.2
Cruising	1.1	2.6	0.5	0.7	0.9	1.2	0.4	0.6
Acceleration	0.5	1.0	0.4	1.1	0.7	1.3	0.4	0.2

carbon content is expressed both as mg./scf. and as the weight per cent of supplied fuel.

At these particular test conditions, that is, with the deceleration starting at 20 mph., the fuel supply to the Diesel engines was not completely shut off. Subsequent tests with vehicle 1 showed that no fuel was supplied to the engine when the deceleration began at 35 mph. Apparently, the position attained by the injector rack when the foot throttle is closed depends upon the vehicle speed.

On the average, higher hydrocarbon contents were observed during deceleration in the exhaust of LPG vehicles than in that of gasoline vehicles. At first thought, this difference might be attributed to fuel or engine type. However, because the passenger car tests showed the hydrocarbon content during deceleration to be greatly dependent upon manifold vacuum, it seems likely that this variable was largely responsible for the observed differences. The fact that the highest hydrocarbon contents were observed with vehicles 7 and 8, which were equipped with standard transmissions, lends support to this belief.

Due to the limited number of commercial vehicles tested, definite conclusions concerning the relative merits of the different engine types should be made with caution. Also, it is difficult to compare Diesel and carbureted engines with respect to total hydrocarbon emission on the basis of exhaust gas analyses alone because the relative air and fuel consumptions vary markedly. However, it is believed that the total amount of hydrocarbon discharged during normal operation would be substantially the same whether the vehicle were equipped with a Diesel, gasoline, or LPG engine, provided the over-all fuel consumption was comparable.

Summary

These investigations have shown that the reductions in exhaust gas hydrocarbon content can be achieved through proper maintenance and design. Mass spectrometer analyses have indicated that the hydrocarbon content of engine exhaust gas varies appreciably with driving condition as shown below:

Test Condition	Hydrocarbon Content—Weight Per Cent of Supplied Fuel	
	Observed Range	Average
Idle	1 to 28	4
Part Throttle	1 to 5	1.5
Simulated Deceleration	1 to 63	12.5

The most important engine-fuel variable affecting the hydrocarbon content at idle was mixture ratio, with the highest hydrocarbon contents being observed at rich mixtures. A substantial reduction in the average hydrocarbon content could be obtained by adjustment of the idle mixture ratio of all cars to the range resulting in best idle operation. The current trend toward the overhead valve V-8 engine should also help to reduce idle hydrocarbon losses since these engines will idle acceptably with leaner mixtures than either 6 cylinder or line 8 engines. Fuel type was found to have essentially no effect on the exhaust gas hydrocarbon content.

None of the engine-fuel variables investigated at part throttle were observed to affect significantly the hydrocarbon content. These included mixture ratio, compression ratio, fuel type, coolant temperature, engine type, engine speed, and engine load.

The most important engine-fuel variable affecting the hydrocarbon content during simulated deceleration was manifold vacuum. The hydrocarbon content was found to increase sharply to high values at manifold vacuums above 21 in. of mercury. Since manifold vacuum during a closed throttle deceleration depends upon engine speed, the trend toward automatic transmissions and lower rear axle ratios made possible by higher output engines tends to

TABLE XII
Comparison of Exhaust Gas Hydrocarbon Content During Deceleration

Vehicle Type	Diesel Coaches		Gasoline Coaches		LPG Coaches			
Number	1	2	3	4	5	6	7	8
Hydrocarbon Content:								
Milligrams Per Standard Cubic Foot	21	13	118	130	237	703	839	1515
Weight Per Cent of Supplied Fuel	23.9	24.3	8.4	18.7	15.4	31.9	34.1	56.2

reduce hydrocarbon losses by reducing engine speed at a given car speed.

Limited studies using gasoline, LPG, and Diesel powered public transit buses have suggested that there is no significant difference in the total amount of hydrocarbon released to the atmosphere by the 3 different engines, provided that the over-all fuel consumption is comparable.

Acknowledgment

The authors wish to express their appreciation to:

(1) The Kansas City Public Service Company, of Kansas City, Missouri, and the Leyden Motor Coach Company, of Franklin Park, Illinois, for their cooperation in the coach tests.

(2) Mr. D. V. Kniebes and co-workers of the Institute of Gas Technology for performing the mass spectrometer analyses.

(3) The members of the Fuels and Lubricants Department, General Motors Research Laboratories, for their assistance in running the tests and their criticisms and suggestions during the preparation of the manuscript.

APPENDIX A

In the twenties and thirties, several investigators[1-2] observed small amounts of hydrocarbons in exhaust gases. Since their methods of analysis could not identify individual hydrocarbons, all the hydrocarbon was arbitrarily reported as methane. The development of more suitable analytical instruments, such as infrared and mass spectrometers, made it possible to measure the concentration of individual components of a gas mixture even though present in very small amounts. Both techniques have been successfully applied to the determination of hydrocarbons in exhaust gases[3-4].

To decide which of the above two analytical methods would be used in this investigation, several comparable exhaust gas samples were analyzed by both methods. These tests and conversations with those familiar with the capabilities of each instrument indicated that the mass spectrometer method would be the more suitable for this investigation. This decision was reached primarily because the mass spectrometer can quantitatively identify most of the hydrocarbons in exhaust gas. The infrared spectrometer, on the other hand, can identify only those hydrocarbons having characteristic structures, such as methane, ethylene, and acetylene. Other hydrocarbons are grouped together and one must assume an average molecular weight to make effective use of this information.

The samples were analyzed by the Institute of Gas Technology in Chicago, Illinois, and thus several days elapsed between sampling and analysis. It is not known how this delay affected the analyses.

---

(1) See footnote 1, page 109.
(2) See footnote 2, page 109.
(3) See footnote 3, page 109.
(4) See footnote 4, page 109.

TABLE XIII
Comparison of Mass Spectrometer Exhaust Gas Analyses Performed by Three Laboratories

Car H	1000 rpm. Downhill		Closed Throttle Operation	
	Concentration—Volume Per Cent			
Constituent	Lab. A	Lab. B	Lab. C	Orsat
Nitrogen	72.8	75.9	75.6	
Carbon Monoxide	2.6	4.8	5.5	4.5
Oxygen	18.8	13.4	13.3	13.8
Argon	0.90	0.9	0.9	
Hydrogen	0.933	1.5	1.2	
Carbon Dioxide	2.58	2.0	1.6	2.6
Water	.....	.....	1.0	
Methane	0.173		0.07	
Ethane	0.052		0.06	
Ethylene		0.1		
Acetylene	0.092	0.2	0.1	
Propane		0.01	0.2	
Propylene	0.096	0.1		
Butanes	0.152	0.1		
Butenes		0.05	0.3	
Butadiene	0.490			
Pentanes	0.108	0.1	0.09	
Pentenes	0.055	0.4		
Hexanes	0.044	0.2		
Hexenes	0.022	0.1	0.05	
Benzene		0.005		
Heptanes	0.026	0.1		
Heptenes	0.016	0.005	(a)	
Octanes	0.014			
Octenes		0.005	0.02	
Total Hydrocarbon Volume Per Cent	1.34	1.47	0.99(a)	
Weight Per Cent of Supplied Fuel	40.7	52.6	31.8	

(a) Probably low because C_7's were present on the spectrum, but not reported in the analysis.

However, the mass spectrometer has limitations that should be recognized. It is difficult to distinguish between carbon monoxide and nitrogen since both have a parent peak at mass 28 and few characteristic secondary peaks. For this reason, duplicate samples were collected and the carbon monoxide determined by Orsat analysis. Simple aldehydes have the same molecular weight at the next higher paraffin. Therefore, their parent peaks coincide and, unless both are present in appreciable concentrations, it is difficult to distinguish between the two. Neither aldehydes nor any other oxygenated organic compounds were detected in these analyses. Oxygen, in concentrations greater than 5%, is troublesome because it may attack the tungsten carbide-coated filament in the ionization chamber. In such cases, the mass spectrometer carbon dioxide and carbon monoxide concentrations are questionable and the Orsat values were assumed to be correct.

The water vapor in exhaust gas has a strong tendency to condense on or be absorbed by the glass surfaces of the sample containers or of the mass spectrometer inlet system. Most of the analyses were reported on a dry basis because only 5 to 10% of the expected water vapor appeared to reach the ionization chamber and contribute to the spectrum. This was true even though the sample containers were heated to 200°F. when transferring the sample to the mass spectrometer. When water condensation occurs, water soluble oxygenated compounds may be lost and recent information[10] has shown that hydrocarbons heavier than C_4 may also disappear.

It is difficult to check the accuracy of the mass spectrometer because no other instrument has the sensitivity required to detect individual hydrocarbons in low concentrations. Although gas mixtures containing various hydrocarbons in low, accurately known concentrations can be prepared, in practice this is very difficult to do. For this reason, it was decided the best approach for this work would be to collect comparable exhaust gas samples, submit them to several laboratories for analysis, and compare the results.

Exhaust gas samples were obtained from a 1953 model car coasting downhill at a constant engine speed of 1000 rpm. at the simulated deceleration condition previously described. The samples were not collected simultaneously, but every attempt was made to maintain comparable operating conditions at the times samples were collected. Portions of the mass spectrometer traces of these gas samples as determined by 3 well-known laboratories are shown in Fig. 7. To make direct comparisons possible, the peak height at mass 57 was arbitrarily assigned a value of 100 in each case, and all other peak heights

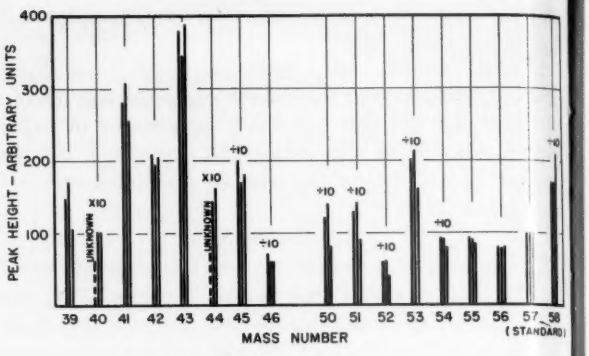

Fig. 7. Comparision of spectra.

between 39 to 46, and 50 to 58 scaled accordingly. Considering that each instrument has its own "cracking pattern" for each hydrocarbon and that one laboratory (c) employed a freeze-out technique, the relative peak heights agree well. This suggests that the true composition of each sample was essentially the same.

The compositions reported by each laboratory differed considerably, however, as may be seen from Table XIII. The concentrations of the major constituents agreed fairly well, but there were some large differences in the reported concentrations of individual hydrocarbons. Despite this, the total hydrocarbon content of each sample, expressed as volume per cent or as per cent unburned fuel, were all of the same order of magnitude. Because of the similarity of the spectral patterns, it seems likely that the large variations in the reported concentrations of individual hydrocarbons were due to different interpretations of the spectral patterns.

The conclusion must be reached that the absolute accuracy of mass spectrometer exhaust gas analyses remains somewhat in doubt. This is due both to the difficulty of getting a representative sample into the ionization chamber and the complex problem of deducing the gas composition from the spectral pattern. To help solve these problems the Coordinating Research Council has recently organized a special group to develop improved methods of sampling and analyzing engine exhaust gas. However, in spite of these difficulties, differences between samples collected in a similar manner and analyzed by one operator on one instrument are significant, and can provide valuable information.

(Continued on next page)

(10) Walker, J. K., and O'Hara, C. L., "Analysis of Automobile Exhaust Gases by Mass Spectrometry," presented at Southern California Air Pollution Foundation Meeting, Pasadena, California, August 18, 1954.

(Continued from page 74)

An Inventory of Automobile Gases

available but the following table covers the years of 1950 through 1953[4].

TABLE III
Gasoline Consumption

Date	Gallons per Year (State)	Percent Los Angeles County	Gallons per Year Los Angeles County	Tons/Day Los Angeles County
1950	3,391,494,666	40.31	1,365,000,000	11,550[a]
1951	3,694,506,374	40.23	1,485,000,000	12,550
1952	3,965,740,762	40.12	1,590,000,000	13,440
1953	4,172,814,857	40.68	1,700,000,000	14,380

(a) Based on 325.14 gal. per 2000 lbs., API gravity 60.

The tabulated data indicate that the consumption of gasoline in Los Angeles County is approximately 40-41% of the total gasoline consumption for the State of California. It therefore seems reasonable to use the State consumption figures as an index of the consumption of gasoline in Los Angeles County during the period 1935-53.

The data shown in Fig. 4 and 5 may therefore be used for estimating the control of automobile exhaust gases that would be required for return to the relatively smog-free years prior to 1945. Based on the hydrocarbon emission from automobiles shown in this study, it may be estimated that the probable hydrocarbon emission in 1945 was about 600 tons/day. Therefore, automobiles should be equipped with devices which will curtail the exhaust content of hydrocarbons by about 60%. It must be recognized that the addition of more automobiles (the trend is upward) would necessitate curtailment of the hydrocarbon content of automobiles by more than 60%. In no case should the total hydrocarbon emission exceed about 600 tons/day. It is believed that devices can be built that will convert 60% of the unburned or partially burned hydrocarbons to inert gaseous products. Research on devices for the latter purpose seems to be of paramount importance in controlling smog of the Los Angeles type.

(4) See footnote 4, page 71.

(Continued from page 118)

Some Effects of Engine-Fuel Variables

APPENDIX B

The hydrocarbon content of an exhaust gas sample was calculated from the mass spectrometer analysis of the sample. The weight of supplied fuel was determined from a carbon balance and the carbon-hydrogen ratio of the supplied fuel, assuming that all the carbon in the exhaust gas sample came from the fuel. A summation of the concentration times the molecular weight for each hydrocarbon gives the weight of unburned hydrocarbons present. The hydrocarbon content in weight per cent of the supplied fuel is then the ratio of the weight of unburned hydrocarbons present to the weight of supplied fuel. The stepwise procedure is outlined below:

Test Conditions: 400 rpm. Idle; 11.7 Air-Fuel Ratio; Isooctane.

Constituent	Concentration Mole Per Cent	x	Mol. Wt.	=	Hydrocarbon, Wt. Per 100 Moles of Sample	Moles Carbon Per 100 Moles of Sample
CO_2	8.63		.....		.....	8.63
CO	8.5		.....		.....	8.5
Methane	0.212		16		3.392	0.212
Ethane	0.023		30		0.690	0.046
Ethylene	0.034		28		0.952	0.068
Acetylene	0.096		26		2.496	0.192
Propylene	0.029		42		1.218	0.087
Butanes	0.002		58		0.116	0.008
Butenes	0.013		56		0.728	0.052
Butadiene	0.013		54		0.702	0.052
Pentanes	0.003		72		0.216	0.015
Hexanes	0.002		86		0.172	0.012
Heptenes	0.002		98		0.196	0.014
Octanes	0.041		114		4.674	0.328
Benzene	0.001		72		0.072	0.006
			Total Unburned Hydrocarbon		15.624	
			Total Carbon			18.222

Weight of Supplied Fuel = Total C x 12 + Total H x 1
= 18.222 [12 + 2.25 (1)] = 259.7

Total Hydrocarbon Content = $\frac{15.624}{259.7}$ x 100 = 6.0% by weight of supplied fuel

Per Cent Unreacted Fuel = $\frac{4.674}{259.7}$ x 100 = 1.8% by weight of supplied fuel

A Rapid General Purpose Centrifuge Sedimentation Method for Measurement of Size Distribution of Small Particles---Apparatus and Method*

K. T. Whitby
University of Minnesota
Minneapolis, Minn.

The rapid increase in industrial development and concentration of urban dwellers has placed increased emphasis on the need for more effective air cleaning.

The air filtration problem generally resolves itself into a need for knowledge of contaminants present in atmospheric air. These contaminants can be broadly classified as particulate matter, gaseous matter, airborne bacteria, viruses and odors.

The American Society of Heating and Air-Conditioning Engineers, Inc., through its Technical Advisory Committee on Air Cleaning fully realizes the magnitude of this air pollution problem. The Society is, however, presently confining its activities to a study of particulate matter which exists in air that ventilates spaces used for human occupancy.

This first paper presents a new method of particle-size measurement which has been found to be of practical value for measurement in the 0.05μ to 100μ range. Part I describes the apparatus and basic method. Part II will describe detailed procedures applicable to a variety of applications.

Problems of particle-size measurement are almost as varied as industry itself. For example, size measurement is important in the production of such substances as flour, paint pigments, powdered sugar and insecticides. In recent years the air pollution problem has received increasing attention, and a need exists for rapid yet comprehensive methods for evaluating atmospheric dust samples.

These and similar needs in other fields of particle technology have generated interest in size analyses because of the fundamental importance of size-distribution data.

The literature in size analysis is voluminous and scattered widely in various scientific journals. Lately this situation has been improved by a number of comprehensive reviews covering all methods of size analysis. Several good ones are given by Schweyer and Work[1], Heywood[2], Stairmand[3], and Rose[4]. Two recent reviews which also have fairly extensive bibliographies are by Herdan[5] and Work and Whitby[6].

Study of the literature shows that only the microscopic and sedimentation methods have been used widely for the subsieve range. Microscopic analysis by electron beam or light can be used from 0.01 μ up but the procedures are tedious and inaccurate except for narrow size ranges. For this reason, sedimentation analysis has been the most widely used. All sedimentation or elutriation methods use the relationship between particle size and settling velocity derived from Stokes' law, Hawksley [7] has given an excellent discussion of the basic principles of sedimentation analysis.

Stokes' law states that the settling velocity of a particle in a fluid is proportional to the square of the particle diameter. For this reason the settling velocity of particles below 5 μ in size becomes rather slow. For example, a 1 μ particle of density 2.5 would require about 24 hr. to settle 10 cm. in water. Thus, for practical reasons, gravity sedimentation is usually limited to 1 μ and larger. By using a centrifuge to increase the force on the particles, the sedimentation analysis may be extended to the finer size ranges. This is the approach used in the development of the method described in this paper.

Basically, the method combines gravity and centrifuge sedimentation to take advantage of the desirable characteristics of each. This approach is not new. For example, Norton and Speil[8] constructed a centrifuge large enough so that standard hydrometers and jars could be used.

(1) Schweyer, H. E., and Work, L. T., in "Symposium on New Methods for Particle Size Distribution in the Subsieve Range," ASTM meeting, Washington, D.C., March 4, 1941.

*This paper is the result of research sponsored by the American Society of Heating and Air-Conditioning Engineers, Inc., in cooperation with the Mechanical Engineering Department, University of Minnesota, Minneapolis, Minn. It was presented at the 61st Annual Meeting of the American Society of Heating and Air-Conditioning Engineers at Philadelphia, Pa., January 1955.

(2) Heywood, H., "The Scope of Particle Size Analysis and Standardization," *Trans. Inst. Chem. Engrs.* (London) and *Soc. Chem. Ind.* (London), Roads and Building Materials Group, Advance Copy, February 4, 1947, pp. 1-11.

(3) Stairmand, C. J., "Some Practical Aspects of Particle Size Analyses in Industry," *Trans. Inst. Chem. Engrs.* (London) and *Soc. Chem. Ind.* (London), Roads and Building Materials Group, Advance Copy, 1947, pp. 58-68.

(4) Rose, H. E., "The Measurement of Particle Size in Very Fine Powders," Constable and Company, Ltd., London, 1953.

(5) Herdan, G., "Small Particle Statistics," The Elsevier Press, Inc., New York, 1953.

(6) Work, L. T., and Whitby, K. T., "Size Measurement of Particles" in "Encyclopedia of Chemical Technology," Vol. 12, Interscience Encyclopedia, Inc., 1954.

(7) Hawksley, P. G. W., "The Physics of Particle Size Measurement—Part I, Fluid Dynamics and the Stokes Diameter," *Bull. Brit. Coal Utilization Research Assoc., 15,* 105 (April 1951).

(8) Norton, F. H., and Speil, S., "The Measurement of Particle Sizes in Clays," *J. Am. Ceram. Soc., 21,* 89 (1938).

Most centrifuge methods start with an initially homogeneous suspension in the tube. Robison and Martin[9] and Kamack[10] describe recent improvements in this approach. The one serious drawback in the use of a homogeneous suspension in a centrifuge is the complication involved in the calculation of results. The fact that various size particles are settling out at any given time, plus the fact that the forces on the particle vary with the radius in the centrifuge, precludes any exact solution to the differential equations that describe the rate of sedimentation. This difficulty can be eliminated by making the radius of the centrifuge large compared to the sedimentation height, or by starting all the particles off in a layer on top of the sedimentation liquid. The latter approach, first used by Marshall[11], is the one used in the method described in this paper.

Several different methods have been used for sensing the rate of sedimentation. Kamack[10] describes an ingenious system of withdrawal pipettes which can be operated while the centrifuge is in motion. Svedberg[12] made extensive use of optical methods in his ultracentrifuges. Norton and Speil[8] used a hydrometer, and Berg[13], a specific gravity diver. However, all of these either require elaborate apparatus or careful technique. For these and other reasons a simple capillary at the bottom of the centrifuge tube has been used to measure sediment height.

(8) See footnote 8, page 120.

(9) Robison, H. E., and Martin, S. W., "Beaker Type Centrifugal Sedimentation of Subsieve Solid-Liquid Dispersions—I, Theory," *J. Phys. & Colloid Chem., 52,* 854 (1948).

(10) Kamack, H. J., "Particle Size Determination by Centrifuge Pipette Sedimentation," **Anal. Chem.**, *23,* 844 (1951).

(11) Marshall, C. E., "A New Method of Determining the Distribution Curve of Polydisperse Colloidal Systems," *Proc. Roy. Soc.* (London), Part A, *126,* 427 (1930).

(12) Svedberg, T., "The Ultracentrifuge and Its Field of Research," *Ind. Eng. Chem., Anal. Ed., 10,* 113 (1938).

(13) Berg, S., "Studies on Particle-Size Distribution," *Ingeniorvidenskabelige Skrifter, 2,* 243 (1940).

Principle of Operation

Basic to the method is the special centrifuge tube and feeding chamber illustrated in Fig. 1. At the beginning of a size analysis the clean tube is filled to the line near the top of the tube with a suitable sedimentation liquid. The tube is then placed in a holding device, which may be simply a laboratory clamp on a ring stand, or may be a more elaborate optical observing device as illustrated in Fig. 2.

Next, a suspension of particles is made up in a liquid that is miscible with the sedimentation liquid and has a slightly lower density and a slightly higher viscosity. The particles must be practically insoluble in either liquid. An aliquot of this suspension is placed in the feeding chamber and the chamber placed in the tube and released in such a way so as to leave a sharp layer of suspension on top of the sedimentation liquid.

Then, at times calculated from Stokes' law for the desired sizes, the height of the sediment in the capillary is read. Sedimentation is allowed to proceed under gravity for 4 to 10 min. depending upon the time schedule that has previously been worked out. Then the tube is transferred to the first and lowest speed centrifuge and run for a precalculated time. The tube is removed to read the sediment height and then is replaced in the centrifuge for the next time interval. This is continued until there is no change in sediment height or until the last centrifuge time in the schedule has been run. During the centrifuge

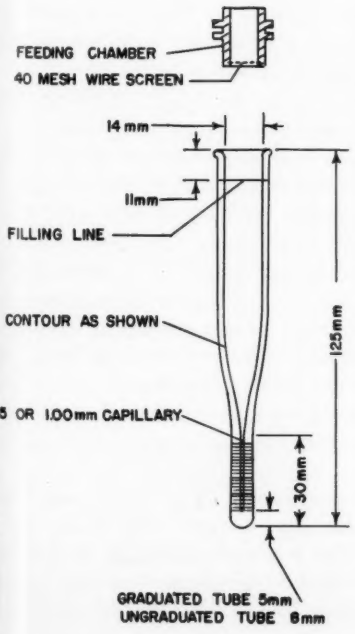

← *Fig. 1. Centrifuge tube and feeding chamber design.*

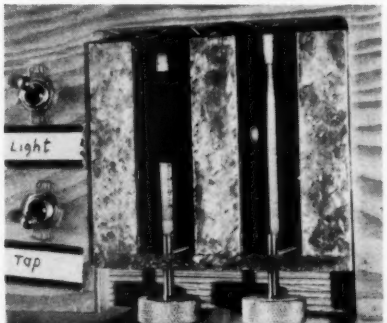

Fig. 4. Projected image of tube. Left—with sediment, Right—empty tube. (Note—image is inverted).

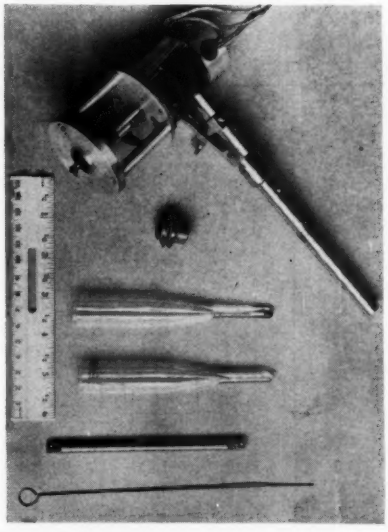

Fig. 6. Miscellaneous equipment. Left to right: Cleaning wire, powder scoop, graduated tube, feeding chamber, and micro stirrer.

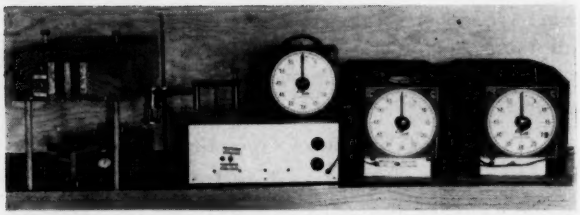

Fig. 2. Complete centrifuge size analysis equipment. Left to right: Projection reading apparatus, tubes in rack, micro stirrer, 300 rpm. centrifuge, 600-1200 rpm. and 1800 rpm. centrifuges.

runs the speed is increased as the settling velocity of the particle decreases.

By proper choice of liquids, centrifuge speeds and reading times, it is possible to determine size distribution at the rate of 2 per hr. on such materials as the A.C. fine test dust, illustrated in Fig. 3 and Table I. If this size analysis had been run by straight gravity sedimentation, it would have required approximately 54 hr. as compared to about 25 min. by centrifugal analysis.

Application of the method has been broad. Equipment and procedures are the result of the combined experience of 6 industrial firms and the University of Minnesota on over 50 materials ranging from paint pigments to D.D.T. insecticide.

Though extensive, the equipment required is simple enough so that some version of the method is within the reach of every laboratory. Fig. 2 illustrates the complete apparatus used in making a size analysis. The method is very flexible. Size analyses can be made on samples as small as 2 mg. One or 20 points on the distribution curve may be determined and the method is especially suitable for obtaining accurate analyses of samples containing a few per cent of large particles.

Calculation of results for routine analyses is simple,

TABLE I
Size Analysis Data for A.C. Fine Test Dust Analyzed Benzene

Particle Size Microns	Reading Time min. sec.	Centrifuge rpm.	Observed Height on Screen	Per Cent Greater Than Size	Per Cent Less Than Size
60	:18		0	0	100
50	:26		0.2	0.8	99.2
40	:40		0.9	3.5	96.5
35	:53		1.3	5.0	95.0
30	1:12		2.0	7.7	92.3
25	1:43		3.0	11.5	88.5
20	2:41		4.5	17.2	82.8
16	4:12		5.9	22.6	77.4
12	:18	300	8.3	31.8	68.2
8	:24	600	11.3	43.4	56.6
4	:38	1200	16.7	64.0	36.0
2	1:03	1800	20.4	78.2	21.8
1	3:22	1800	22.4	85.8	14.2
0.5	12:34	1800	23.8	91.4	8.6
±0	15:00	4000	26.1	100.0	0

Note: Room Temperature = 80° F; Sedimentation Liquid = Benzene; Feeding Liquid = 40% Benzene + 60% Naphtha; Dispersing Agent = 0.1% Twitchell 8240; $\rho = 2.52$ gm/cm³; $\rho_o = 0.87$; $\eta_o = 0.00582$ poise; $K = 6.45 \times 10^4$. Dispersed 2 min. in a blender.

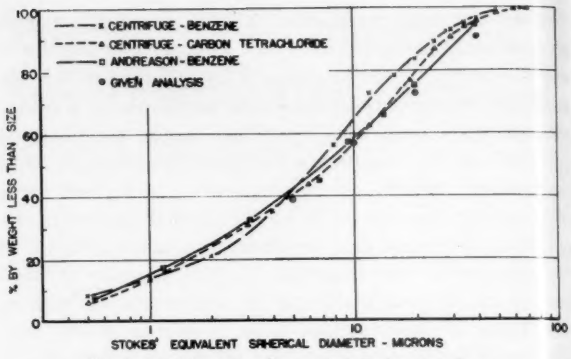

Fig. 3. Particle size analyses of A.C. fine test dust.

requiring only a few calculations on a slide rule. Details of the calculations involved and preparation of schedules will be described later. Selection of liquids, dispersing agents and dispersion methods will be discussed in Part II (to be published).

Apparatus

Centrifuge Tubes

The tube design that has been developed is illustrated in Fig. 1. The graduated tubes, which can be read without any optical accessories, are necessary for the analysis of certain materials. Ungraduated tubes are satisfactory for most materials. Paint pigments and other submicron materials form an optically opaque suspension in the capillary above the sediment. Though it is possible to see the line of demarcation with the unaided eye, it is often impossible when using the projection system.

The ungraduated tubes used with a suitable projection system are desirable for most size-analysis work. Magnification of the capillary image 6 times, as in Fig. 4, permits easier, more accurate reading of sediment height. The magnified image also makes it easy to see if dispersion is satisfactory and to see the actual shape and number of the few largest particles.

Tube size is such as to fit the standard 15 ml. tube shields and heads available on most small centrifuges. Other tube dimensions have been worked out from experiment and from consideration of what it is practical to make from glass. It has been found that the 2 parts of the tube most difficult to make, and also the most important, are the transitions from the cylindrical portion to the capillary and the flat bottom of the capillary.

In addition to the tube design shown in Fig. 1, a special open-ended design having a bore of 0.17 mm. is under development for use with impinger dust samples and other applications where the concentration of dust in the feeding liquid is very low.

Centrifuges

Early attempts to use ordinary laboratory centrifuges showed that while they can be used, they have many serious drawbacks. The major disadvantage is lack of speed stability. Acceleration rates are too low at the low speeds and too high at the high speeds. Also it is

very difficult to control these rates without major reconstruction of the centrifuges.

Some of the smaller commercial centrifuges can be used if an accurate stroboscope is available and if they are operated with covers open in order to keep the tubes at room temperature and to increase aerodynamic resistance.

Considerable experimentation has established the following centrifuge characteristics as necessary:

1. Speed must be constant within 1% of the values used in calculating the tables.
2. Maximum rate of acceleration during starting and stopping must be less than 5 rad. per (sec.) (sec.)
3. Speed *vs.* time curves during starting and stopping must be known and constant enough so that starting and stopping correction will not vary more than ±0.5 sec.
4. It is desirable to have a 300-600 rpm. range for the slowest centrifuge.
5. For ease of operation it is desirable that no adjustment of rheostats or other speed control equipment be necessary during the starting and stopping period of the centrifuge. This is to permit the centrifuge to be started and stopped by an automatic timer of suitable accuracy.

The foregoing requirements dictated the design of the special centrifuges illustrated in Fig. 2. These centrifuges are powered by multi-speed hysteresis-type synchronous motors. Three centrifuges have been developed so far. A 300-600 rpm. unit is powered by a 600-1200 rpm. motor with a 2 to 1 gear reduction between motor and head. A 600-1200 rpm. unit is direct driven, as is an 1800 rpm. unit. Starting and stopping characteristics are controlled by a combination of an inertia disk on the motor shaft and a variable resistor in series with one winding of the motor. For some locations, a wave-form correcting-type voltage regulator is necessary to obtain constant starting characteristics.

For convenience, a 1-sec. to 1-hr. timer is built into each centrifuge. All of the work to date has been done with centrifuges equipped with small commercial heads. These two-place heads were used because they were the smallest standard heads available. Use of other heads with slightly different trunnion radii would have no effect other than to change the radii used in the calculation of time schedules.

Tube-Reading Equipment

It was found desirable to tap the tube gently on the tip along the axis of the tube during the gravity portion of the run. Therefore, for both the graduated tubes and the projection tubes, the tube holder is provided with a cam operated tapper which strikes the tube a light blow on the tip 40 times/min.

For the ungraduated tubes a special projection system is used to read the tubes. Fig. 4 is a close-up of the screen and illustrates the type of scale and image obtained. Fig. 5 illustrates in schematic form an improved version of the optical unit which is now under construction. The tube should be out in the open so that sedimentation can be observed in the whole tube and so that the lamp heat will not cause convection currents. Space for more than one tube is provided in a sliding rack so that more than one analysis can be run at the same time. This is also the reason for the double optical system of the instrument illustrated in Figs. 2 and 4.

Miscellaneous Equipment

Several small but essential items go to complete the apparatus as follows:

1. *Feeding chamber*—as illustrated in Fig. 1—is essential for obtaining a uniform layer of suspension on the surface of the sedimentation tube.
2. Fig. 6 illustrates a *cleaning wire* and *powder scoop*. Closed end tubes are cleaned by pumping this wire rapidly in and out of capillary with the tube full of liquid. The *powder scoop* is used for measuring out a given volume of powder when the dispersion is made directly in the feeding chamber. This is particularly convenient for routine analyses on materials reasonably easy to disperse.
3. Fig. 6 also illustrates a *special micro-stirrer* that can be used to stir the suspension in the feeding chamber. This makes it unnecessary to make up a separate suspension in a blender or other stirring device. Using a motor that will develop at least 10,000 rpm., this microstirrer will disperse all but the most difficult materials.
4. *High-speed commercial centrifuge*—A commercial centrifuge that will develop approximately 2,000 g's is useful for obtaining end points on very fine materials such as paint pigments. A small medical centrifuge is satisfactory for this purpose.

Calculation of Tables

Because this method combines both gravity and centrifugal sedimentation, it is most convenient to calculate

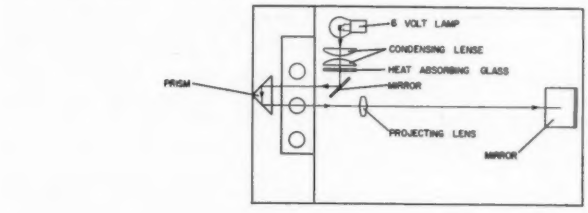

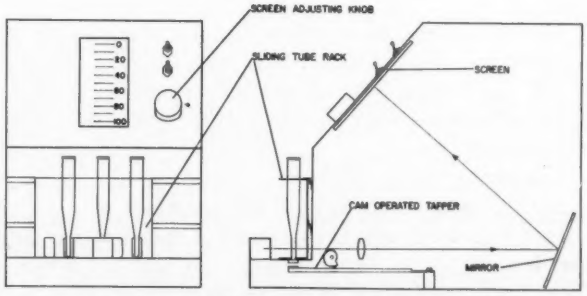

Fig. 5. Schematic diagram of improved projection unit.

TABLE II
Values of $1/d^2$ Used in Table III

d - microns	$1/d^2$
70	2.04×10^{-4}
60	2.78×10^{-4}
50	4.00×10^{-4}
40	6.25×10^{-4}

the reading times completely before a run is begun. Though there are several ways of doing this, only one procedure will be given here. Developed in collaboration with Dr. M. A. Knight, this procedure is particularly adapted to industrial laboratory operations since it reduces the decisions that must be made during the computation.

Gravity Portion of Tables

The time for a particle to settle a given distance in a fluid under the influence of gravity can be calculated from the usual form of Stokes' law.

$$t_g = (18 \times 10^8\ \eta_o\ h)/[(\rho - \rho_o)\ g\ d^2] \quad (1)$$

where

t_g = time in seconds for a particle to settle a distance h under the influence of gravity.
d = particle diameter, μ.
h = settling height, centimeters (10 cm. for all tubes).
ρ = true density of particles, gm./cm.^{3}
ρ_o = density of sedimentation liquid, gm./cm.^{3}
η_o = absolute viscosity of sedimentation liquid, poise.
g = gravitational constant.

if we let

$$K = (18 \times 10^8\ \eta_o\ h)/[(\rho - \rho_o)\ g] \quad (2)$$

then Equation 1 becomes:

$$t_g = K/d^2 \quad (3)$$

Since K will be a constant for a given material in a given sedimentation liquid, the gravity reading times may be calculated by multiplying the calculated K value by $1/d^2$ values pre-calculated in tabular form. Table II illustrates a few $1/d^2$ values used in calculating the time schedule of Table III.

Centrifuge Portion of Table

Centrifuge settling times can be calculated by a form of Stokes' law for a centrifugal field that is derived as follows:

Let r represent the radius of rotation of a particle of mass m rotating about an axis with angular velocity ω. At equilibrium, two forces will be acting on the particle: a frictional force determined by Stokes' law, and a centrifugal force.

Equating these we obtain:

$$3\ \pi\ \eta_o d\ (dr/dt) \times 10^8 = m\ \omega^2\ r.$$

In a liquid the effective mass of a spherical particle will be:

$$m = (\pi/6)\ d^3\ (\rho - \rho_o)$$

Therefore:

$$dr/dt = [(\rho - \rho_o)\ \omega^2 d^2 r]/(18 \times 10^8\ \eta_o)$$

Integrating between the starting radius r_1, and the final radius r_2 we obtain:

$$t_c = t_2 - t_1 = \left\{(18 \times 10^8\ \eta_o)/[(\rho - \rho_o)\ \omega^2\ d^2]\right\} \log_e (r_2/r_1) \quad (4)$$

where

t_c = the centrifuge running time necessary to centrifuge a particle of size d from r_1 to r_2.

In both Equations (3) and (4), the slightly different density and viscosity of the feeding and sedimentation liquid have been neglected. This approximation is valid because the thickness of the feeding layer is small and usually the density and viscosity differences are small.

The K-values may also be defined from Equation (4) if the centrifuge speeds are selected. If we let K_s represent the K-value associated with a given centrifuge speed s, then:

$$K_s = (18 \times 10^8\ \eta_o)/[\rho - \rho_o)\ \omega_s^2] \quad (5)$$

Equation (4) becomes:

$$t_c = (K_s/d^2) \log_e (r_2/r_1) \quad (6)$$

By equating Equations (2) and (5), K_s may be expressed in terms of K as shown in Table III.

In Equation (6), r_2 is a constant for a given tube and head design, but r_1 will depend not only on the radius of the top of the tube but on how far the particle has already settled under the influence of gravity.

TABLE III
Calculation of Reading Schedule of K = 6.45 x 10^4

RPM	Values of Ks	Values of Js
300	0.0992 $K = 0.640 \times 10^4$	100 $1/K = 0.00155$
600	0.0248 $K = 0.160 \times 10^4$	525 $1/K = 0.00814$
1200	0.0062 $K = 0.040 \times 10^4$	2,900 $1/K = 0.0450$
1800	0.00276 $K = 0.0178 \times 10^4$	14,500 $1/K = 0.225$

d_g, in Microns	t_g, in Seconds	d_g, in Microns	t_g, in Seconds	
70	13.2	30	71.7	
60	17.9	25	103.3	$t_g = K/d_g^2$
50	25.8	20	161.0	
40	40.3	16	252.0	
35	52.6			

d_c	t_c*	C_s	t_{ct}	RPM	Q
12	17.7	0	17.7	300	0.00277
8	18.0	+ 6.0	24.0	600	0.0130
4	25.4	+12.4	38.0	1200	0.0764
2	46.7	+16.0	63.0	1800	0.337
1	186.0	+16.0	202.0	1800	1.383
0.5	738.0	+16.0	754.0	1800	5.576

RPM	*$t_{cn} = (Q_n - Q_{n-1})\ K_s$, Seconds
300	$0.00277 \times 0.640 \times 10^4 = 17.7$
600	$(0.0130 - 0.00277)\ (0.160 \times 10^4) = 18.0$
1200	$(0.0764 - 0.0121)\ (0.040 \times 10^4) = 25.4$
1800	$(0.337 - 0.0764)\ (0.0178 \times 10^4) = 46.7$
1800	$(1.383 - 0.337)\ (0.0178 \times 10^4) = 186.0$
1800	$(5.576 - 1.383)\ (0.0178 \times 10^4) = 738.0$

TABLE IV
Portion of a Table of Q Values used to Calculate Centrifuge Running Times (a)

de, microns	dg, microns			
	16	15	14	13
14	0.00099	0.0052		
13	0.00175	0.00123	0.000649	
12	0.00277	0.00219	0.00159	0.000842
11	0.00417	0.00353	0.00281	0.00199
10	0.00613	0.00542	0.00459	0.00367
9	0.00892	0.00811	0.00719	0.00614
8	0.0130	0.0121	0.0110	0.00984
7	0.0191	0.0181	0.0169	0.0156
6	0.0288	0.0278	0.0264	0.0249
5	0.0454	0.0442	0.0427	0.0410
4	0.0764	0.0749	0.0733	0.0713
3	0.144	0.142	0.140	0.138
2	0.337	0.336	0.334	0.331
1	1.383	1.381	1.379	1.376
0.5	5.576	5.576	5.576	5.576

(a) Q valves calculated for $r_o = 3.30$ cm. and $r_2 = 13.30$ cm.

Therefore

$$r_1 = r_o + 10\ (t_g/t_{cg}) \quad \ldots\ldots (7)$$

where

t_g = time for last gravity particle size d_g to settle 10 cm. under gravity.

t_{cg} = time for first centrifuge particle size d_c to settle 10 cm. under gravity.

r_o = starting radius of all particles in the feeding layer at $t = 0$.

If Equation (3) is substituted into Equation (7)

$$r_1 = r_o + 10\ (d_c^2/d_g^2) \quad \ldots\ldots (8)$$

We see that r_1 is a function only of the last gravity size and of the centrifuge size under consideration. This makes it convenient to set up a simple calculation scheme for the centrifuge portion of the run in which use is made of a calculation constant tabulated as a function of d_g and d_c.

In Equation (6), define Q by:

$$Q = (1/d_c^2)\ \log_e\ (r_2/r_1) \quad \ldots\ldots (9)$$

then

$$t_c = K_s\ Q \quad \ldots\ldots (10)$$

Substitution of Equation (8) into Equation (9) yields:

$$Q = (1/d_c^2)\ \log_e \left\{ r_2/[r_o + (10 d_c^2/d_g^2)] \right\} \quad \ldots\ldots (11)$$

Equation (11) may then be used to calculate a table of Q values such as in Table IV, for apparatus with given r_o and r_2 values.

Before illustrating how a table of Q's is used to calculate a complete reading schedule, it is convenient to define one other constant. When preparing a reading schedule such as in Table III, the question arises as to just what particle-size intervals and centrifuge speeds are desirable.

There is not too much of a problem during the gravity portion of the run because practically any size intervals may be used. However, during the centrifuge portion, a number of factors must be considered. Due to computational difficulties, it is impractical to have a centrifuge running time less than the starting time of the centrifuge at that speed. In Table III for example, the first centrifuge time at 12 μ is 17.8 sec. For this centrifuge the minimum useful timer setting is 10 sec. If the centrifuge time for a size of say 14 μ was to be calculated, it would be found that the centrifuge time would be only 6.3 sec., which is below the useful time and therefore impractical. The same problem exists when changing to higher speeds.

To aid in selecting the best combination of sizes and speeds, it is convenient to define the minimum useful increment in Q that can be used for each centrifuge speed.

In Equation (10), t_c is the centrifuge running time assuming that the centrifuge runs at the given speed for the whole interval. Actually a starting and stopping correction is necessary because in most cases it is inconvenient to balance the starting time against the stopping time. Later it will be shown how this correction is obtained but for the present it is sufficient to say that it is a constant which is added algebraically to t_c in order to get the timer setting t_{ct}.

Therefore,

$$t_{ct} = t_c + C_s = K_s Q + C_s \quad \ldots\ldots (12)$$

where

C_s = the starting-stopping correction at speed S.

t_{ct} = the centrifuge timer setting necessary.

The minimum useful increment in Q may now be calculated by setting t_{ct} equal to the starting time of the centrifuge.

$$t_{ct} = t_{starting} = K_s\ J_s + C_s$$

or

$$J_s = (t_{starting} - C_s)/K_s \quad \ldots\ldots (13)$$

where

J_s is the minimum useful increment in Q at the speed s. As an example, for the 600 rpm. centrifuge $C_s = +6$ sec., and t starting = 19 sec.,

therefore

$$J_{600} = (19 - 6/K_{600}) = (13/0.0248K) = (525/K)$$

Table III illustrates how these Q and J values are used to calculate a complete schedule. A convenient step-by-step procedure is outlined:

1. Using Equation (2), calculate K for the given conditions of density and viscosity.

2. Calculate $1/K$, K_s and J_s values as at the top of Table III.

3. Calculate the gravity portion of Table VI from Equation (3) and a suitable table of $1/d^2$ values. It is best to terminate the gravity portion of the run between 4 and 10 min. The minimum gravity time permissible will depend on the centrifuge equipment available and the size interval from the last gravity to the first centrifuge size.

4. Select the first centrifuge size so that $Q_1 > J_{s1}$. In the example $J_{300} = 0.00155$ and therefore for $d_g =$

16 μ it is seen from Table IV that $d_c = 13$ μ is the maximum particle size that could be selected for the first centrifuge size. In this case 12 μ was selected because the interval from 12 to 16 μ was small enough. Calculate t_c from Equation (10), using a Q value corresponding to $d_g = 16$ and $d_c = 12$ and K_{300}. Add the appropriate start stop correction to get the time setting t_{ct}.

$$t_{ct} = Q_1 K_s^1 + C_s^1$$

5. Select the next centrifuge size so that $Q_2 > Q_1 + J_{s2}$. The problem now arises as to whether to use the centrifuge speed used for d_{c1} or go to a higher speed. In this case $Q_1 + J_{300} = 0.00432$ and $Q_1 + J_{600} = 0.0109$. From Table IV it is seen that the maximum d_{c2} that could be used with 300 rpm. centrifuge is 10 μ and with the 600 rpm. centrifuge, 8 μ. Since the interval from 12 to 8 μ is satisfactory, we choose the 600 μ rpm. centrifuge in order to save time. Then for the example:

$$\begin{aligned} t_{ct} &= Q_2 K_{600} - Q_1 K_{600} + C_{600} \\ &= 0.0130 \times 0.160 \times 10^4 - 0.00277 \\ &\quad \times 0.160 \times 10^4 + 6.0 = 24 \text{ sec.} \end{aligned}$$

6. Subsequent centrifuge size intervals and centrifuge times are calculated using the same procedure. Because the starting and stopping of the centrifuges and the handling of the tube causes a small amount of mixing in the tube, centrifuge reading sizes should be limited to a maximum of 7. Actual experience has indicated that 5 is usually sufficient.

Where many size analyses must be run on a variety of materials it is convenient to make up tables of appropriate reading schedules calculated for increments of K. Tables calculated for successive increments having a ratio of 1.025 over a range from 5 x 10^4 to 25 x 10^4 will cover most used range.

Determination of Starting and Stopping Correction

Due to the short runs that are made with the centrifuge, the starting and stopping correction becomes an appreciable fraction of the running time. This makes a precise determination of the correction necessary. The following scheme has been found to be satisfactory.

A stroboscope is used to obtain accurate angular velocity time data during starting and stopping. This is accomplished by observing the time at which the centrifuge reaches a speed preset on the stroboscope.

From Equation (4), it is apparent that the settling velocity at a given radius is proportional to the angular velocity is squared. Therefore, if the angular velocity squared is plotted against the time during starting and stopping (Fig. 7), the area under the starting and stopping curves will be proportional to the distance settled during the respective times. The net correction is, therefore:

$$\text{Net correction} = \frac{\text{Area } A - \text{Area } B}{Y \text{ (to same scale as } T)}$$

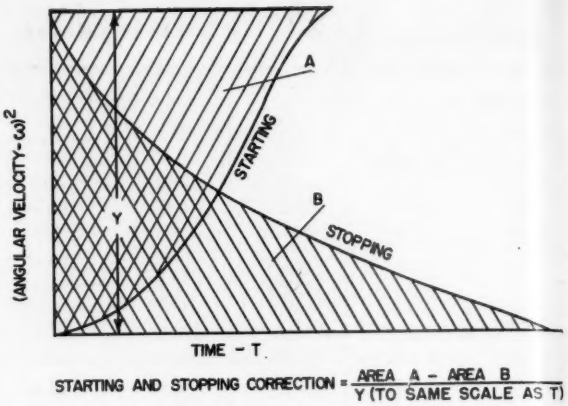

Fig. 7. Typical starting and stopping curves.

Calculation of Results

Calculation of results from the sediment height *vs.* time data is simple. The percentage of particles by weight larger than a given size is obtained by dividing the sediment height at that size by the total sediment height. For example in Table I the percent larger than 12 μ is

$$(8.3/26.1) \times 100 = 31.8\%$$

The percent undersize, or the frequency distribution may be obtained in the usual manner from the percent larger than distribution.

Typical Data

Fig. 3 illustrates a typical particle-size analysis obtained with this method as compared to the standard Andreason pipette and the size analysis supplied by the makers of the dust. At this time it will merely be stated that reproducibility and agreement with other methods have been found to be entirely satisfactory for all but a few unusual situations. Considering the compromises that have been made in the development of the method, agreement with other methods is good.

Summary

This paper describes the apparatus and basic principle of a new method of centrifuge sedimentation analysis which has been found to be of great practical value for measurement of size distribution of dusts in the 0.05 to 100 micron size range. Extensive use by six different industrial firms has demonstrated that the method for the first time permits economical and rapid size analysis in the 0.05 to 5 micron size range occupied by most atmospheric dusts.

Included are descriptions of apparatus, basic derivations and outlines for practical methods of calculation of necessary tables and results.

Acknowledgment

The author is grateful for the suggestions of the following individuals during the development of this method: Dr. R. C. Jordan, head of the Mechanical Engineering Department, University of Minnesota, for making laboratory facilities available; Prof. A. B. Algren, head of the

(Continued on page 132)

A Technique For the Rapid Solution of An Air-Pollution Equation*

F. T. Bodurtha, Jr.
Engineering Service Division
Engineering Department
E. I. duPont de Nemours and Company
Wilmington, Delaware

A technique for the rapid solution of the Bosanquet and Pearson formula for atmospheric gas concentrations is developed in this paper. The equations and graphs presented refer to stack gases at or near atmospheric density. General consideration is given to stack gases whose density differs from atmospheric. It is indicated that the total plume rise may decrease with increasing stack gas velocity when the effluent density is less than atmospheric.

Nomenclature

a=Velocity rise factor, dimensionless.
C_o=Ground level concentration,
for gas of emission rate Q_m, ppm. by volume,
for particulate matter, mg./ft.^{3}
$C_{o(max)}$=Maximum concentration at ground level, (same as C_o).
e= Natural logarithmic base, 2.718.
G=Gradient of potential atmospheric temperature, deg. C/ft.
g=Acceleration due to gravity, 32.2 ft./sec.^{2}
H=Effective stack height, ft.
h_s=Stack height above grade or other reference level, ft.
$h_{v(max)}$=Maximum velocity rise, ft.
h_v=Velocity rise at distance x, ft.
$h_{t(max)}$=Maximum thermal rise, ft.
h_t=Thermal rise at distance x, ft.
J=Parameter for calculation of thermal rise, dimensionless.
p, q=Diffusion coefficients, dimensionless.
Q_m=Emission rate at atmospheric temperature,
for gas concerned with, cfs.
for particulate matter, kg./sec.
Q_{T1}=*Total* gas emission rate at temperature T_1, cfs.
T=Atmospheric temperature, deg. K or deg. R.
T_s=Stack gas temperature, deg. K or deg. R.
T_1=Temperature at which stack gas and atmospheric densities are equal,
($T_1 = \frac{\text{(Mol. Wt. Stack Gas) (T)}}{29}$ for gases at atmospheric pressure), deg. K. or deg. R.
u=Mean horizontal wind speed, fps.
u_c=Wind speed at which maximum concentration occurs at a specified distance x (critical wind speed), fps.
u_{cm}=Wind speed at which maximum concentration occurs (critical wind speed), fps.
V_s=Stack gas exit velocity, fps.
x=Downwind distance from emission source, ft.
x_m=Distance from stack to point of maximum ground level concentration, ft.
Z=Parameter for calculation of thermal rise, dimensionless.
$\Delta = T_s - T_1$, deg. C or deg. F.

*Presented at the Annual Meeting of the American Society of Mechanical Engineers, New York, N. Y., November 28 to December 3, 1954.

Introduction

The current emphasis on the abatement of air pollution makes it necessary in many instances to provide means to keep the ground level concentration of effluent gases below specified values. Stacks are commonly used for this purpose. Necessary stack heights for single sources may be calculated from formulas developed by Bosanquet and Pearson[1] and Sutton[2]. A comprehensive discussion on the application of these formulas has been given by Helmers[3].

The Bosanquet and Pearson equation for the average gas concentration at ground level beneath the plume axis is

$$C_o = \frac{Q_m \times 10^6 \times e^{-\frac{H}{px}}}{\sqrt{2\pi}\, pqux^2} \qquad (1)$$

where

$$H = h_s + h_v + h_t \qquad (2)$$

C_o in Equation (1) is representative of average concentrations for 30 min. or longer[3]. Peak 1 min. concentrations are about 10-20 times those of Equation (1) while instantaneous concentrations may be 50 times the average concentration[4-5].

Bosanquet, Carey, and Halton[6] have given the following equations for the rise of the plume caused by the velocity of the stack gases:

(1) Bosanquet, C. H., and Pearson, J. L., "The Spread of Smoke and Gases from Chimneys," *Trans. Faraday Soc., 32,* 1249 (1936).
(2) Sutton, O. G., "The Theoretical Distribution of Airborne Pollution from Factory Chimneys," *Quart. J. Roy. Meteorol. Soc., 73,* 426 (1947).
(3) Helmers, E. N., "The Meteorology of Air Pollution," Chapter 8 in "Air Pollution Abatement-Manual," Manufacturing Chemists Association, Inc., Washington, D. C., 1951.
(4) Falk, L. L., et. al., "Development of a System for Predicting Dispersion from Stacks," *Air Repair, 4,* 35 (1954).
(5) Gosline, C. A., "Dispersion from Short Stacks," *Chem. Eng. Progr., 48,* 165 (1952).
(6) Basanquet, C. H., Carey, W. F., and Halton, E. M., "Past Desposition from Chimney Stacks," *Inst. Mech. Engrs (London),* 1949.

$$h_{v(max)} = \frac{4.77\sqrt{Q_{T_1} V_s}}{(1+0.43\frac{u}{V_s})u} \quad (3)$$

$$h_v = h_{v(max)}(1-0.8\frac{h_{v(max)}}{x}) \quad (4)$$

when $x > 2h_{v(max)}$. Their equation for the additional rise due to buoyancy (i.e., thermal rise) is

$$h_{t(max)} = \frac{6.37 g Q_{T_1} \Delta}{u^3 T_1} Z \quad (5)$$

where

$$Z = \ln J^2 + \frac{2}{J} - 2 \quad (6)$$

and

$$J = \frac{u^2}{\sqrt{Q_{T_1} V_s}}(0.43\sqrt{\frac{T_1}{gG}} - \frac{0.28 V_s T_1}{g\Delta}) + 1 \quad (7)$$

The foregoing equations are functions of the wind speed, u. Maximum values of C_o occur at a certain u, the critical wind speed. This is true since $e^{-\frac{h^2}{2\sigma^2}}$ increases with increasing wind velocity in Equation (1) while

$$\frac{Q_m \times 10^6}{\sqrt{2\pi} pqux^2}$$

decreases. A trial-and-error technique is generally used to calculate this critical wind speed.

The purpose of the present analysis is to develop a rapid method for the solution of the Bosanquet and Pearson formula, Equation (1), for effluent gases at or near atmospheric density. The method is based on the fact that the total height, H, of a gas after exit from a stack is a function of u. Consequently, the basic equations can be partially differentiated with respect to u. The critical wind speed is obtained if the resulting equation is set equal to zero. Other investigators have similarly calculated critical wind speeds using Sutton's equations and other plume rise formulas[7]. Thermal rise is not included in this rapid method because of the unwieldy character of the resulting equations.

Methods for the solution of 3 commonly required calculations are given below.

Case I. The Maximum Ground Level Concentration From a Given Stack Height

It is indicated in Bosanquet and Pearson[1] that by partial differentiation of Equation (1) with respect to x and setting the result equal to zero,

$$x_m = \frac{H}{2p} \quad (8)$$

and

(1) See footnote 1, page 127.

(7) "A Meteorological Survey of the Oak Ridge Area," U. S. Atomic Energy Commission, *ORO--99*, 1953.

TABLE I
Values of p and q for Stated Degrees of Atmospheric Turbulence

Turbulence	p	q	p/q	x_m
Low	0.02	0.04	0.50	$25H$
Average	0.05	0.08	0.63	$10H$
Moderate	0.10	0.16	0.63	$5H$

$$C_{o(max)} = \frac{2.15 \times Q_m \times \frac{p}{q} \times 10^5}{uH^2} \quad (9)$$

Rational values of p and q, for stated degrees of atmospheric turbulence are given in Table I[3].

The maximum ground level gas concentration, occurring with average or moderate turbulence, downwind from a given source, consequently becomes

$$C_{o(max)} = \frac{1.35 \times Q_m \times 10^5}{uH^2} \quad (10)$$

By partial differentiation of Equation (10) with respect to u it can be derived that the wind speed resulting in the greatest value of $C_{o(max)}$ is

$$u = -\frac{H}{2\frac{\partial H}{\partial u}} \quad (11)$$

It is usually sufficient and desirable to express the velocity rise of a gas as a fixed ratio of the maximum velocity rise at x_m. 85% of the maximum theoretical velocity rise will be attained where $x = 5.3h_{v(max)}$. [See Equation (4)] The closest location of maximum concentration from the stack will be $5H$ with moderate turbulence when $p = 0.1$. At x_m, therefore, nearly the full rise will always be attained. The stated fixed ratio is to allow for inaccuracies in the theoretical velocity rise and will usually be based on judgment and the problem under consideration. Thus,

$$H = h_s + h_v = h_s\left(1 + \frac{2.38a\sqrt{Q_{T_1}} V_s^{\frac{3}{2}}}{(V_s + 0.43u)uh_s}\right) \quad (12)$$

where

$a = 1$ for $\frac{1}{2}\ h_{v(max)}$
$a = 1\frac{1}{2}$ for $\frac{3}{4}\ h_{v(max)}$
$a = 2$ for $h_{v(max)}$

Therefore,

$$\frac{\partial H}{\partial u} = -\frac{2.38a\sqrt{Q_{T_1}} V_s^{\frac{3}{2}}(V_s + 0.86u)}{(V_s + 0.43u)^2 u^2} \quad (13)$$

Substitution of Equations (12) and (13) into Equation (11) and rearrangement give*

(3) See footnote 3, page 127.

*Critical wind speeds less than 1.5 fps. (1 mph.), resulting from equations developed in this analysis, are assumed equal to 1.5 fps.

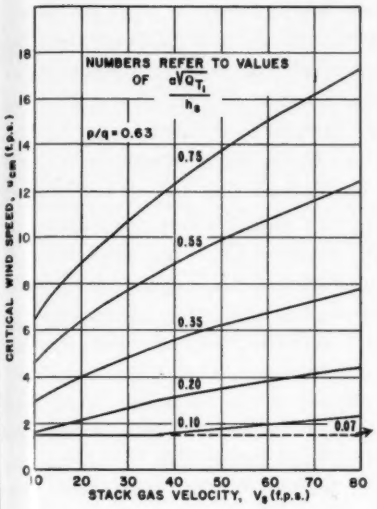

Fig. 1. Critical wind speed as a function of stack gas velocity when stack height is defined. Whenever $V_s \leq 80$ *and* $a\frac{\sqrt{Q_{T_1}}}{h_s} \leq 0.07$, *then* $u_{cm} = 1.5^{(2)}$.

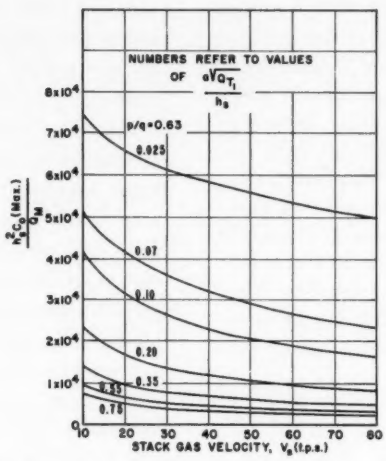

Fig. 2. $\frac{h_s^2 C_{o(max)}}{Q_m}$ *as a function of stack gas velocity when stack height is defined.*

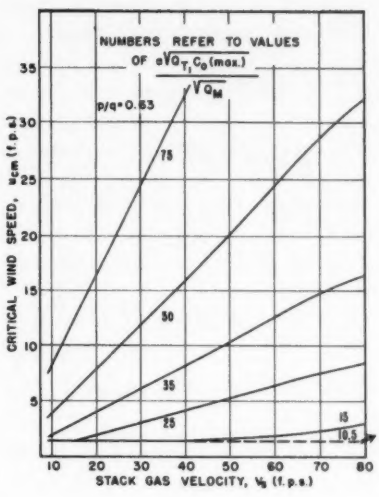

Fig. 3. Critical wind speed as a function of stack gas velocity when allowable maximum concentrations, $C_{o(max)}$, *is defined. Whenever* $V_s \leq 80$ *and* $a\frac{\sqrt{Q_{T_1}C_{o(max)}}}{\sqrt{Q_m}} \leq 10.5$ *then* $u_{cm} = 1.5^{(2)}$.

$$u_{cm}^3 + 4.65V_s u_{cm}^2 + \left[5.40V_s^2 - 16.62a\frac{\sqrt{Q_{T_1}}}{h_s}V_s^{\frac{3}{2}}\right]u_{cm} - 12.95a\frac{\sqrt{Q_{T_1}}}{h_s}V_s^{\frac{5}{2}} = 0 \qquad (14)$$

Fig. 1 depicts u_{cm} vs. V_s for assigned values of $\frac{a\sqrt{Q_{T_1}}}{h_s}$

Appropriate values of u_{cm} can be substituted into Equations (12) and (10). It is possible to further reduce the length of necessary computations for $C_{o(max)}$, however, by substituting Equation (12) into Equation (10). The following results:

$$\frac{h_s^2}{Q_m} \times C_{o(max)} = \frac{1.35 \times 10^5}{u_{cm}\left[1 + \frac{2.38a\sqrt{Q_{T_1}}V_s^{\frac{3}{2}}}{(V_s + 0.43u_{cm})u_{cm}h_s}\right]^2} \qquad (15)$$

Fig. 2 is a representation of Equation (15). The maximum average concentration, $C_{o(max)}$, therefore, may be ascertained directly by multiplying the ordinate determined from Fig. 2 by Q_m/h_s^2.

The selection of the maximum stack gas velocity represented in Fig. 1 and 2 (and others referred to later) is an arbitrary one. Most stack gas velocities will be below 80 fps., however.

If it is assumed,

$$h_{v(max)} = \frac{2.38a\sqrt{Q_{T_1}V_s}}{u} \qquad (16)$$

the resulting maximum velocity rise will never be more than 10% greater than that given by the complete formula, if $u_{cm} \leq 0.23V_s$. This will most often be the case when $V_s > 80$ fps.,

For the determination of critical wind speeds when $V_s > 80$ fps.,

$$H \cong h_s + \frac{2.38a\sqrt{Q_{T_1}V_s}}{u} \qquad (17)$$

From Equations (11) and (17), therefore,

$$u_{cm} \cong \frac{2.38a\sqrt{Q_{T_1}V_s}}{h_s} \qquad (18)$$

Case II. Stack Heights to Keep Concentration of Effluent Gases Below Specified Values at Given Levels

If it is necessary to keep the concentration of effluent gases below specified values, $C_{o(max)}$, it is evident from Equation (10) that

$$H = \sqrt{\frac{1.35 \times 10^5 \times Q_m}{uC_{o(max.)}}} \qquad (19)$$

[2] See footnote 2, page 127.

Substitution of Equations (19) and (13) into Equation (11) and rearrangement yields

$$u_{cm}^{\frac{5}{2}} + 4.65 V_s u_{cm}^{\frac{3}{2}} - 6.04 \times 10^{-2} a \frac{\sqrt{Q_{T_1} C_{o(max)}}}{\sqrt{Q_m}} V_s^{\frac{3}{2}} u_{cm} + 5.40 V_s^2 u_{cm}^{\frac{1}{2}} - 7.01 \times 10^{-2} a \frac{\sqrt{Q_{T_1} C_{o(max)}}}{\sqrt{Q_m}} V_s^{\frac{5}{2}} = 0 \quad (20)$$

Fig. 3 shows u_{cm} versus V_s for assigned values of

$$\left[a \frac{\sqrt{Q_{T_1} C_{o(max)}}}{\sqrt{Q_m}} \right]$$

It is possible as in Case I to further simplify necessary calculations for h_s by equating Equations (12) and (19). Thus,

$$h_s \times \frac{\sqrt{C_{o(max)}}}{\sqrt{Q_m}} = \frac{3.68}{\sqrt{u_{cm}}} - \frac{2.38 V_s^{\frac{3}{2}} a \sqrt{Q_{T_1} C_{o(max)}}}{(V_s + 0.43 u_{cm}) u_{cm} \sqrt{Q_m}} \quad (21)$$

Fig. 4 is a graph of Equation (21). The required stack height, h_s, may be found directly by multiplying the ordinate determined from Fig. 4 by $\frac{\sqrt{Q_m}}{\sqrt{C_{o(max)}}}$

For $V_s > 80$ fps. and from Equations (11), (17), and (19) with a development the same as that above

$$u_{cm} \cong \frac{16.7 a^2 Q_{T_1} C_{o(max)} V_s \times 10^{-5}}{Q_m} \quad (22)$$

It is apparent from Fig. 4 that relatively high stack gas velocities permit comparatively lower stack heights (and smaller diameters). It can be shown that the thermal rise obtained from Equations (5) to (7) decreases with increasing stack gas velocity, V_s, when the stack gas density is less than atmospheric, i.e., $T_s > T_1$. (These equations are not applicable in a neutral or unstable atmosphere because $G \leqq 0$ for these situations). This effect is evidently due to the greater entrainment of ambient air at the higher stack gas velocities. Under some atmospheric conditions, therefore, the *total* plume rise, $h_{v(max)} + h_{t(max)}$ for stack gases when $T_s > T_1$ may decrease with increasing stack gas velocity (for constant Q_{T_1}) Maximum velocity rise, thermal rise, and combined rise indicated in Table II for reasonable meteorological and stack parameters emphasize this point. It is desirable, however, that the stack gas velocity exceed a certain minimum value to prevent "downwash" of the effluent to the lee of the stack. This minimum value depends on the physical environment and can be determined from wind tunnel tests[8-9]. Increasing the stack gas velocity beyond this minimum value may not be advisable when $T_s > T_1$.

When the stack gas density is greater than that of the atmosphere ($T_s < T_1$) the effluent may sink rather than rise. Chesler and Jesser[10] have stated that heavy hydrocarbon vapors have been observed to drop towards the ground at refineries. The writer, too, has observed heavy gases sinking rapidly to the ground when the stack exit velocity was low. When $T_s < T_1$, therefore, it is apparent that high stack velocities *are* advisable to provide air entrainment and mixture with consequent reduction in both plume density and undesirable settling.

Case III. Critical Wind Velocity for a Specified Distance from the Stack

The foregoing considerations have been based on maximum concentrations. A requirement may arise, however, where it is necessary to deal only with concentrations at a specific distance, x, from a stack. It can be derived that

(8) von Hohenleiten, H. L. and Wolf, E. F., "Wind-Tunnel Tests to Establish Stack Heights for Riverside Generating Station," *Trans. ASME., 64,* 671 (1942).

(9) Sherlock, R. H., and Lesher, E. J., "Role of Chimney Design in Dispersion of Waste Gases," *Air Repair, 4,* 13 (1954).

(10) Chesler, S., and Jesser, B. W., "Some Aspects of Design and Economic Problems Involved in Safe Disposal of Inflammable Vapors from Safety Relief Valves," *Trans. ASME., 74,* 229 (1952).

TABLE II

Plume Rises for Stated Meteorological and Stack Parameters

V_s, fps.	u, fps.	Q_{T1}, cfs.	$h_{v(max)}$, ft.	$h_{t\ (max)}$, ft.	$h_{v(max)} + h_{t(max)}$, ft.
30	4	300	108	907	1,015
60	4	300	155	669	824
30	20	300	17	32	49
60	20	300	28	29	57

(a) $\Delta = 175°$ C; $T_1 = 300°$ K; $G = 0.003°$ C/ft.

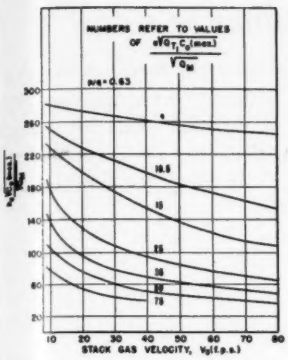

Fig. 4. $\frac{h_s\sqrt{C_{o(max)}}}{\sqrt{Q_m}}$ *as a function of stack gas velocity when allowable maximum concentration;* $C_{o(max)}$, *is defined.*

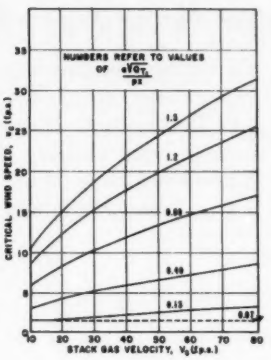

Fig. 5. Critical wind speed as a function of stack gas velocity for defined degree of turbulence and given distance from stack for $X >$ *about* $2.65\,ah_{v(max)}$. *Whenever* $V_s \leq 80$ *and* $a\frac{\sqrt{Q_{T_1}}}{px} \leq 0.07$ *then* $u_c = 1.5$[2].

for this case the maximum concentration at x will occur when

$$u = -\frac{px}{\frac{\partial H}{\partial u}} \qquad (23)$$

On substitution of Equation (13) into (23), where $x >$ about $2.65ah_{v(max)}$, the following results:

$$u_c^3 + 4.65V_s u_c^2 + \left[5.40V_s^2 - 11.1a\frac{\sqrt{Q_{T_1}}}{px}V_s^{\frac{3}{2}}\right]u_c - 12.9a\frac{\sqrt{Q_{T_1}}}{px}V_s^{\frac{5}{2}} = 0 \qquad (24)$$

A graph of u_c versus V_s for asigned values of

$$\left(a\frac{\sqrt{Q_{T_1}}}{px}\right)$$

is presented in Fig. 5. Consistent values of parameters can be substituted in Equations (1) and (12) to find C_o at x from a given stack height, or h_s required to keep effluent concentrations below specified values at x.

For $V_s > 80$ fps. and with the approximation of Equation (17)

$$u_c \cong \frac{2.38a\sqrt{Q_{T_1}V_s}}{px} \qquad (25)$$

(2) See footnote 2, page 127.

Conclusion

Methods for rapid solution of the Bosanquet and Pearson formula, Equation (1), have been developed for use with stack gases at or near atmospheric density. It is emphasized, however, that the present status of knowledge on atmospheric turbulence is not complete. The above equations, therefore, should not be interpreted as exact indicators of gas concentrations or necessary stack heights. It is advisable to use them only with consideration of their accuracy. These considerations are discussed by Helmers[3]. With regard for the referred limitations, the present method should materially aid the solution of some problems concerned with air pollution.

Appendix

Example

3,000 cfm. of an air-gas mixture at atmospheric temperature containing 120 cfm. of contaminant gas is discharged through a stack 1 ft. in diameter. What height should the stack be so that the average ground level concentrations of the contaminant do not exceed a given maximum allowable concentration of 10 ppm. by vol.? (Take ¾ of maximum velocity rise.)

Solution

Since the mixture contains 96% air it can be assumed that $T_s = T_1$. From the given conditions:

$Q_{T1} = 50$ cfs.
$Q_m = 2$ cfs.
$V_s = 64$ fps.
$C_{o(max)} = 10$ ppm. by vol.
$a = 1\frac{1}{2}$

$$a\frac{\sqrt{Q_{T_1}C_{o(max)}}}{\sqrt{Q_m}} = 23.5$$

Enter Fig. 4 with $V_s = 64$ and

$$a\frac{\sqrt{Q_{T_1}C_{o(max)}}}{\sqrt{Q_m}} = 23.5.$$

The value of $h_s\frac{\sqrt{C_{o(max)}}}{\sqrt{Q_m}}$ is 80. The required stack height, therefore, is

$$80\frac{\sqrt{Q_m}}{\sqrt{C_{o(max)}}} = 36 \text{ ft.}$$

Peak 1-min. concentrations from a 36-ft. stack could be expected to be 100-200 ppm. Momentary concentrations might equal 500 ppm.

The critical wind speed obtained directly from Fig. 3 is 6.5 fps. (4.5 mph).

(3) See footnote 3, page 127.

(Continued from page 126) *A Rapid General Purpose Centrifuge Method*

Heating, Ventilating and Refrigeration Division of the Mechanical Engineering Department for activating the research project; Ralph Gracza of Pillsbury Mills, Inc., relative to its application in the flour milling industry; Dr. M. A. Knight of Minnesota Mining and Manufacturing Co. for valuable suggestions on the methods of calculating tables; Arie Galswick of the Engineering Research and Development Division of General Mills for certain data on reproducibility; J. A. Becket of the Research and Engineering Division of the Fram Corp. for data on certain problems of reproducibility.

AIR POLLUTION CONTROL ASSOCIATION

President

H. KENNETH KUGEL '56
Chief Engineer
Division of Smoke Regulation and Boiler Inspection
District of Columbia
Washington, D. C.

First Vice President

BENJAMIN LINSKY '57
Chief, Smoke Abatement Bureau
City of Detroit
Detroit, Michigan

Vice Presidents

RALPH W. BOURNE '56
Chief Combustion Engineer
Louisville Smoke Commission
Louisville, Kentucky

H. L. WAGNER '56
Vice President in Charge of Engineering
Detroit Stoker Company
Detroit, Michigan

ELMER P. WHEELER '57
Assistant Director, Medical Department
Monsanto Chemical Company
St. Louis, Missouri

Past President

GORDON P. LARSON '56
Air Pollution Control District of Los Angeles County
Los Angeles California

DIRECTORS

JOHN E. BROWN '56
Air Pollution Control Engineer
County of Milwaukee
Milwaukee, Wisconsin

MILLER G. STEWART '56
Road Foreman of Engines
Washington Terminal Company
Washington, D. C.

R. L. IRELAND '56
Chairman, Executive Committee
Pittsburgh Consolidation Coal Company
Cleveland, Ohio

HERBERT H. ULRICH '57
Chief Smoke Regulation Engineer
Sanitation Commission
Omaha, Nebraska

BASIL HORSFIELD '58
Vice President
Reynolds Metals Company
Sheffield, Alabama

ARNOLD ARCH '58
Director, Air Pollution Control Dept.
City of Niagara Falls
Niagara Falls, New York

EDGAR C. BAIN '58
Vice President
United States Steel Corporation
Pittsburgh, Pennsylvania

R. M. LANDON '58
Executive Assistant
Gulf Oil Corporation
Pittsburgh, Pennsylvania

HARRY M. PIER '58
Special Assistant
Research-Cottrell, Inc.
Basking Ridge, New Jersey

W. A. QUEBEDEAUX '58
Director, Stream and Air Pollution Control
Harris County Health Department
Houston, Texas

MILTON REIZENSTEIN '58
Smoke Abatement Engineer
City of Baltimore
Baltimore, Maryland

Treasurer
H. C. DAVIES

Executive Secretary
HARRY C. BALLMAN

4400 FIFTH AVENUE - PITTSBURGH 13, PA.